SEE
FOLLOWING
NOTE

PARTS OF THE ORIGINAL DOCUMENT

ARE OF POOR REPRODUCTIVE QUALITY

-------------------------------------

CERTAINES PARTIES DU DOCUMENT ORIGINAL

SONT DE PIÈTRE QUALITÉ DE REPRODUCTION

CA1
DTC 801
85
T115
c.2

Department of Mechanical Engineering
University of New Brunswick
Fredericton, N.B.

89-02027/

TP 7518E

# TANK CAR THERMAL RESPONSE ANALYSIS: VOLUME 5

## SUPPORTING STUDIES

J.E.S.Venart, A.C.M.Sousa, F.R. Steward, et al

**Prepared For:**

TRANSPORT CANADA
TRANSPORTATION DEVELOPMENT CENTER
Montreal, Quebec  H3A 2R3

**Prepared By:**

University of New Brunswick
Department of Mechanical Engineering
P.O. Box 4400
Fredericton, NB E3B 5A3

Library an [illegible]
Centre d [illegible]
REC[illegible]
JUL 29 1987
Transport Canada / Transports Canada

THE CONTENTS OF THIS REPORT REFLECT
THE VIEWS OF THE CONTRACTOR AND NOT
NECESSARILY THE OFFICIAL VIEWS OR
POLICIES OF THE TRANSPORTATION
DEVELOPMENT CENTER

# REPORT DOCUMENTATION FORM

| | | |
|---|---|---|
| 1. Transport Canada Report No.<br>TP 7518E | 2. TDC Project No.<br>4727 | 3. Recipient's Catalogue No. |
| 4. Title and Subtitle<br>Tank Car Thermal Response Analysis: Volume 5 Supporting Studies | | 5. Report Date<br>March 1985<br>6. Performing Organization Report No.<br>UNB-ME-TF 28 |
| 7. Author(s)<br>J.E.S. Venart, A.C.M. Sousa, F.R. Steward, et al | | 8. Transport Canada File No.<br>D1465-302-2 |
| 9. Performing Organization Name and Address<br>Fire Science Centre<br>University of New Brunswick<br>P.O. Box 4400<br>Fredericton, N.B. E3B 5A3 | | 10. DSS File No.<br>11SD.T8200-2-2509<br>11. DSS or Transport Canada Contract No.<br>OSD82-00085 |
| 12. Sponsoring Agency Name and Address<br>Transportation Development Centre (TDC)<br>Guy Favreau Complex<br>200 Dorchester Blvd. West., Suite 601, West Tower<br>Montreal, Quebec H2Z 1X4 | | 13. Type of Report and Period Covered<br>14. Sponsoring Agency Code<br>TDC 4727 |
| 15. Supplementary Notes<br>See also "Tank Car Thermal Response Analysis: Executive Summary", by J.E.S. Venart, March 1985 TP 6809E. | | 16. TDC Project Officer<br>D.W. Dibble |

17. Abstract

This collection of supporting studies relating to tank car thermal response includes three study papers, three draft manuscripts, and two computer programmes, as listed below:

1. "Transient Laminar Free Convection in Horizontal Cylinders" - draft manuscript.
2. "Three Dimensional Formulation of the Radiant Heat Flux Variation in a Cylinder Engulfed in Flames" - draft manuscript.
3. "Nucleate and Film Pool Boiling in R11: The Effects of Inclination Angle and Surface Enhancement" - draft manuscript.
4. "Rail Tank Car Geometry" - computer programme.
5. "Design, Construction and Testing of a Cylindrically Surfaced Calorimeter" - study paper.
6. "Report on the Significance of Flare Radiation on Railway Cars Containing LPG" - study paper.
7. "Report on Pool Fire Experiments Related to Tank Car Modelling" - study paper.
8. "Development of Computer Code to Determine the Thermodynamic and Transport Properties of Propane"- computer programme.

| | |
|---|---|
| 18. Key Words<br>Accidents, BLEVE, Boiling, Fires, Pool, Propane, Railway, Tank Car, Thermal Response, Protection | 19. Distribution Statement<br>Limited number of copies available from the Transportation Development Centre |

| | | | |
|---|---|---|---|
| 20. Security Classification (of this report)<br>Unclassified | 21. Security Classification (of this page)<br>Unclassified | 22. No. of Pages<br>180 | 23. Price<br>— |

TDC CDT 79-005

# FORMULE DE DOCUMENTATION POUR RAPPORT

1. Nº du rapport Transports Canada
TP 7518E

2. Nº de l'étude — CDT
4727

3. Nº de catalogue du destinataire

4. Titre et sous-titre
Tank Car Thermal Response Analysis: Volume 5
Supporting Studies

5. Date du rapport
mars 1985

6. Nº du rapport de l'organisme exécutant
UNB-ME-TF 28

7. Auteur(s)
J.E.S. Venart, A.C.M. Sousa, F.R. Steward, et al

8. Nº de dossier Transports Canada
D1465-302-2

9. Nom et adresse de l'organisme exécutant
Fire Science Centre
Université du Nouveau-Brunswick
C.P. 4400
Fredericton, N.B. E3B 5A3

10. Nº de dossier — ASC
11SD.T8200-2-2509

11. Nº de contrat — ASC ou Transports Canada
OSD82-00085

12. Nom et adresse de l'organisme parrain
Centre de développement des transports (CDT)
Complexe Guy-Favreau
200 ouest, boul. Dorchester, Suite 601, Tour Ouest
Montréal, Québec H2Z 1X4

13. Genre de rapport et periode visée

14. Code de l'organisme parrain
CDT 4727

15. Remarques additionnelles
Voir aussi "Tank Car Thermal Response Analysis: Executive Summary", par J.E.S. Venart, mars 1985 TP 6809E.

16. Agent de projet — CDT
D.W. Dibble

17. Resumé

La nomenclature des études découlant de la recherche sur le comportement thermique des wagons-citernes comprend trois études proprement dites, trois avant-projets manuscrits et deux programmes informatiques, comme suit:

1. "Transient Laminar Free Convection in Horizontal Cylinders": avant-projet manuscrit.
2. "Three Dimensional Formulation of the Radiant Heat Flux Variation in a Cylinder Engulfed in Flames: avant-project manuscrit.
3. "Nucleate and Film Pool Boiling in R11: The Effects of Inclination Angle and Surface Enhancement": avant-projet manuscrit.
4. "Rail Tank Car Geometry": programme informatique.
5. "Design, Construction and Testing of a Cylindrically Surfaced Calorimeter": étude.
6. "Report on the Significance of Flare Radiation on Railway Cars Containing LPG": étude.
7. "Report on Pool Fire Experiments Related to Tank Car Modelling": étude.
8. "Development of Computer Code to Determine the Thermodynamic and Transport Properties of Propane:"programme informatique.

18. Mots-clés
Accidents, BLEVE, ébullition, flammes enveloppantes, propane, rail, wagon-citerne, comportement thermique, protection

19. Diffusion
Le Centre de développement des transports dispose d'un nombre limité d'exemplaires.

20. Classification de sécurité (de ce rapport)
non classifié

21. Classification de sécurité (de cette page)
non classifiée

22. Nombre de pages
180

23. Prix
—

## TABLE OF CONTENTS

PAGE

I DRAFT MANUSCRIPT
"Transient Laminar Free Convection in Horizontal Cylinders"........................ 1-1

II DRAFT MANUSCRIPT
"Three Dimensional Formulation of the Radiant Heat Flux Variation in a Cylinder Engulfed in Flames"........................ 2-1

III DRAFT MANUSCRIPT
"Nucleate and Film Pool Boiling in R11: The Effects of Inclination Angle and Surface Enhancement"......... ............ 3-1

IV COMPUTER PROGRAMME
"Rail Tank Car Geometry".................... 4-1

V STUDY PAPER
"Design, Construction and Testing of a Cylindrically Surfaced Calorimeter......... 5-1

VI STUDY PAPER
"Report on the Significance of Flare Radiation of Railway Cars Containing LPG".. 6-1

VII STUDY PAPER
"Report on Pool Fire Experiments Related to Tank Car Modelling"....................... 7-1

VIII COMPUTER PROGRAMME
"Development of Computer Code to Determine the Thermodynamic and Transport Properties of propane"........ ....................... 8-1

# TRANSIENT LAMINAR FREE CONVECTION IN HORIZONTAL CYLINDERS

N.U. Aydemir*, A.C.M. Sousa** and J.E.S. Venart***
Department of Mechanical Engineering
University of New Brunswick
Fredericton, N.B.
Canada E3B 5A3

## ABSTRACT

A numerical study of laminar natural convection inside uniformly heated, partially or fully filled horizontal cylinders is made. A coordinate transformation which simplifies the discretization of the equations of motion and energy is utilized. The resulting system of partial differential equations with their boundary conditions is solved using central differences for various Prandtl and Grashof numbers for two different grid sizes. The flow in completely filled cylinders for which experimental data are available is predicted. Close agreement between steady-state predictions and experiments is obtained for temperature and velocity profiles as well as for the streamline contours and isotherms. The technique is further demonstrated by solving the transient natural convection flow inside a partially filled horizontal cylinder with an adiabatic free surface and subjected to uniform wall heating.

* Research Assistant
** Associate Professor
*** Professor

## NOMENCLATURE

| | |
|---|---|
| $g$ | acceleration due to gravity, $m/s^2$ |
| $Gr_R^*$ | modified Grashof number $= \frac{g\beta qR^4}{k\nu^2}$ |
| $Gr_R$ | Grashof number $= \frac{g\beta\Delta TR^3}{\nu^2}$ |
| $\vec{H}$ | heat function vector, dimensionless |
| $k$ | thermal conductivity, W/mK |
| $L(Y)$ | cord length associated with coordinate Y, dimensionless |
| Pr | Prandtl number $= \frac{\nu}{\alpha}$ |
| $q$ | wall heat flux, $W/m^2$ |
| $R$ | radius, m |
| $r(X,Y,Z)$ | distance of a boundary point from the reference axis, dimensionless |
| $\vec{S}$ | vector derived from the flow field solution, dimensionless |
| $T$ | temperature, K |
| $T_w$ | wall temperature, K |
| $T_\infty$ | reference temperature, K |
| $t$ | time, s |
| $u$, $v$ | velocity components in x, y direction, m/s |
| $U,V$ | dimensionless velocity components in X- and Y-direction normalized with $U_\infty$ |
| $U_\infty$ | reference velocity $= \sqrt{g\beta qR^2/k}$ or $\sqrt{g\beta\Delta TR}$, $\frac{m}{s}$ |
| $\vec{V}$ | velocity vector, dimensionless |
| $\vec{W}$ | vorticity vector, dimensionless |
| $W$ | vorticity, dimensionless |
| $x,y,z$ | cartesian coordinates, m |
| $X,Y,Z$ | cartesian coordinates normalized with a reference length, dimensionless |

## Greek Letters

| | |
|---|---|
| $\alpha$ | thermal diffusivity, $m^2/s$ |
| $\beta$ | coefficient of thermal expansion, $K^{-1}$ |
| $\zeta, \eta, \zeta', \eta'$ | non-dimensional coordinates in the transformed domain |
| $\Theta$ | non-dimensional temperature = $\frac{(T-T_\infty)}{qR}k$ or $\frac{T-T_\infty}{T_w-T_\infty}$ |
| $\nu$ | kinematic viscosity, $m^2/s$ |
| $\tau$ | non-dimensional time = $\frac{\nu}{R^2}\sqrt{Gr_R}\ t$ or $\frac{\nu}{R^2}\sqrt{Gr_R^*}\ t$ |
| $\phi$ | angle measured from the bottom of the cylinder, rads. |
| $\phi^*$ | angle measured from the $\zeta$ axis on $(\zeta-\eta)$ plane, rads. |
| $\vec{\Phi}$ | heat potential, dimensionless |
| $\Phi$ | angle of incidence of the heat flux vector, rads. |
| $\psi$ | non-dimensional stream function |
| $\vec{\Psi}$ | vector potential, dimensionless |
| $\Delta\zeta$ | grid size, dimensionless |
| $\nabla^2$ | Laplacian operator |
| $\vec{\nabla}$ | gradient vector |

## 1. Introduction

The present work is part of a research program whose objective is to understand and model the behaviour of fluids inside horizontal cylindrical or elliptical containers subjected to circumferential heating. Of particular interest are those cases where the tank is partially filled.

In the past, a number of workers have studied natural convection in completely filled cylinders experimentally [3,4,5] as well as numerically and analytically with boundary conditions of the first kind, [1,2,3].

Ostrach [1] in reviewing the existing work in enclosures also solved analytically the horizontal cylinder problem for a high Prandtl number of 20,000 and a low Grashof number of 1.1. For this particular study the governing equations were simplified in two steps, namely: (i) an order-of-magnitude analysis was applied and as a result of the large Prandtl number the advective terms of the equation of motion were neglected, and (ii) a modified Oseen linearization was utilized leading to the uncoupling of the energy equation from the equation of motion. His results compare reasonably well with the experimental data obtained from a cylinder whose walls were set at a cosine varying temperature around the circumference, but constant with time. The theory, however, leads to an incorrect flow field for those cases $\phi=0$ ($\phi$ is the angle as defined in [1]) and cannot predict the shape of the streamlines for $\phi$ larger than zero. A suitable adjustment of the Oseen constant, however, leads to the excellent agreement of the analytical prediction with the experimental data.

Hellums and Churchill [2] have solved the same problem numerically for air (Pr=0.7) enclosed in a cylinder whose half sides were kept at different constant temperatures for a Grashof number range from $4.5 \times 10^4$ to $10^7$. The results reported compare well with Martini and Churchill's data [4].

The numerical or analytical solution of the flow inside a partially filled horizontal cylinder is involved since one has to deal with an irregular domain whose boundaries are not parallel to the coordinate system (Figure 1.a). To the authors' knowledge the only study on this topic [6] utilized an integral method of analysis along with a new stability analysis. Their results compare favourably with experimental data obtained in a partially filled tank of Freon 11 ($Pr = 3.4$) with heat fluxes between 20 to 40 $kW/m^2$. This integral analysis, however, provides only limited information about the flow and cannot for instance predict it in regions outside the boundary layer. A complete numerical integration is therefore required to obtain more information about the flow field.

It is known that the growth of thermally stratified layers inside closed containers may lead to dangerous vapor pressures when they are heated either by solar radiation or a fire surround. An example for the latter case is a derailed railroad tank car loaded with self pressurized liquid fuel exposed to a pool fire. The consequences of such an accident are discussed in detail elsewhere [7]. The initial heat transfer mechanism to the fluid is by natural convection and the prediction of the fluid temperature and flow field is important in order to evaluate pressures and develop internal or external protection methods.

In the following section a technique will be introduced to obtain an orthogonal coordinate system which enables discretization in a rectangular domain. The governing equations will next be stated along with the method of solution, the treatment of boundary conditions will also be discussed in this section. In the following section the results of test runs for completely and partially filled tanks are presented and compared with data and observations.

The computed flow patterns and temperature fields will be given in streamline and isotherm contour plots. A new technique of computational flow visualization introduced by [8] will also be applied to the case of partial filling to determine the regions dominated by convection or conduction.

## 2. The Coordinate Transformation

Methods of coordinate transformation are not new, however, they are problem dependent; one must use special transforms for different problems. One such example is that of Yao [9], where natural convection along a vertical wavy surface was considered and transformed to that of a flat surface. A similar method to that introduced in this paper was discussed by [10] who considered a trapezoidal domain. The method introduced in this study is also special but it can be further applied to other geometries provided certain requirements are met. Extension to three dimensions is reasonably straightforward.

The method is indeed a stretching of the X-coordinate* by normalizing it using the cord length associated with the Y-coordinate of an arbitrary point (Figure 1a). In this way, an orthogonal system can be obtained in $(\zeta,\eta)$ where

$$\zeta = \frac{X}{\sqrt{1-Y^2}} \quad \text{and} \quad \eta = Y \tag{1}$$

noting that $-1\leq\zeta\leq 1$ and $-1<\eta<1$.

This transformation maps a circular domain into a square or a normal cross-section of a partially filled cylinder into a rectangle (Figure 1b). It can be seen that $L(Y) = \sqrt{1-Y^2}$ is the associated cord length which varies with height.

---

* Cartesian coordinates are used to describe the physical domain instead of polar coordinates, since expressed in the latter, the transformed equations are extremely involved.

The above technique can be applied to any domain whose boundaries are expressed by a continuous function with continuous first derivatives in the domain of interest.

The singularity points of the proposed transformation are those where the cord length vanishes. At these points the mapping is not one-to-one and a special treatment for these regions is necessary.

Relations similar to eqn. (1) can be found for those containers whose cross-section boundary can be represented with a function meeting the above continuity requirements. For instance for a parabola given by

$$Y = aX^2 \qquad Y > 0, \quad a > 0$$

we can write

$$\zeta = \frac{X}{\sqrt{\frac{Y}{a}}}, \qquad \eta = Y \tag{2}$$

or for an ellipse given by

$$\frac{X^2}{a^2} + \frac{Y^2}{b^2} = 1,$$

we can show that

$$\zeta = \frac{X}{\sqrt{a^2 - (\frac{a}{b} Y)^2}}, \qquad \eta = Y \tag{3}$$

It should be noted that if the containers were full, it would be much easier to use conventional coordinate systems, however if they are partially filled then the above transformations permit some simplification of the problem.

Generalization of the technique to three dimensions can also be made since if $F(X,Y,Z) = 0$ defines a surface in space (Figure 2a), a transformation may be obtained with

$$\zeta = \frac{X}{r(X,Y,Z)}, \quad \eta = \frac{Y}{r(X,Y,Z)}, \quad Z = Z \tag{4}$$

where $r(X,Y,Z)$ is a function whose value is the distance between the vertical Z-axis and the boundary point $P(X,Y,Z)$, measured along the line perpendicular to the axis and passing through the point. This transformation maps the 3-dimensional surface to a cylinder. Equation (1) can be applied to eqns.(4) to obtain a cube (whereas in 2-dimensions a square is generated) to give (Figure 2b, 2c)

$$\zeta' = \frac{\zeta}{\sqrt{1-\zeta^2}}, \quad \eta' = \eta, \quad Z = Z \tag{5}$$

This method can in principle be applied to any 3-dimensional body as long as F(X,Y,Z) is a smooth function with continuous derivatives in every direction.

Note that for bodies of revolution like a sphere, ellipsoid, cone, etc., the intermediate transformation $(\zeta,\eta)\to(\zeta',\eta')$ is not required.

One particular difficulty with the method, however, is the additional complication caused by the transformed equations of motion. These must be developed according to the relations given by eqn. (1) or eqns. (4) and (5). The new forms of the relevant differential operators in the $(\zeta-\eta)$ plane are given in Appendix A for 2-dimensions.

The Jacobian of the mapping given by eqn. (1) is

$$|J| = 1-Y^2 \tag{6}$$

which vanishes at $Y = \mp 1$. The transformation is therefore not unique at the top and bottom of the cylinder since the vertical lines in the $(\zeta-\eta)$ plane meet at a single point in the X-Y plane, that is as $\eta$ approaches the values $\pm 1$. The singularity at $\eta=1$ is avoided in this instance since the problem is for a partially filled vessel. The singularity at $\eta = -1$ may be excluded from the domain by a horizontal cut at $\eta = -0.99$. For completely filled cylinders a cut above $\eta = 0.99$ is taken similar to $\eta = -0.99$. As it will be shown these approximations do not appear to significantly affect the results.

## 3. The Mathematical Problem

The equations of motion are the transient, incompressible, two-dimensional Navier-Stokes equations linked to the energy equation by the Boussinesq approximation.

Eliminating pressure by cross-derivation we obtain in dimensionless form:

Vorticity Transport Equation:

$$\frac{\partial W}{\partial \tau} + U\frac{\partial W}{\partial X} + V\frac{\partial W}{\partial Y} = \frac{\partial \Theta}{\partial X} + \frac{1}{\sqrt{Gr_R}}\nabla^2 W \tag{7a}$$

Energy Equation:

$$\frac{\partial \Theta}{\partial \tau} + U\frac{\partial \Theta}{\partial X} + V\frac{\partial \Theta}{\partial Y} = \frac{1}{Pr\sqrt{Gr_R}}\nabla^2 \Theta \tag{7b}$$

Stream Function - Vorticity Equation:

$$\nabla^2 \psi = -W \tag{7c}$$

Velocity Relations:

$$U = \frac{\partial \psi}{\partial Y}, \quad V = -\frac{\partial \psi}{\partial X} \tag{7d}$$

where

$$U = u/u_\infty, \quad V = v/u_\infty, \quad X = x/R, \quad Y = y/R$$

$$\Theta = (T-T_\infty)\frac{k}{qR} \text{ if } Gr_R = \frac{g\beta qR^4}{k\nu^2}$$

with $U_\infty = \sqrt{\frac{g\beta qR^2}{k}}$

or $\Theta = \frac{T-T_\infty}{T_\omega - T_\infty}$ if $Gr_R = \frac{g\beta\Delta TR^3}{\nu^2}$

with $U_\infty = \sqrt{g\beta\Delta TR}$

and $\tau = \frac{\nu}{R^2}\sqrt{Gr_R}\, t$

The transformed equations of motion are given in Appendix B.

Extension of the present computations to three dimensions is possible using a vector potential in the definition of the velocity vector as $\vec{V} = \vec{\nabla} \times \vec{\psi}$, which results in three vorticity transport and three vorticity-stream function equations. Including the energy equation, the system is closed with seven unknowns and seven equations [11]. Obviously, for the horizontal cylinder no additional transformation is necessary in the Z-direction since the axis of the cylinder is parallel to the coordinate axis. The resulting solution domain will be a rectangular box and can be discretized in a cartesian coordinate system using a uniform grid spacing. The assumption of an infinitely long cylinder makes the computations two dimensional.

No difficulties arise with Dirichlet type boundary conditions since these can be set up by imposing the scalar value along the boundary of the physical or mathematical domains (e.g. presumed temperature or homogeneous stream function along the impermeable walls).

Neumann boundary conditions require additional manipulation however. The wall values of vorticity are computed from the stream function values in the usual way but the treatment is different due to cross derivative appearing in the Laplacian (eqn. A1)).

Noting that

$$V = \frac{1}{\sqrt{1-Y^2}} \frac{\partial \psi}{\partial \zeta} = 0 \quad \text{and} \quad U = \frac{\partial \psi}{\partial \eta} = \frac{\partial^2 \psi}{\partial \zeta^2} = 0 \qquad (8)$$

along the walls of the rectangle, we can write eqn.(B.3) using eqn.(8) as,

$$\left[\frac{1}{1-\eta^2} + \frac{\zeta^2 \eta^2}{(1-\eta^2)^2}\right] \frac{\partial^2 \psi}{\partial \zeta^2} + \frac{2\zeta\eta}{1-\zeta^2} \frac{\partial^2 \psi}{\partial \zeta \partial \eta} = -W \qquad (9)$$

$\frac{\partial^2\psi}{\partial\zeta^2}$ can be approximated with third order accuracy using using eqn. (8) and Taylor series expansion as

$$\frac{\partial^2\psi}{\partial\zeta^2} = \frac{8\psi_{i+1,j} - \psi_{i+2,j}}{2\Delta\zeta^2} \tag{10}$$

similarly,

$$\frac{\partial^2\psi}{\partial\zeta\partial\eta} = \frac{\partial}{\partial\zeta}\left(\frac{\partial\psi}{\partial\eta}\right).$$

Expanding in Taylor series again, having i located at the left wall, (i.e. i = 1),

$$\left.\frac{\partial\psi}{\partial\eta}\right|_{i+1} = \left.\cancelto{0}{\frac{\partial\psi}{\partial\eta}}\right|_i + \left.\frac{\partial}{\partial\zeta}\left(\frac{\partial\psi}{\partial\eta}\right)\right|_i \Delta\zeta + \left.\frac{\partial^2}{\partial\zeta^2}\left(\frac{\partial\psi}{\partial\eta}\right)\right|_i \frac{\Delta\zeta^2}{2!} + 0(\Delta\zeta^3)$$

$$\left.\frac{\partial\psi}{\partial\eta}\right|_{i+2} = \left.\cancelto{0}{\frac{\partial\psi}{\partial\eta}}\right|_i + \left.\frac{\partial}{\partial\zeta}\left(\frac{\partial\psi}{\partial\eta}\right)\right|_i 2\Delta\zeta + \left.\frac{\partial^2}{\partial\zeta^2}\left(\frac{\partial\psi}{\partial\eta}\right)\right|_i \frac{(2\Delta\zeta)^2}{2!} + 0(\Delta\zeta^3) \tag{11}$$

Eliminating $\left.\frac{\partial^2}{\partial\zeta^2}\left(\frac{\partial\psi}{\partial\eta}\right)\right|_i$ in the above, we obtain,

$$\frac{\partial}{\partial\zeta}\left(\frac{\partial\psi}{\partial\eta}\right)_i = \frac{4\left.\frac{\partial\psi}{\partial\eta}\right|_{i+1} - \left.\frac{\partial\psi}{\partial\eta}\right|_{i+2}}{2\Delta\zeta} \tag{12}$$

with second order accuracy. A similar expression can be written for the right wall with i+1→k-1, i+2→k-2 and i→k where k is the total number of nodes in the ζ direction.

Note that at the bottom and top of the fully filled cylinder we have,

$$\frac{\partial^2\psi}{\partial\eta^2} + \frac{2\zeta\eta}{1-\eta^2}\frac{\partial^2\psi}{\partial\zeta\partial\eta} = -W \tag{13}$$

since the derivatives $\frac{\partial}{\partial\zeta}$ vanish at the horizontal boundaries ($\psi$ = const.). At the shear free surface eqn. (13) simplifies to $W = 0$. Discretization of eqn. (12) with central differences requires 9 nodal points at every station along the wall, whereas in a real rectangular enclosure only three nodes need to be considered.

The Neumann conditions introduced by a constant heat flux condition can also be handled similarly.

Considering the temperature normalized with respect to heat flux, i.e. $\Theta = (T-T_\infty)\frac{k}{qR}$, the constant heat input boundary conditions are introduced as in the non-transformed domain by

$$\frac{\partial\theta}{\partial X} = \cos\Phi \quad \text{and} \quad \frac{\partial\Theta}{\partial Y} = \sin\Phi \qquad (14)$$

where $\Phi$ is the angle of incidence of the heat flux vector whose magnitude is assumed to be constant. The assumption of normal heat flux vector is a reasonable one, i.e. $\Phi = \phi^*$ along the circumference. Utilizing eqns. (A2) and (A3) along with eqn. (1), eqn. (14) can be rewritten as:

$$\frac{1}{\sqrt{1-\eta^2}}\;\frac{\partial\theta}{\partial\zeta} = \zeta\sqrt{1-\eta^2} \;\rightarrow\; \frac{\partial\theta}{\partial\zeta} = \;(1-\eta^2) \qquad (15)$$

and

$$\frac{\zeta\eta}{1-\eta^2}\,\frac{\partial\theta}{\partial\zeta} + \frac{\partial\theta}{\partial\eta} = \eta \qquad (16)$$

Substituting eqn. (15) in eqn. (16) results in

$$\frac{\partial\theta}{\partial\eta} = \eta(1-\zeta^2) \qquad (17)$$

That is, in the transformed domain, along the vertical walls at $\zeta = \mp 1$, the temperature gradient in the direction of $\eta$ vanishes. This is consistent with the fact that if heat flux vector is normal to the boundary, then the surface is isothermal. Eqn. (15) along with eqn. (17) constitute therefore the boundary conditions of the second type.

Eqns. (B1) to (B4) in Appendix B are discretized using central differences with an implicit formulation in time. Transient as well as steady-state solutions are obtained through a time marching process. For each time step the governing equations in transformed form, eqns. (B1) to (B4), are solved using point-by-point iteration with a single pass per equation in each iterative cycle. In the present context the convergence of the computations is based on the convergence of the vorticity field such that the criterion

$$\max\left|\frac{W_{i,j}^{n+1} - W_{i,j}^{n}}{W_{i,j}^{n+1}}\right| \times 100 \leq 0.001, \text{ is satisfied,}$$

with n representing the iteration level.

## 4. Test Runs

Published experimental data for the completely filled cylinder are available for Prandtl numbers 19950 and 0.7, silicone oil [5] and air [4], respectively. Data are given for a case where the walls of the cylinder were kept at time constant temperature with a sawtooth distribution [5]. The computed steady state velocity and temperature profiles are plotted here against the experimental values in Fig. 3 and Fig. 4. The comparison is good and reveals that the flow field difficulties for $\phi \geq 0$ as reported in [1] have been successfully overcome.

The results of the computations for $Pr=0.7$, $Gr=4.5\times10^4$ are shown in Fig. 5 and Fig. 6 where the temperature and velocity profiles are compared with the data of [4]. In this case, the cylinder halves were kept at two different temperatures. The agreement with the steady state temperature profiles is favorable but the computed velocities show deviations as high as 40% from the experimental data close to the wall. This may possibly be due to errors introduced during measurements and interpretations of velocities. In

Fig. 6 of [4], the scatter in the velocity measurements can be observed to be as high as 30% at a distance of 16% of the radius away from the wall. The present computations should be judged on this basis.

For the case of the partially filled vessel, which is the main objective of this study, glycerine was chosen for the simulation runs. It should be noted that the solution domain for the results shown here is $-1 \leq \zeta \leq 1$, $-0.99 \leq \eta \leq 0.4$ where $\eta = 0.4$ corresponds to a 75% filling. The flow conditions are such that $Gr_R = 114$ and $Pr = 6380$ and since the properties are assumed constant along with the heat flux, these values do not change in the computation.

The simulated flow starts with two small eddies at the tank walls close to $\phi = 90°$ (Fig. 7.a). Eventually the two rotating cells join at the centre (Fig. 7.b) and a distortion is observed along the line of their contact (Fig. 7.c).

The shape of the innermost eddies before and after the contact can be explained by considering only the developing cell in one-half of the cylinder. In this region the cell would continue to grow indefinitely with flow velocities increasing if there were no other cell in the other half of the cylinder. When the two counter-rotating cells meet at the centre however, they cannot continue to grow further and hence must adjust themselves. It should be noted that since the wall heat flux is constant this results in a continuously accelerating flow.

The isotherms shown in Figs. 8(a), (b) and (c) indicate the time dependent thermal stratification of the liquid and also the isothermal nature of the horizontal core temperatures.

In Fig. 9, the downward velocity along the vertical radius has been plotted for several times. The velocities in this direction start from zero, pass through a maximum and decreases to zero at the bottom of the tank again where $r/R = 1$. However as the eddies meet at the center at $t = 4.6$ mins, this regular pattern changes and two maximums are observed in the downward velocities. This is also evidenced by the expansion of streamlines (Fig. 7.c) as discussed previously.

A flow visualization (Fig. 10) qualitatively verifies the above results. Here a tracer was injected into a glass vessel of aspect ratio (length to diameter) of 2, allowed to diffuse and mix uniformly with the glycerine inside. The vessel was filled to about 60% compared to the 75% in the numerical simulation. Computations for 62% also displayed the same characteristics as in Fig. 7.c, that is, streamline distortion occurred close to the centre between the interface and the bottom. The figure also shows a similar development of the streamlines which appear to buckle inwards. This photograph was taken approximately twenty hours after test initiation since a long time is required for the dye to mix completely with the liquid glycerine.

Further information about the flow can be obtained through the visualization of 2 dimensional heat flow lines, introduced by [8]. The technique of computational heat flow visualization is analogous to the streamline visualization where contours of constant stream values are drawn. The difference is that the stream function satisfies the continuity equation while the "heat function" satisfies the energy equation.

Contours of the heat function indicate the actual lines of heat flow whereas conventional isotherms can only reveal heat conduction lines. The convective term in the definition of the heat function takes into account any heat flow due to convection. Further details of the method can be found in the original paper [8], where only two dimensions are considered. It is, however, possible to extend the definition of the heat function to a "heat potential," as follows:

The energy equation can be rewritten as

$$\vec{\Phi} = \vec{V}\Theta - \frac{1}{Pr\sqrt{Gr_R}}\vec{\nabla}\Theta \qquad (18a)$$

where $$\vec{\nabla}\cdot\vec{\Phi} = 0 \qquad (18b)$$

It can be shown that the above relations are equivalent to the energy equation in three dimensions. Now we can define a vector heat function as

$$\vec{\Phi} = \vec{\nabla} \times \vec{H} \qquad (19)$$

Such an $\vec{H}$ can easily be shown to exist if eqn. (18b) is considered. Multiplying both sides of eqn. (18a) with the curl operator, $\vec{\nabla}$ and rearranging, we have

$$\vec{\nabla}(\vec{\nabla}\cdot\vec{H}) - \nabla^2 H = (\vec{\nabla}\Theta) \times \vec{V} + \Theta\vec{W} \qquad (20)$$

since $\vec{\nabla}\times(\vec{\nabla}\Theta) \equiv 0$.

Eqn. (20) can be presented in the form

$$\nabla^2 H - \vec{\nabla}(\vec{\nabla}\cdot\vec{H}) + \vec{S} = 0 \qquad (21)$$

with $\vec{S} = (\vec{\nabla}\Theta) \times \vec{V} + \Theta\vec{W}$.

Consequently $\vec{S}$ is a known vector from the solution of the flow field. Therefore it is possible to extend the definition of the "heat function" from two to three dimensions through the solution of eqn. (21) subject to appropriate boundary conditions depending on the nature of the problem.

Applications of this method to the previously computed partially filled case show the conduction-convection dominated regimes of the flow field in Fig. 11. In Fig. 11.a, near the walls the heat lines are inclined in the flow direction hence the flow is convection dominated (see the flow field in Fig. 7.a). Near the interface however, these lines are perpendicular (especially at the corners) to the isotherms indicating that the heat transfer is by conduction only (Fig. 8.a). This is to be expected since the inward velocities are very small near the corners where the upward flow arrests and turns towards the center.

For later times, as the two rotating cells join, the heat flow in the cylinder becomes very complex. The steep gradients mentioned above still remain (Fig. 11.b) but in addition, two closed loops of heat lines form, resembling the flow lines of mass. Thus, we can say that these are showing the convection dominated regions.

## 5. Conclusions and Recommendations

Natural convection inside a partially filled, heated horizontal cylinder has been simulated numerically.

The coordinate transformation technique introduced in the solution of this problem may be generalized to three dimensions.

The algorithm and method have been tested with the data available in the literature and satisfactory agreement was observed.

The complex flow pattern and heat transfer inside the partially filled horizontal cylinder have been described using conventional contour maps of temperature and the stream function in addition to a recently introduced technique called a "heat line" visualization method. The different heat flow lines obtained were compared to those indicated by isotherm mapping.

Qualitative agreement has been observed with the experiments carried out in a partially filled cylinder of glycerine.

It is recommended that future studies include the three-dimensional effects introduced by the end effects if the cylinder considered is of finite length.

Also, the vector heat function discussed in section 4 should be investigated further by applying it to different problems and comparing with traditional isotherm maps.

## Acknowledgement

This work was supported by the Natural Sciences and Engineering Research Council of Canada and The Transportation Development Centre, Transport Canada.

## APPENDIX A

$$\nabla^2_{X,Y} = \zeta\frac{(1+2\eta^2)}{(1-\eta^2)^2}\ \frac{\partial}{\partial\zeta} + \left[\frac{1}{1-\eta^2} + \left(\frac{\zeta\eta}{1-\eta^2}\right)^2\right]\frac{\partial^2}{\partial\zeta^2} + \frac{\partial^2}{\partial\eta^2} + \frac{2\zeta\eta}{1-\eta^2}\ \frac{\partial^2}{\partial\zeta\partial\eta} \tag{A1}$$

$$\frac{\partial}{\partial X} = \frac{1}{\sqrt{1-\eta^2}}\ \frac{\partial}{\partial X} \tag{A2}$$

$$\frac{\partial}{\partial Y} = \frac{\zeta\eta}{1-\eta^2}\ \frac{\partial}{\partial\zeta} + \frac{\partial}{\partial\eta} \tag{A3}$$

## APPENDIX B

Equations (7) can be rewritten using eqns. (A1) to (A3) as follows:

Vorticity Transport Equation:

$$L_1W = L_2\theta + \frac{L_3W}{\sqrt{Gr^*_R}} \tag{B1}$$

Energy Equation:

$$L_1\theta = \frac{1}{Pr\sqrt{Gr^*_R}}\ L_3\theta \tag{B2}$$

Stream Function-Vorticity Equation:

$$L_3\psi = -W \tag{B3}$$

Velocity Relations:

$$U = \frac{\zeta\eta}{1-\eta^2}\ \frac{\partial\psi}{\partial\zeta} + \frac{\partial\psi}{\partial\eta},\quad V = \frac{1}{(1-\eta^2)^{\frac{1}{2}}}\frac{\partial\psi}{\partial\zeta} \tag{B4}$$

where

$$L_1 = \frac{U}{(1-\eta^2)^{\frac{1}{2}}}$$

$$L_2 = \frac{1}{(1-\eta^2)^{\frac{1}{2}}}$$

$L_3 = \nabla^2_{X,Y}$ as given in eqn. (A1).

# References

1. Ostrach, S.: Natural convection in enclosures. Advances in Heat Transfer, 8(1972) pp. 161-227.

2. Hellums, J.D.; Churchill, S.W.: Transient and Steady State, Free and Natural Convection, Numerical Solutions: Part 1. AIChE J. 8 (1962) pp. 690-692.

3. Maahs, G.H.: Transient Natural Convection Heat Transfer in a Horizontal Cylinder. Ph.D. Thesis, University of Washington (1964).

4. Martini, W.R.; Churchill, S.W.: Natural Convection Inside a Horizontal Cylinder. AIChE J. 6 (1960), pp. 251-257.

5. Brooks, I.; Ostrach, S.: An Experimental Investigation of Natural Convection in a Horizontal Cylinder. J. Fluid Mechanics 44 (1970), pp. 545-561.

6. Aydemir, N.U.; Sousa, A.C.M.; Venart, J.E.S.: Transient Thermal Stratification in Heated Partially Filled Horizontal Cylindrical Tanks. The 22nd ASME/AIChE National Heat Transfer Conference, ASME Paper No. 84-HT-60 (1984).

7. Venart, J.E.S.; Sousa, A.C.M.; Steward, R.D.; Prasad, R.C.: Experiments on the Physical Modelling of LPG Tank Car under Accident Conditions. Symposium Transport and Storage of LPG and LNG, Brugge (1984)

8. Kimura, S.; Bejan, A.: The Heatline Visualization of Convective Heat Transfer. J. Heat Transfer 105 (1983) pp. 916-919.

9. Yao, L.S.: Natural Convection along a Vertical Wavy Surface. J. Heat Transfer, 105(1983) pp. 465-468.

10. Lee, T.S.: Computational and Experimental Studies of Convective Fluid Motion and Heat Transfer in Inclined Non-Rectangular Enclosures. Int. J. Heat and Fluid Flow 5 (1984) pp. 29-36.

11. Aziz, K.; Hellums, J.D.: Numerical Solutions of the Three-Dimensional Equations of Motion for Laminar Natural Convection. Physics of Fluids 10 (1967) pp. 314-324.

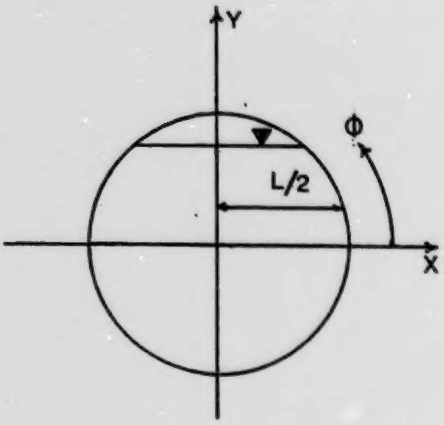

Figure 1.a. Physical plane.

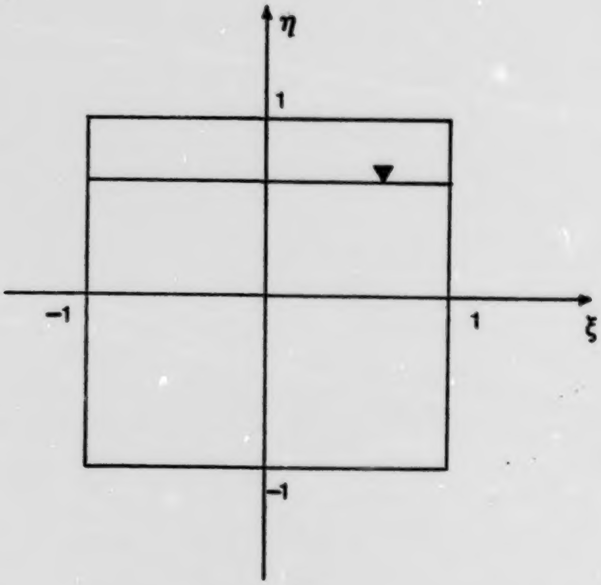

Figure 1.b. Mathematical plane.

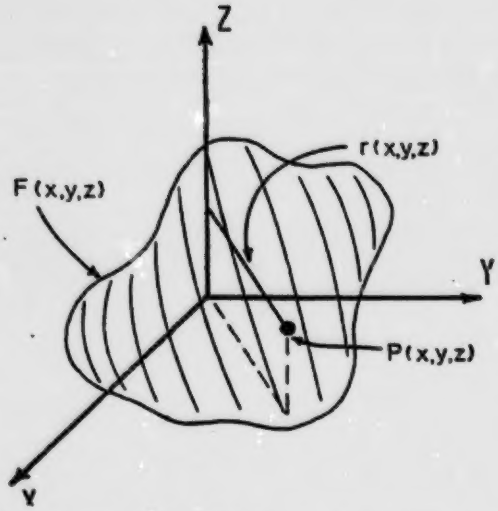
Z
r(x,y,z)
F(x,y,z)
Y
P(x,y,z)
Y

gure 2.a. Arbitrary domain in 3-D space.

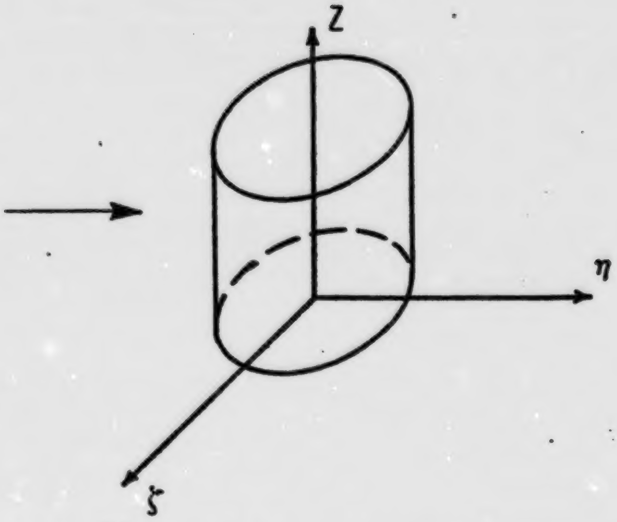

Figure 2.b. Intermediate transformation to ζ-η plane.

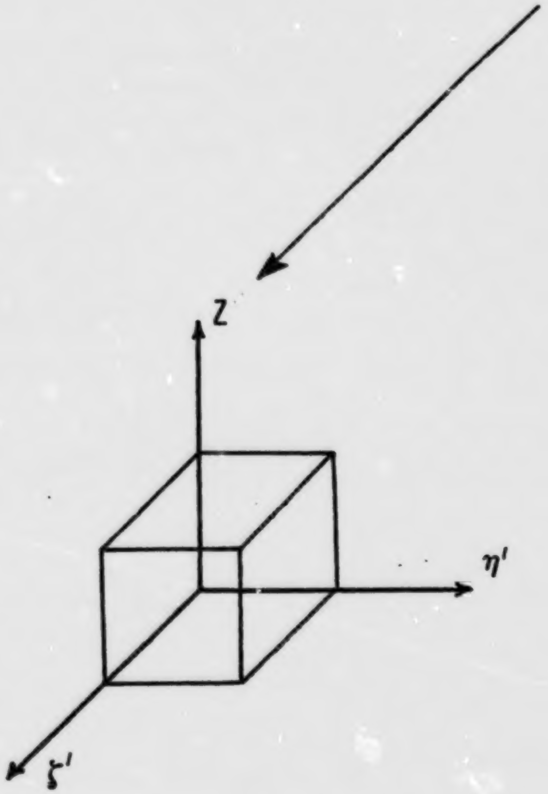

Figure 2.c. Final transformation to ζ'-η' plane.

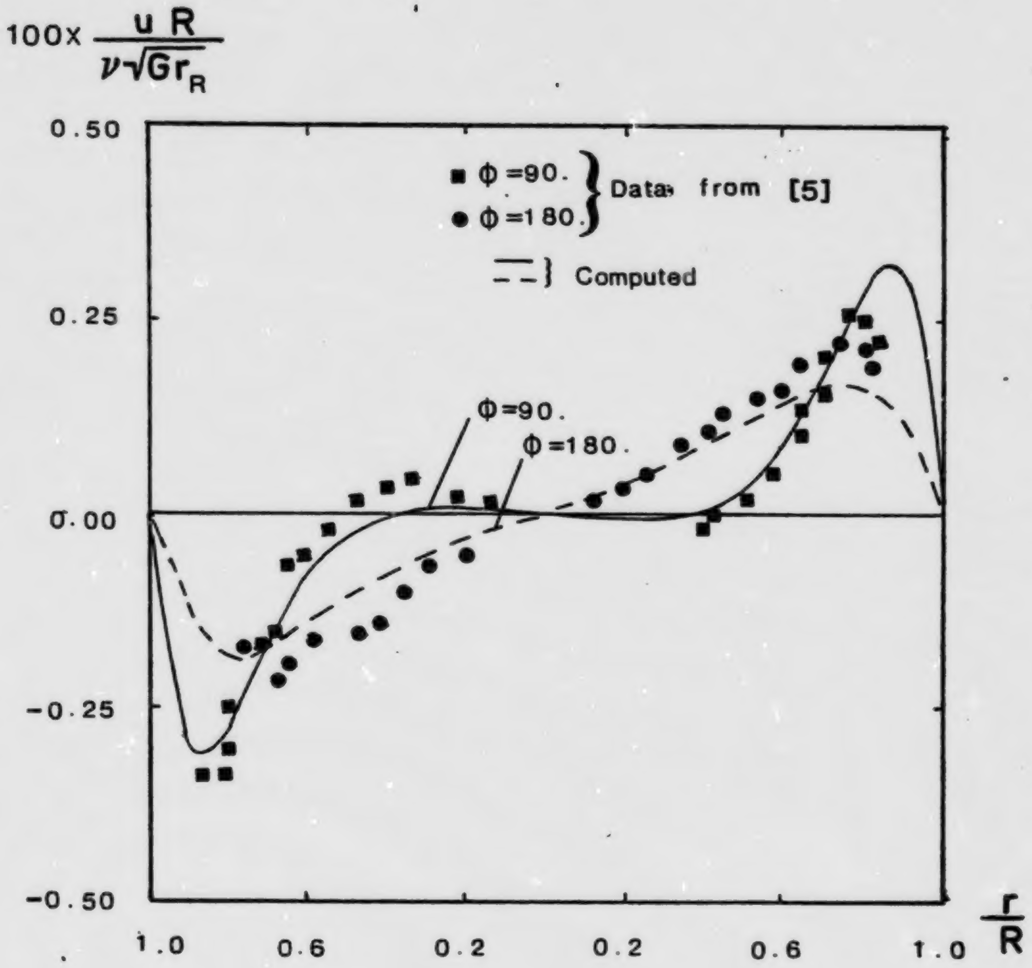

Figure 3. Velocity profiles for Pr=19950. and $Gr_R$=1.1.

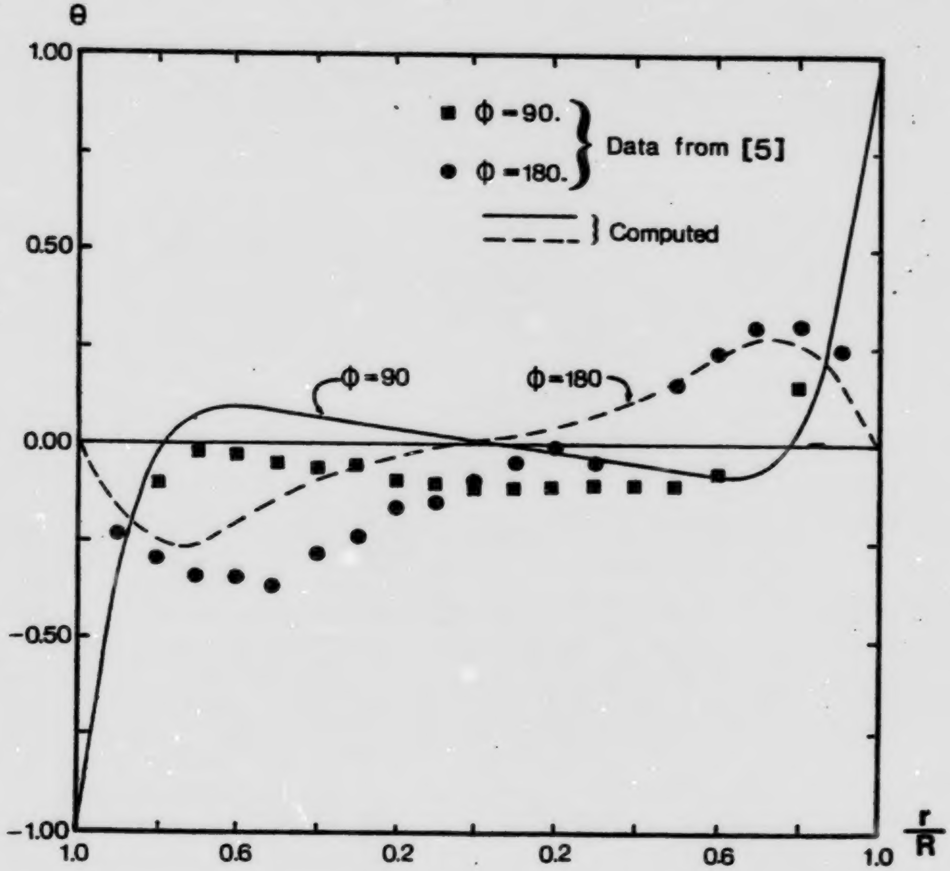

Figure 4. Temperature profiles for Pr=19950. and $Gr_R$=1.1.

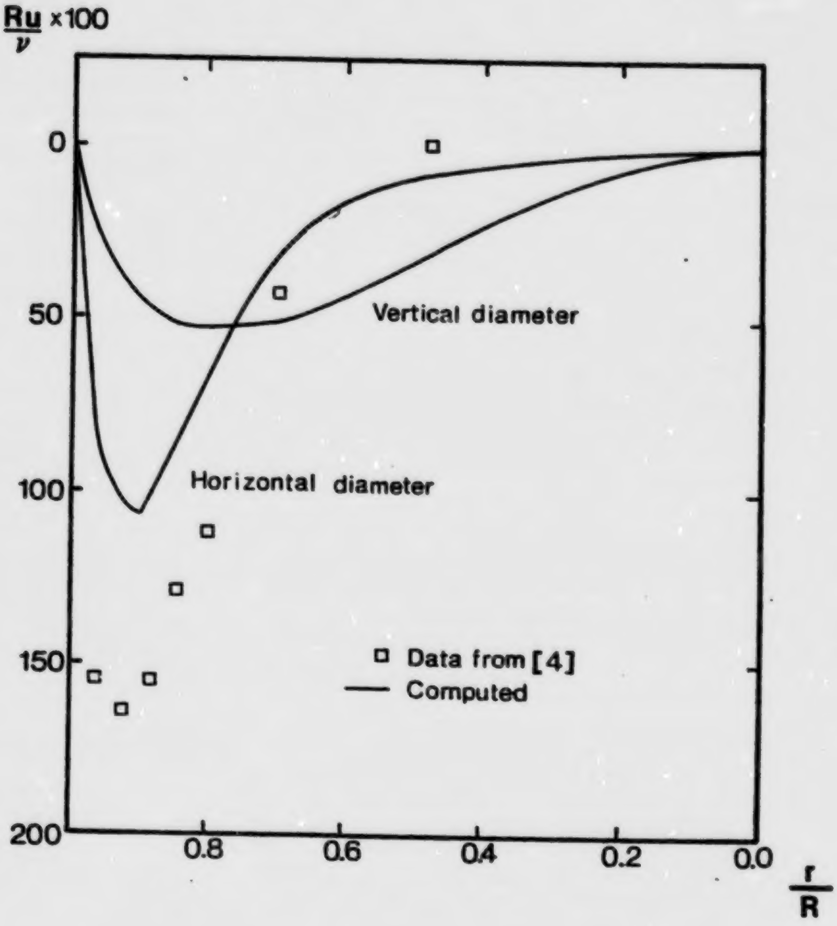

Figure 5. Velocity profiles for Pr=0.7 and $Gr_R=4.5*10^7$.

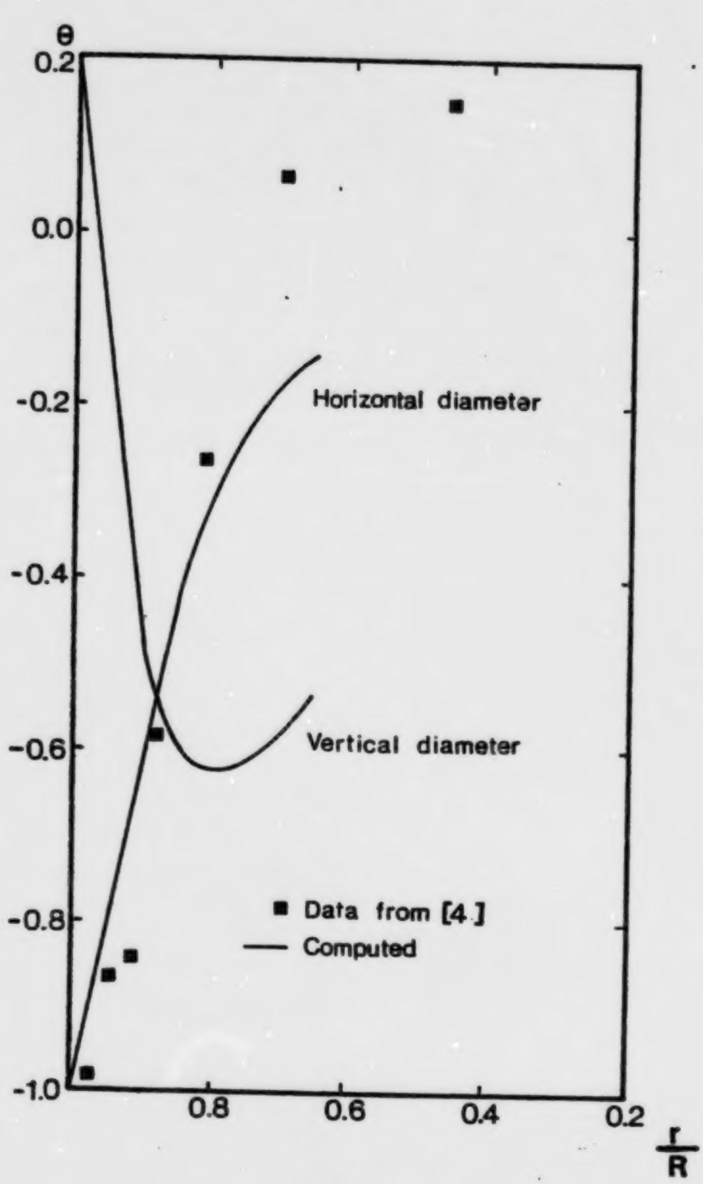

Figure 6. Temperature profiles for Pr=0.7 and $Gr_R=4.5*10^7$ .

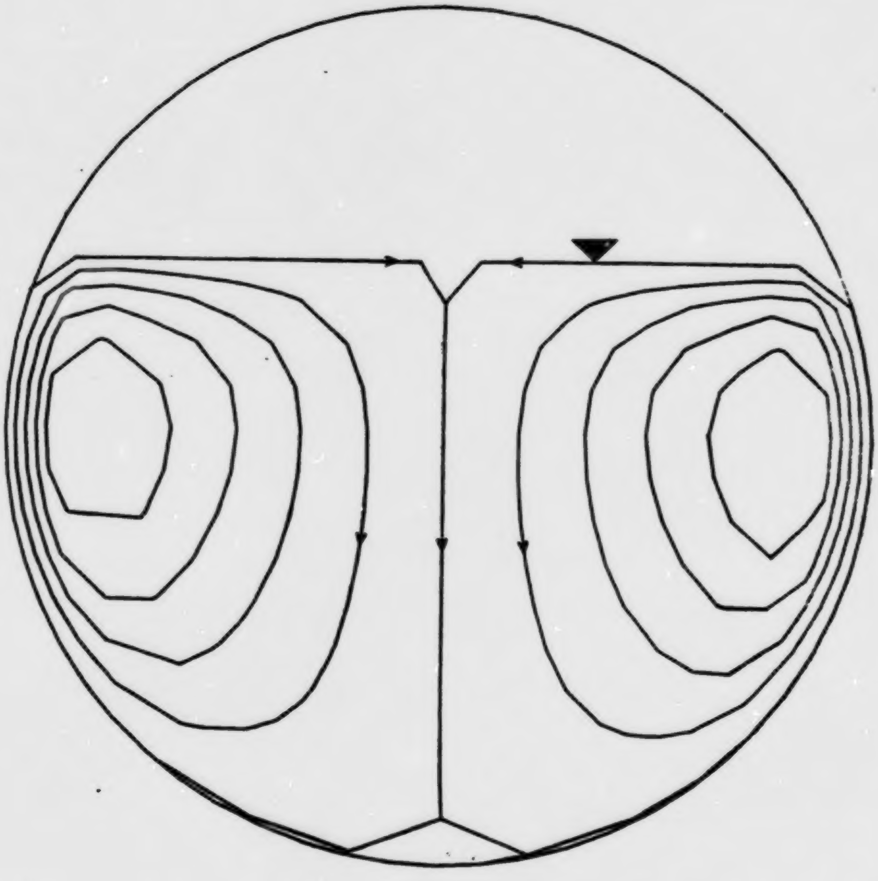

Figure 7.a. Streamlines in transient computation, $t=0.7$ minutes, $Gr_R^*=114.$ and $Pr=6380.$ .

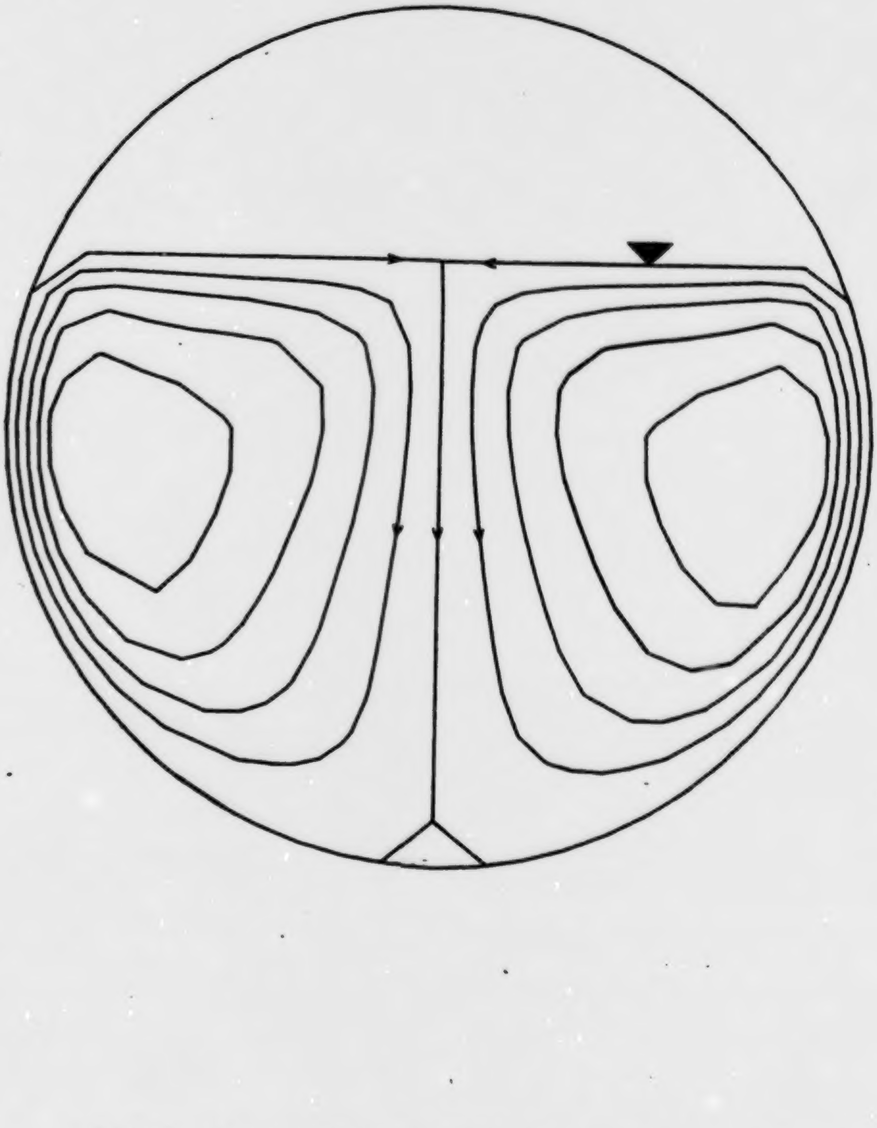

Figure 7.b. Streamlines in transient computation, t=3.3 minutes, $Gr_R^*$=114. and Pr=6380.

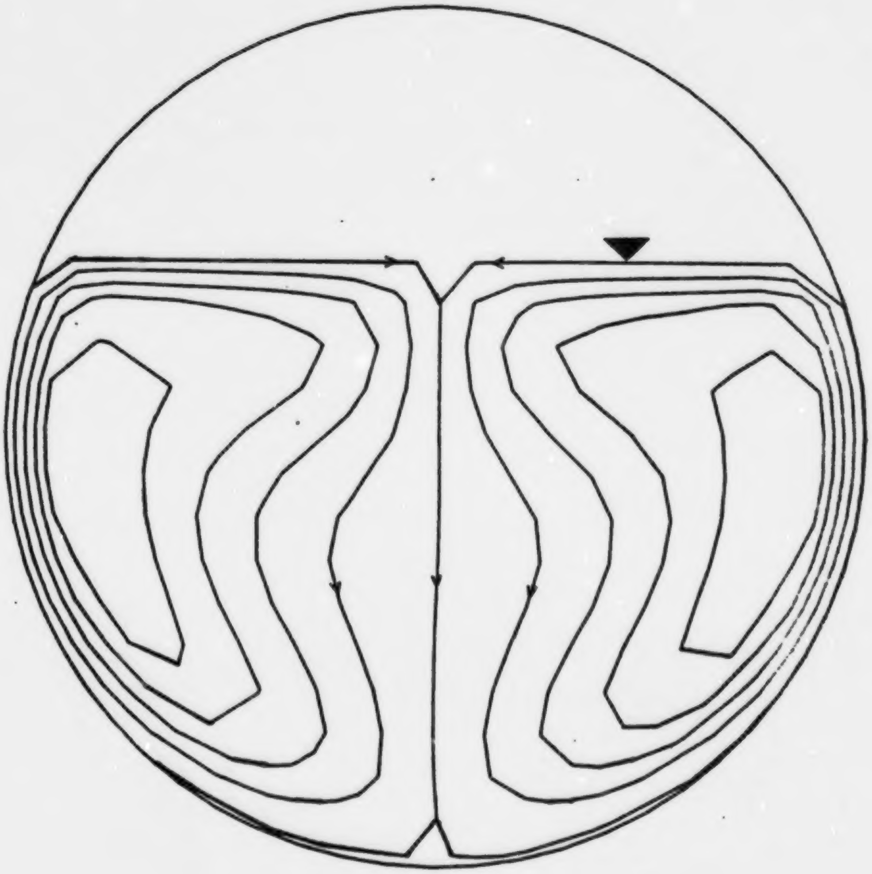

Figure 7.c. Streamlines in transient computation, t=4.6 minutes, $Gr_R^*$=114. and Pr=6380. .

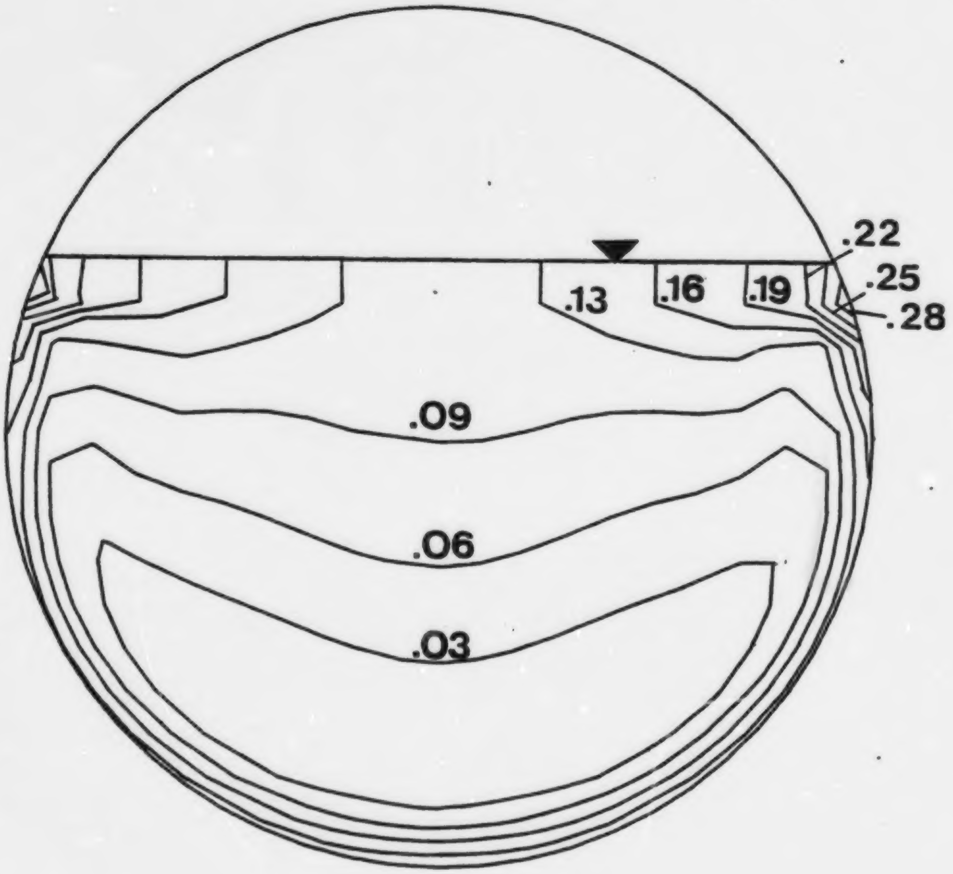

Figure 8.a. Isotherms in transient computation, t=0.7 minutes, $Gr_R^*$=114. and Pr=6380. .

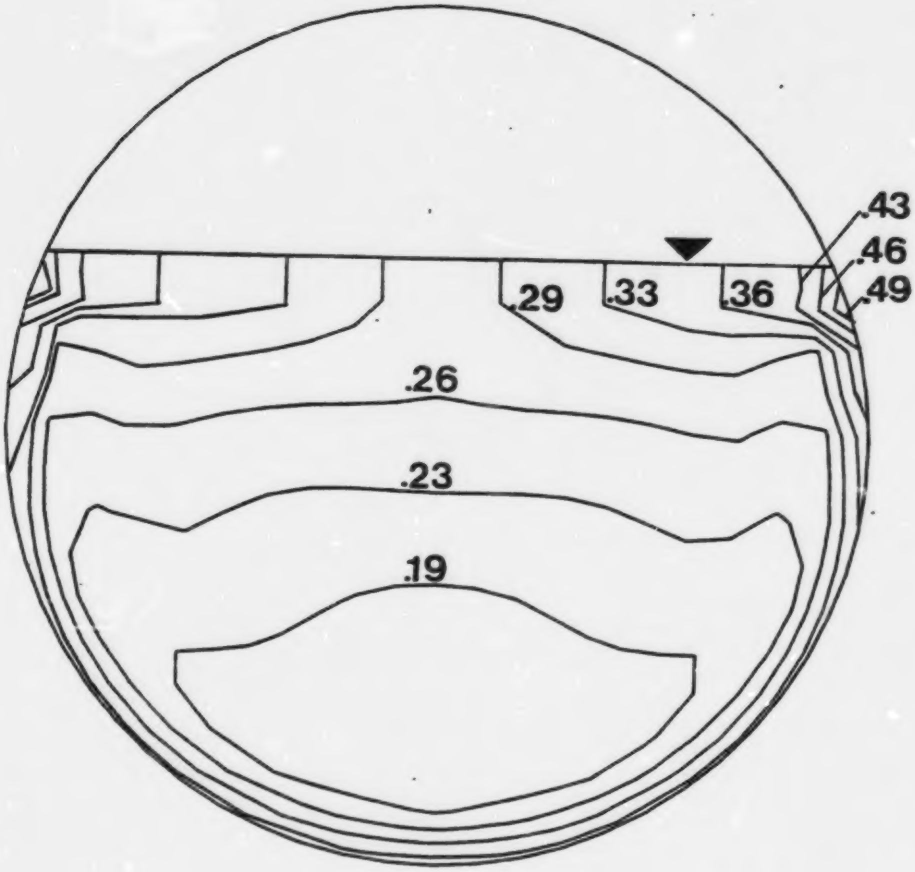

Figure 8.b. Isotherms in transient computation, t=3.3 minutes, $Gr_R^*$=114. and Pr=6380. .

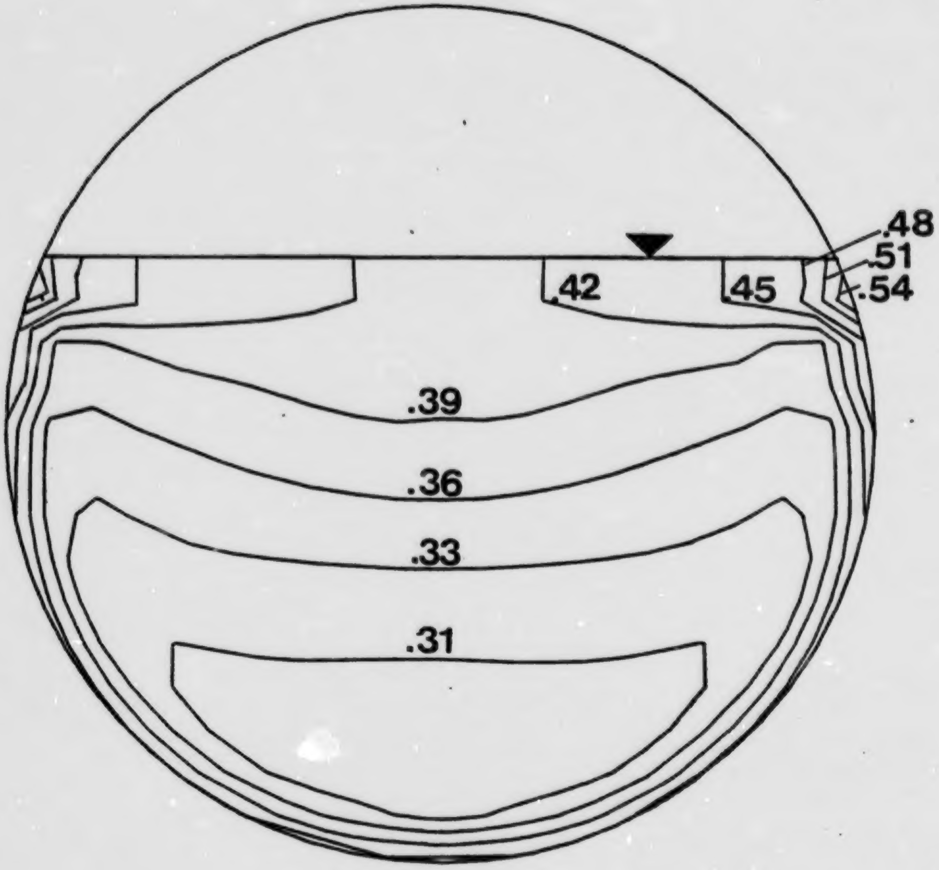

Figure 8.c. Isotherms in transient computation, t=4.6 minutes, $Gr_R^*$=114. and Pr=6380. .

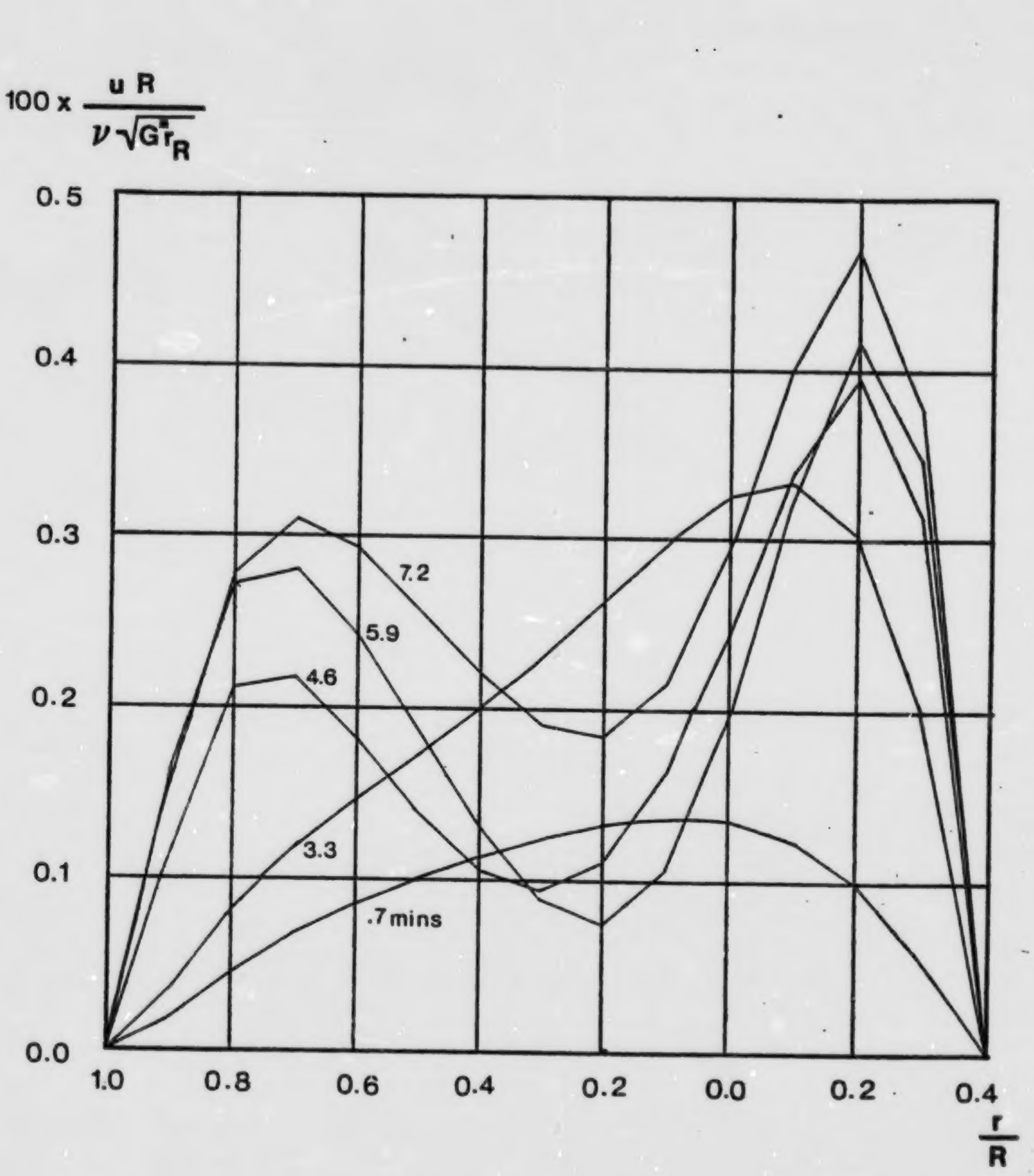

Figure 9. Transient central velocities for Pr=6380. and $Gr^*_R$=114. ($\phi$=180°).

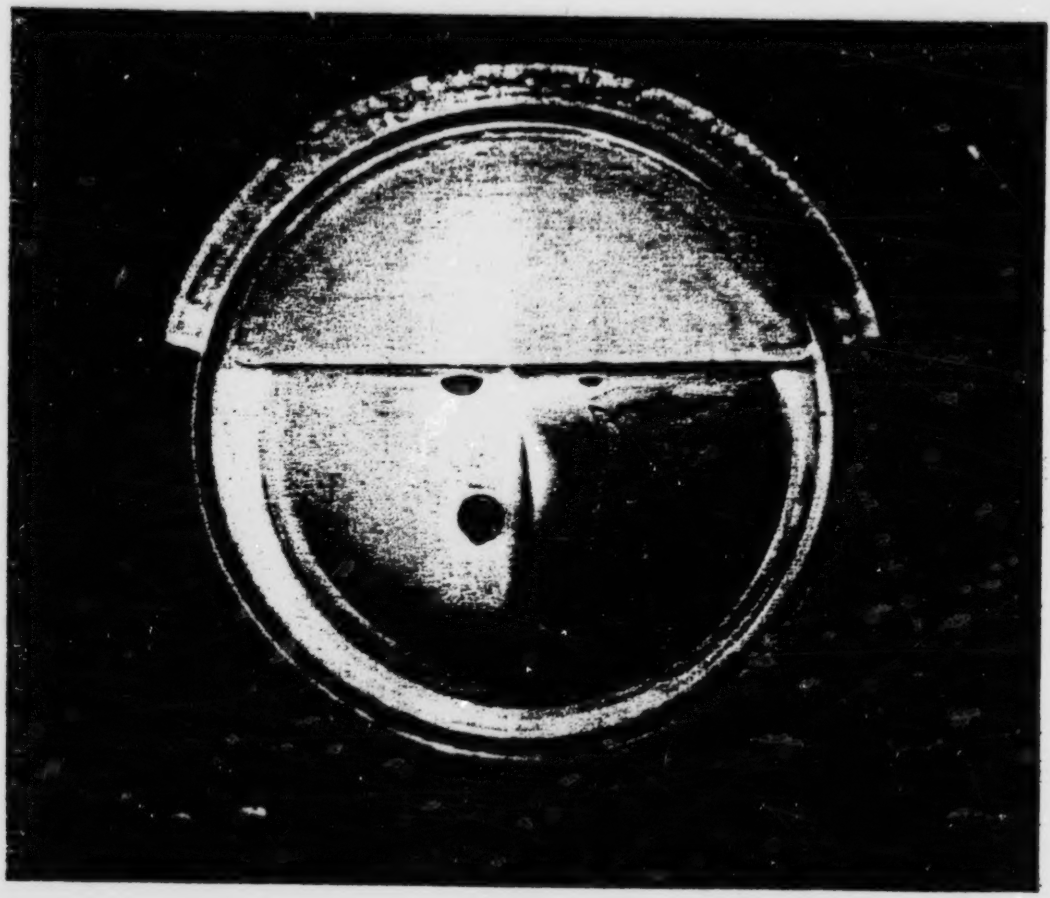

Figure 10. Experimental flow pattern for 60% full tank ($Pr=6380.$, $Gr_R^*=35.$).

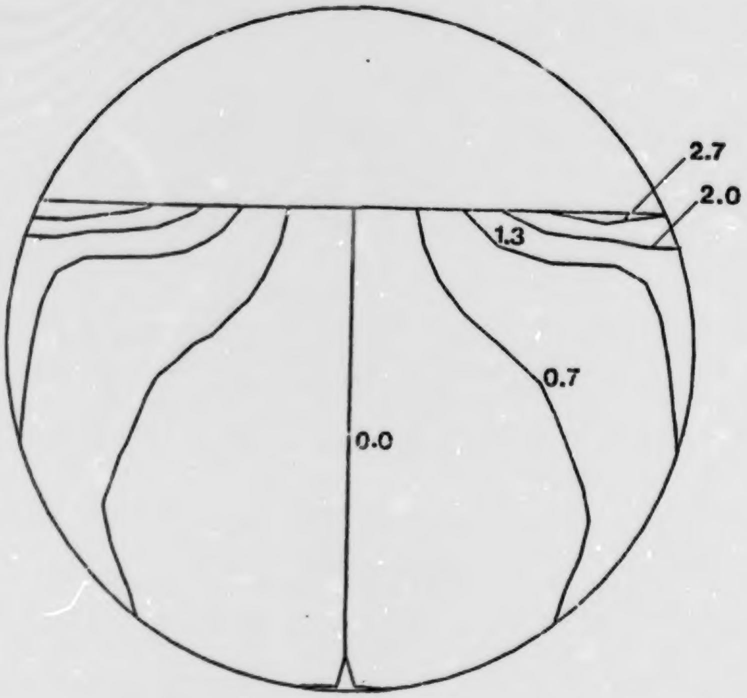

(a) t=0.7 minutes

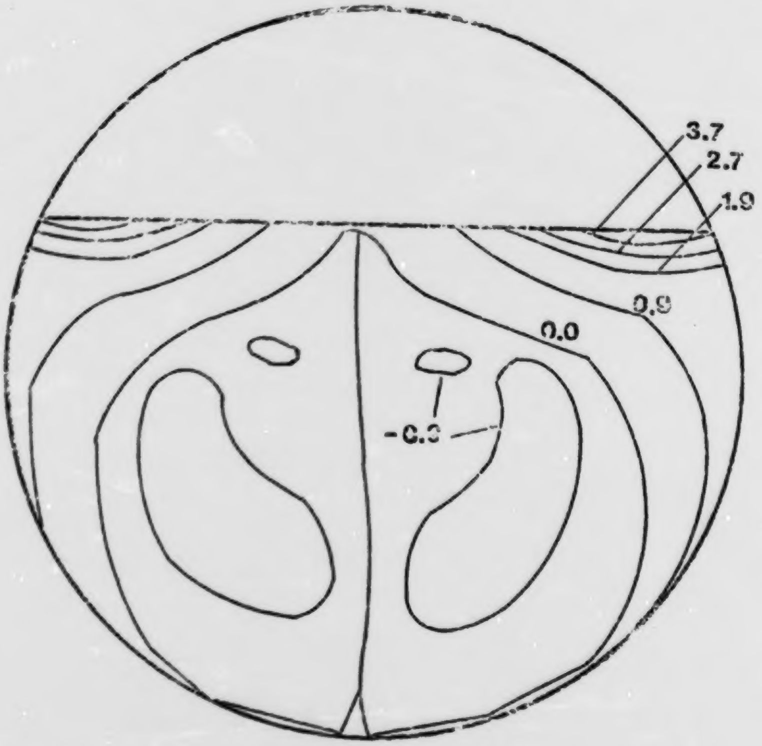

(b) t=4.6 minutes

Figure 11. Heat lines for Pr=6380. and $Gr_R^*$=114. .

# THREE DIMENSIONAL FORMULATION OF THE RADIANT HEAT FLUX VARIATION ON A CYLINDER ENGULFED IN FLAMES

M.M. TUNÇ
Assoc. Member of ASME
Assis.Prof.

Technical University of Istanbul
Mechanical Eng. Faculty, Gümüşsuyu
Istanbul, TURKEY

# ABSTRACT

A three dimensional formulation is used to determine the incident radiant heat flux on a cylinder surface which is engulfed in flames. For an axisymmetric horizontal pool fire of a specified flame shape,effective flame radiation temperature and a gray flame absorbtion coefficient, this analysis computes the variation of the incident radiant heat flux along the length and around the circumference of the tank, portrayed as a cylinder,engulfed in flames.

The radiant flux density from the flame to the cylinder becomes maximum toward the center of the pool and decreases markedly toward the edges.The points which are receiving the maximum amount of radiation heat flux around the circumference of the cylinder are also determined.

# NOMENCLATURE

$A$ = surface area, $m^2$

$a$ = the distance between the point under consideration and the top center point on the cylinder surface, m

$D$ = The diameter of the cylinder, m

$E_\lambda$ = Monochromatic emissive power of a black body at wavelength, $\lambda$

$H$ = The height of the combustion zone, m

$h_1$ = The distance between the top of the cylinder and the ground, m

$h$ = The distance between the bottom of the cylinder and ground, m

$K$ = The mean absorption coefficient of the combustion gases. $m^{-1}$

$K_\lambda$ = Monochromatic absorption coefficient, $m^{-1}$

$L$ = The length of the cylinder, m

$Q$ = The radiant flux exchanged between an element of volume and a surface element, W

$q$ = The radiative flux density on a surface received from a finite source, $W/m^2$

$r$ = The radius of the cylinder, m

$R(z)$ = Flame radius, m

$S$ = The absorbing path length, m

$T$ = Temperature, K

$V$ = Volume, $m^3$

$W$ = The width of the pool fire, m

$T_f$ = Flame Temperature, K

$x$ = Horizontal axis

$z$ = Vertical axis

## Greek Symbols

$\theta$ = Angular coordinate,rad

$\theta_1$ = The angle between the vertical vector and the vector between the center of the cylinder and the point of interest on the circumference of the cylinder, rad

$\lambda$ = Wavelength

$\rho$ = Radial coordinate, m

$\sigma$ = Stefan Boltzmann constant, $5.66 \times 10^{-8}$ $W/m^2 K^4$

$\tau_{\lambda(Sij)}$ = Transmittance

$\phi$ = The angle between the connecting vector and the vector normal to the surface element, rad

# INTRODUCTION

Under certain accident conditions, cylindrical tanks containing liquified gases, in particular LPG, may be exposed to enveloping pool fires.The primary objective of this paper is to determine the variation of the incident radiant heat flux along the length and around the circumference of the tank, portrayed as a cylinder, engulfed in flames.

There are numerous studies concerned with the properties of pool fires and the resulting radiant heat flux to external targets and to the pool surface. A mathematical model was developed by Masliyah and Steward (1) to calculate the radiative emission from the flame. The radiative interchange between the flame and the plane surrounding its base was determined by assuming the flame to be a gray emmitter. To compute the radiative heat flux from a luminous pool fire to an arbitrarily located target surface,either within or external to the fire, a general calculation procedure has been presented by Modak (2). Recently Birk and Oosthuizen (3) estimated the radiant heat transfer to a long horizontal cylinder engulfed in flames. In their two dimensional analysis the cylinder is considered to be of infinite length and the combustion gases which surround the cylinder, occupy a space which can be represented by a rectangle. The walls of this rectangle are represented by an infinite but stagnant media.The model estimates the various surface to surface and surface to volume exchange factors as a function of position around the circumference of the cylinder. This method is not able to determine the radiant heat flux variation along the length of the cylinder.

The present study presents a three dimensional formulation to determine the variation of incident radiant heat flux along the length and around the circumference of the tank, portrayed as a cylinder, engulfed in flames. The effects of the effective flame temperature and the absorption coefficient on the incident radiant heat flux are investigated.

## THE CALCULATION OF THE INCIDENT RADIANT HEAT FLUX ALONG THE LENGTH AND AROUND THE CIRCUMFERENCE OF THE CYLINDER

The radiation interchange between an elemental volume $dV_i$ of radiating gas in the flame and an arbitrary surface element $dA_j$ on the cylinder surface is depicted in Fig.1.

The following assumptions are made in the present analysis.

a) The effect of scattering has been acepted to be negligible. (8).

b) The effect of convective heat transfer is neglected (2).

c) The shape of flame is an important parameter and controls the radiative heat flux coming to the cylinder surface. This analysis avoids arbitrary assumptions regarding shapes (such as conical, rectangular or cylindrical flames, etc.) and instead characterizes the flame shape by means of axisymmetric flame contours obtained from actual photographs and other experimental evidence from large ($W \geq 4.5$ m) JP - 4 jet fuel pool fires (5). In this work a fourth order polynomial is fitted to the contours of the flame to describe the radius of the flame as a function of height :

$$R(z) = a_0 + a_1 z + a_2 z^2 + a_3 z^3 + a_4 z^4 \qquad (1)$$

The flame shape corresponding to Eq.(1) is shown in Figure 2.

A three dimensional computer model for the pool fire and the cylinder is shown in the Figure 3.

d) The cylinder surface is a black body. Several geometrical dimensions the pool fire and the cylindrical tank and $a_0, a_1, a_2, a_3, a_4$ constants are given in Table - 1.

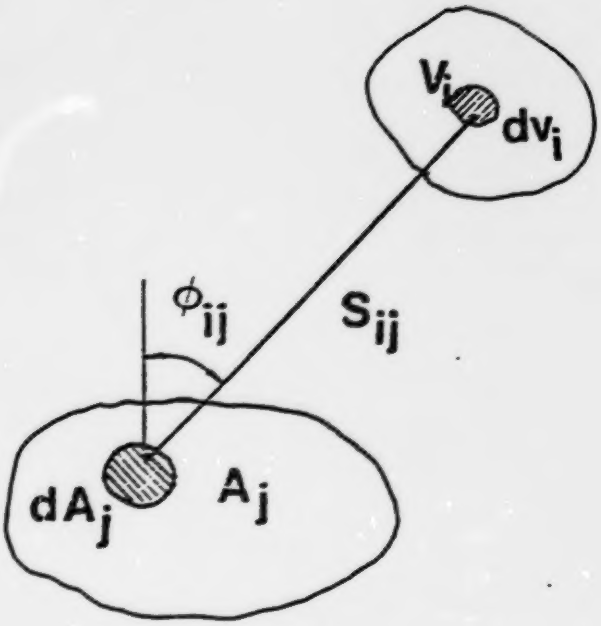

Fig.1.Exchange between gas volume $V_i$ and surface $A_j$

Let $V_i$ and $A_j$ be any arbitrary volume and surface respectively . The monochromatic emmissive power from a volume element $dV_i$ is

$$4K_{\lambda i}E_{\lambda i}dV_i d\lambda \qquad (2)$$

The fraction of emmission directed towards $dA_j$ is

$$\frac{dA_j \text{ Cos } \phi_{ij}}{4\pi S^2_{ij}} \qquad (3)$$

The fraction of radiation transmitted through the path length $S_{ij}$ is $\tau_\lambda(S_{ij})$ which can be expressed as

$$\exp \left| - \int_{S_i}^{S_j} K_{\lambda i}(S)dS \right| \qquad (4)$$

The spectral radiation energy emitted from a volume element $dV_i$ and arriving at a surface element $dA_j$ can be written as

$$dq_{\lambda i,j} = \frac{K_{\lambda i}E_{\lambda i}\text{Cos } \phi_{ij}}{\pi S^2_{ij}} \cdot \exp\left| -\int_{S_i}^{S_j} K_{\lambda i}(S)ds \right| dV_i dA_j d\lambda \qquad (5)$$

If we integrate this relation over $V_i$,$A_j$ and over all wavelengths, the following equation can be obtained

$$Q = \int_{\lambda=0}^{\infty} \int_{V_i} \int_{A_j} \frac{K_{\lambda i}E_{\lambda i}\text{Cos } \phi_{ij}}{\pi S^2_{ij}} \cdot \exp\left| -\int_{S_i}^{S_j} K_{\lambda i}(S)dS \right| dV_i dA_j d\lambda \qquad (6)$$

By using gray gas approximation, the foregoing equation takes the following form, (4,8)

$$Q = \int_{V_i}\int_{A_j} \frac{K_i \sigma T_i^4}{\pi} \; \frac{\cos\phi_{ij}}{S_{ij}^2} \exp\left| -\int_{s_i}^{s_j} K(S)\, ds \right| dV_i\, dA_j \qquad (7)$$

Eq.(6) is the general relation. In this study as the first step, the emitting and absorbing radiating flame is considered to be an isothermal gas (2,4). If we assume that the absorption coefficient is constant through out the flame, we will obtain the following equation.

$$Q = \frac{K\sigma T^4}{\pi} \int_{V_i}\int_{A_j} \frac{\cos\phi_{ij}}{S_{ij}^2} \exp\left| -\int_{s_i}^{s_j} K\, ds \right| dV_i\, dA_j \qquad (8)$$

(a) The longitudinal radiant heat flux variation

The radiation interchange between an elemental volume dV of radiating gas in the flame and an arbitrary surface element dA on the top line of the cylinder ($h_1$ $h$ $2r$), is depicted in figure 2 a from the same figure the following relationships may be obtained.

$$dV = \rho\, d\theta\, d\rho\, dz \qquad (9a)$$

$$\cos\phi = \frac{z-h_1}{S} \qquad (9b)$$

$$S^2 = a^2 + (z-h_1)^2 + \rho^2 + 2a\rho \cos\theta \qquad (9c)$$

Substituting the above quantities into equation (8) and integrating over the proper limits yields the total flux density received by the area element dA from the flame.

$$q = \int_{h_1}^{H}\int_{0}^{R(z)}\int_{0}^{\pi} \frac{2\sigma K T^4 \rho (z-h_1)\, e^{-KS}}{\pi S^3}\, d\theta\, d\rho\, dz \qquad (10)$$

The triple integral above was solved numerically using Simpson's rule.

### (b) The circumferential radiant heat flux variation

The radiation interchange between an elemental volume dV of the radiating gas and the surface element dA located on the yz plane with an arbitrary angle $\theta_1$ is shown in Figure 2.b. For $0 < \theta_1 < \pi$ and $\theta \neq \pi/2$

$$
\begin{aligned}
\mathrm{Cos}\phi = {} & \frac{\mathrm{Cos}\,\theta_1}{2S\,|z-(h+r+r\mathrm{Cos}\,\theta_1)|} \cdot \Bigg[ \left[\frac{|z-(h+r+r\mathrm{Cos}\theta_1)|}{\mathrm{Cos}\theta_1}\right]^2 \\
& + S^2-\rho^2-a^2-\left\{r\sin\theta_1 + \tan\theta_1 \cdot |z-(h+r+r\mathrm{Cos}\theta_1)|\right\}^2 \\
& +2\rho \cdot \left\{a^2+\left[r\sin\theta_1+\tan\theta_1 \cdot |z-(h+r+r\mathrm{Cos}\theta_1)|\right]^2\right\}^{1/2} \cdot \\
& \cdot \cos\left\{\theta-\tan^{-1}\left[\frac{r\sin\theta_1+\tan\theta_1 \cdot |z-(h+r+r\mathrm{Cos}\theta_1)|}{a}\right]\right\}\Bigg] \qquad (11)
\end{aligned}
$$

$$
\begin{aligned}
S^2 = {} & |z-(h+r+r\mathrm{Cos}\theta_1)|^2+\rho^2+a^2+r^2\mathrm{Sin}^2\theta_1 \\
& -2 \cdot \rho \cdot (a^2+r^2\mathrm{Sin}^2\theta_1)^{1/2} \cdot \mathrm{Cos}\left(\theta-\tan^{-1}\left(\frac{r\mathrm{Sin}\theta_1}{a}\right)\right) \qquad (12)
\end{aligned}
$$

The calculation procedure of the above equations is explained in Fig.4. In evaluation of heat flux integral, the calculation of $\mathrm{Cos}\phi_{ij}$ with the independent variables, $\theta_1$, $\rho, \theta, z$ has a singular value for $\theta_1 = \pi/2$.

For $\theta_1 = \pi/2$, the following equations will be used.

$$
\mathrm{Cos}\phi = \frac{(a^2+\rho^2-2a\,\mathrm{Cos}\theta)^{1/2} \,.\mathrm{Sin}\theta - r}{S} \qquad (13)
$$

$$
S^2 = (z-(h+r))^2+\rho^2+r^2+a^2-2\rho r\mathrm{Sin}\theta-2a\rho\mathrm{Cos}\theta \qquad (14)
$$

Substituting the above into equation(8) and integrating over proper limits yields the total heat flux density received by the area element $dA_j$ on the circumference of the cylinder, located by the $\theta_1$ angle

$$\sigma = \int_{h_1}^{H} \int_{0}^{R(z)} \int_{0}^{2\pi} \frac{-KT^4 \rho e^{-KS} \mathrm{Cos}\phi}{\pi S^2}\, d\theta d\rho dz \qquad (15)$$

Only the portion of the pool fire which is above a tangent plane to the point of interest on the circumference of the cylinder, has to be considered in the above integration , so always $\phi < \pi/2$.

## RESULTS

Figure 5 shows the variation of incident radiant heat flux longitudinally on the top surface of the cylinder for different K values.The flame temperature and the wall temperature are assumed to be 1200 K and 550 K respectively.The surface temperature of the cylinder varies circumferentially.But due to the intense heat flow, from the surface of the cylinder to the inside contained LPG, 550 K is taken as a average circumferential value (5). It is clear from Figure 5 that the radiant flux density from the flame to the cylinder becomes maximum toward the center of the pool and decreases markedly toward the edges.

The variation of the incident radiant heat flux is circumferentially shown in Fig.6. The flame temperature and the wall temperature are assumed to be 1200 K and 550 K respectively. The circumferential heat flux variation is depicted for three different locations along the length of the cylinder. From this figure it is clearly seen that, the parts of the circumferential surface element which receives maximum amount of the radiation,approximately corresponds to $\theta_1 = 0$ and incident heat flux varies considerably around the circumference of the cylinder near the center of the pool fire. Toward the edges of the cylinder the circumferential temperature variation becomes less important.

# REFERENCES

1. Masliyah,J.H.,and Steward,F.R., "Radiative Heat Transfer from a Turbulent Diffusion Buoyant Flame With Mixing Controlled Combustion".Combustuon and Flame, Vol.13,1969, pp.613 - 625
2. Modak,A.T., "Thermal Radiation from Pool Fires." Combustion and flame. Vol.29, 1977 ,pp.177 - 192
3. Birk,A.M. and Oosthhuize,P.H., "Model for the Prediction of Radiant Heat Transfer to a Horizontal Cylinder Engulfed in Flames." ASME Paper 82-WA/HI - 52.
4. Hottel,H.C. and Sarofim,A.D., "Radiative Transfer." McGraw - Hill, 1967.
5. Appleyard,R.D.,"Testing and Evaluation of EXPLOSAGE System as a Method of Controlling the Boiling Liquid Expanding Vapour Explosion." Transport Canada Report No.TP 2740,1980.
6. Ömer,A.D. and Cedmmir,M.S., "Effect of wind on buoyant diffusion flames." I EC Fundamentals, Vol.3,No.2, 1964 , pp.147 - 154
7. Charles ,A., "The effects of a fire environment and rail tank car filled with LPG." U.S. Department of Transporta - tion, PB - 241358, 1974.
8. Siegel,R. and Howell,J.R., "Thermal Radiation Heat Transfer" Mc Graw - Hill, 1972
9. Private Comminacations with F.R.Steward.

TABLE 1 Geometrical Parameters of the pool fire and the cylindirical tank.

| Quantity | |
|---|---|
| $a_o$ (m) | 2.24 |
| $a_1$ | -0.3806 |
| $a_2 (m^{-1})$ | $0.6202.10^{-1}$ |
| $a_3 (m^{-2})$ | $0.1219.10^{-1}$ |
| $a_4 (m^{-3})$ | $-0.3706.10^{-2}$ |
| D (m) | 0.61 |
| H (m) | 6 |
| h (m) | 0.31 |
| L (m) | 3.66 |
| W (m) | 4.5 |

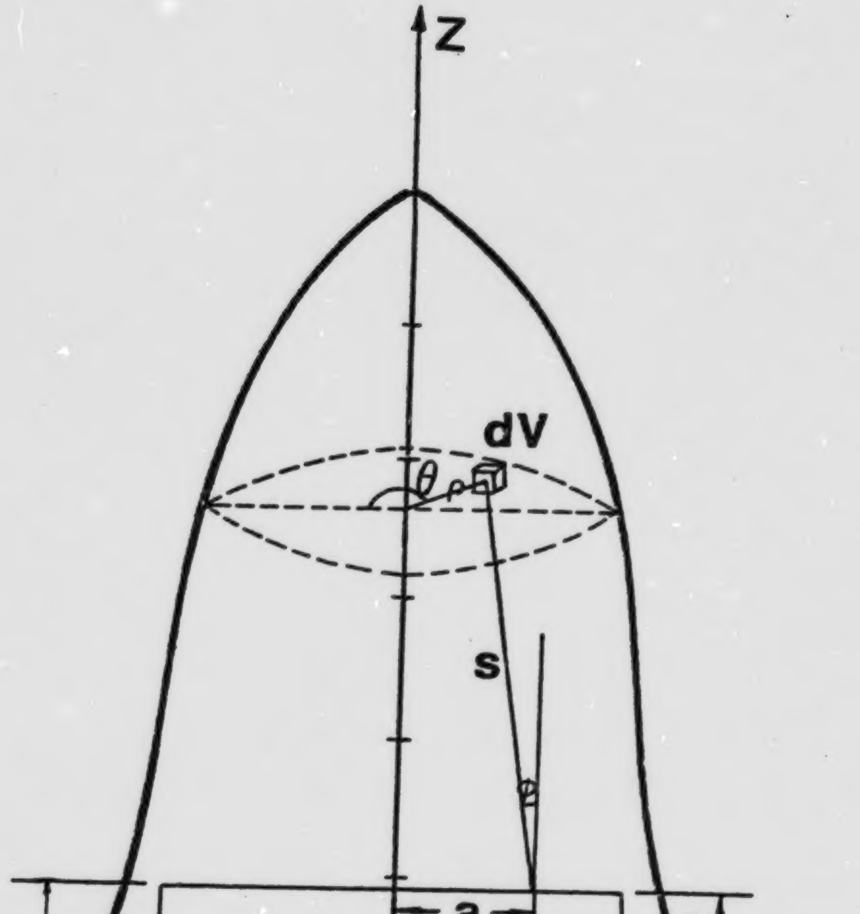
Z
dV
θ
ρ
s
θ
a
h1
2r
X
1
2
3

Fig. 2 a   Geometry of gas radiation interchange between a flame volume and an element of area located on the top plane of the cylinder.

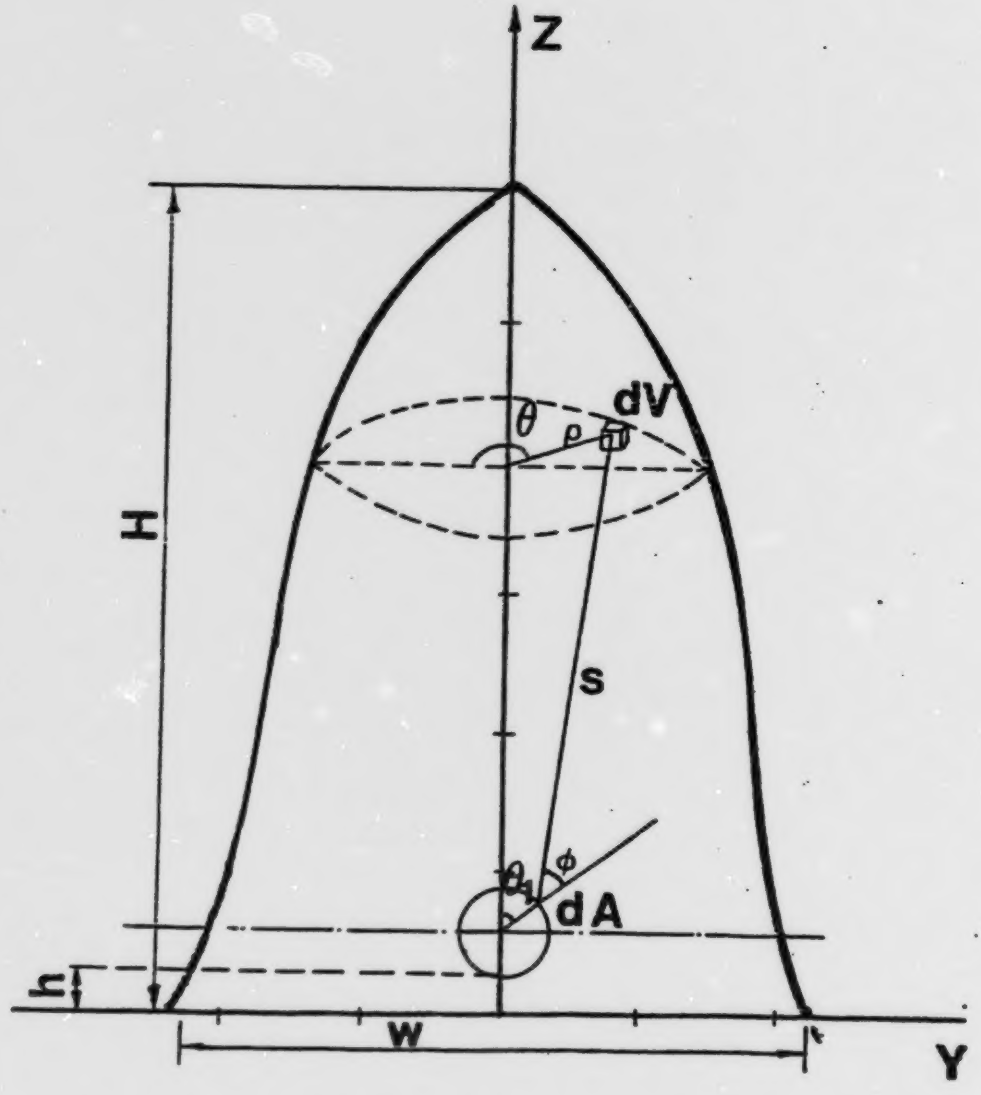
Z
dV
θ
ρ
H
s
θ1
ϕ
dA
h
w
Y

Fig. 2 b Geometry of gas radiation interchange between a flame volume on an element of area located by the $\theta_1$ angle on the circumference of the cylinder.

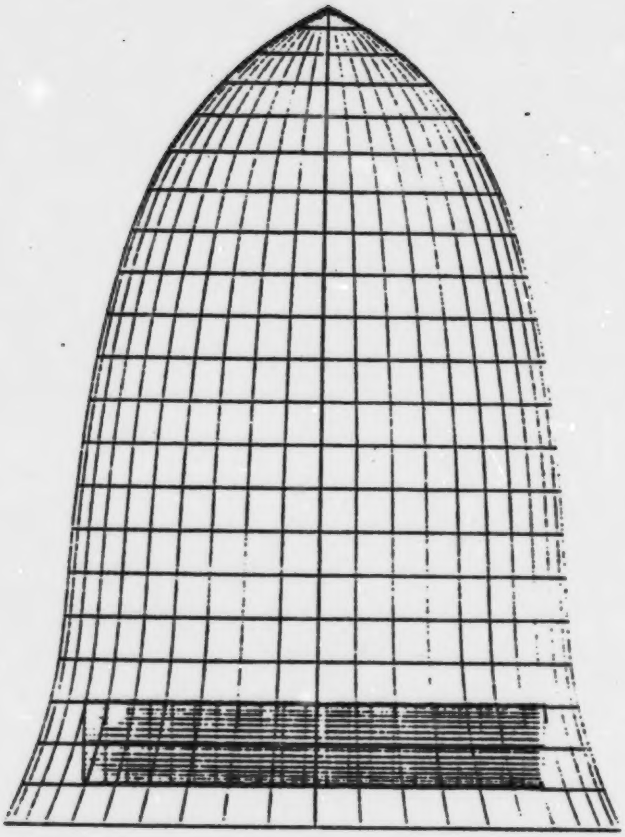

Fig. 3 A three dimensional computer model for the pool fire and the cylinder.

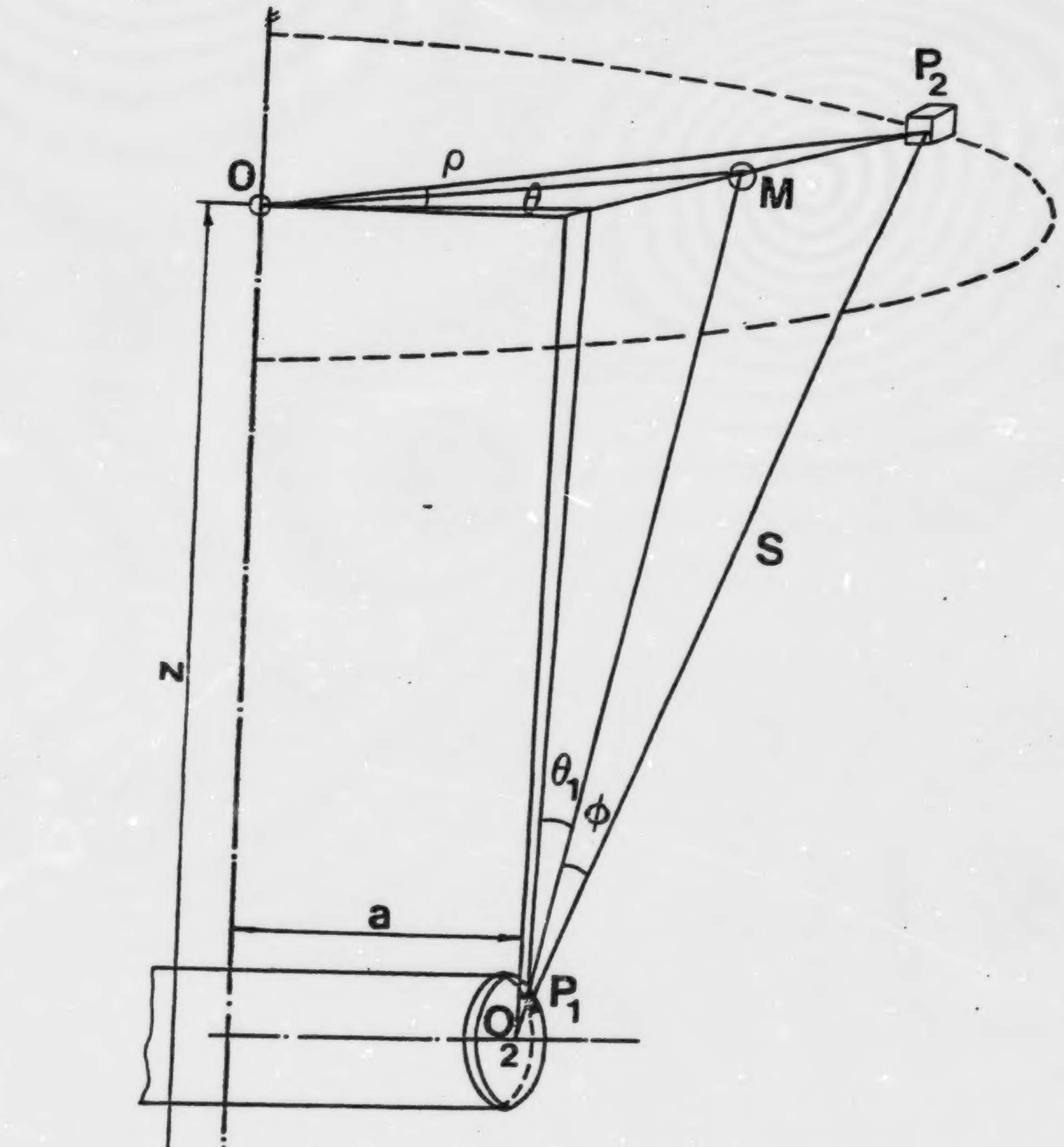
P2
O
ρ
θ
M
z
S
θ1
φ
a
P1
O2

Fig. 4 Geometry for determining the absorbing path length s and the $\theta'$.

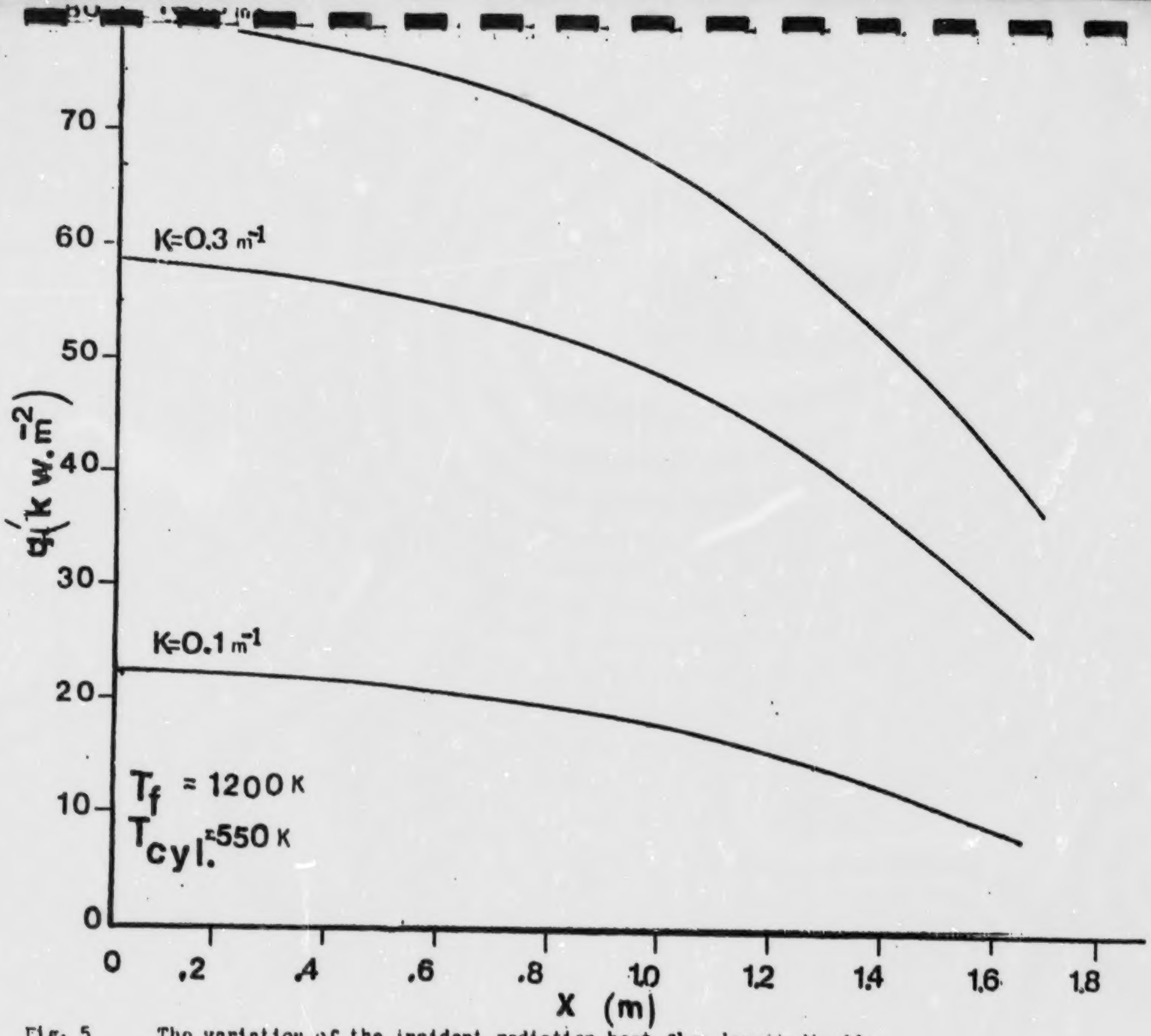

Fig. 5 The variation of the incident radiation heat flux longitudinally on the top surface of the cylinder.

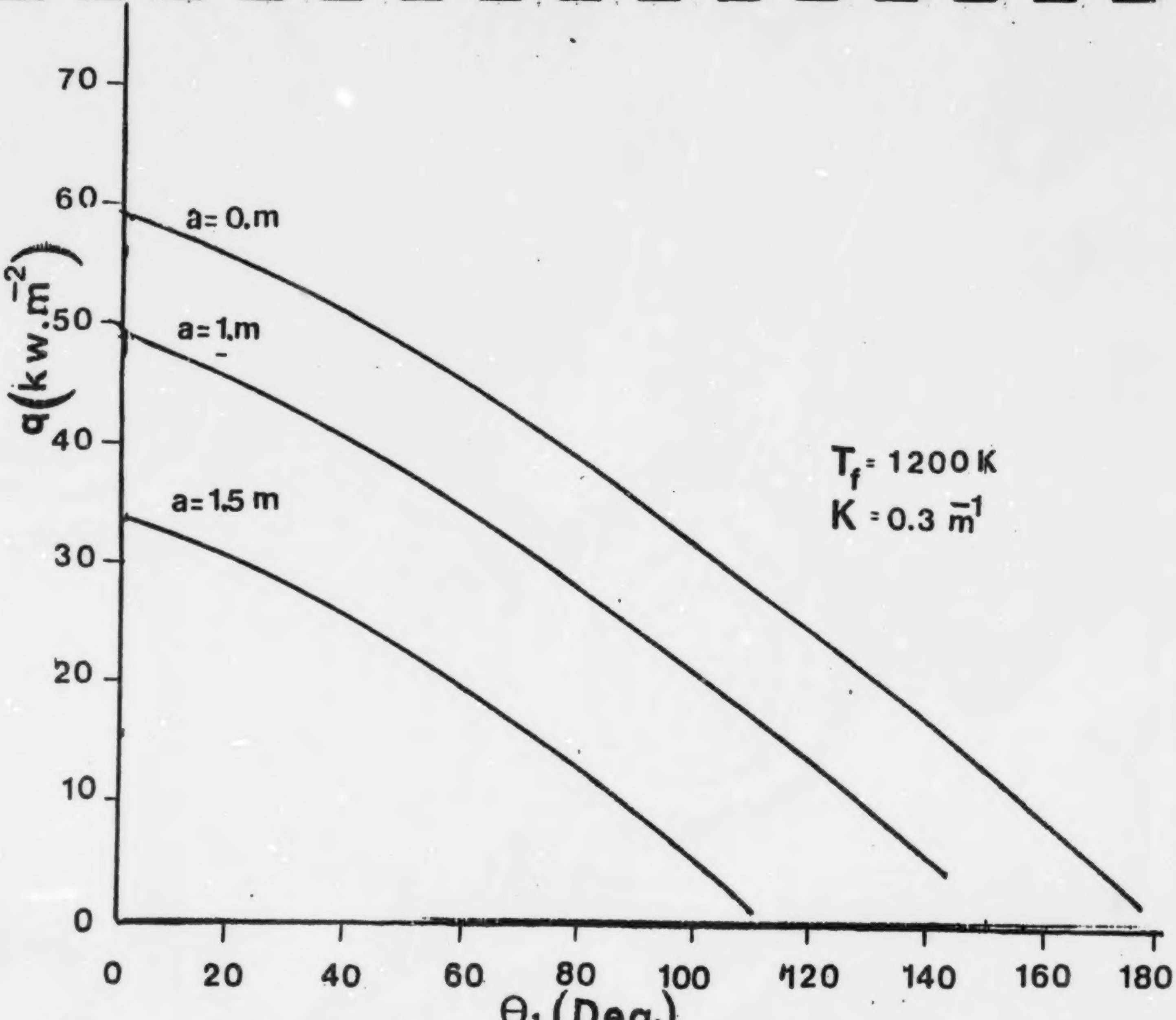

Fig.6 Circumferential variation of the incident radiant heat flux for three different locations.

COMPUTER OUTPUTS FOR THE FIG - 5

NRC= 15 (Number of Grid point in r direction)
NT= 36 ( " " " " " θ " )
DZ=10cm ( " " " " " Z " )

```
ECUTION BEGINS...
K(ABSORBTION COFFICIENT)=0.0010(1/cm)
   A(CM)=         0.0000     Q(KW/M**2)=    0.22152E+05
   A(CM)=        19.1724     Q(KW/M**2)=    0.22033E+05
   A(CM)=        38.3447     Q(KW/M**2)=    0.21753E+05
   A(CM)=        57.5171     Q(KW/M**2)=    0.20651E+05
   A(CM)=        76.6895     Q(KW/M**2)=    0.19361E+05
   A(CM)=        95.8618     Q(KW/M**2)=    0.17923E+05
   A(CM)=       115.0342     Q(KW/M**2)=    0.16422E+05
   A(CM)=       134.2065     Q(KW/M**2)=    0.14216E+05
   A(CM)=       153.3789     Q(KW/M**2)=    0.11532E+05
   A(CM)=       172.5513     Q(KW/M**2)=    0.79536E+04
   A(CM)=       191.7236     Q(KW/M**2)=    0.42804E+04
K(ABSORBTION COFFICIENT)=0.0030(1/cm
   A(CM)=         0.0000     Q(KW/M**2)=    0.58825E+05
   A(CM)=        19.1724     Q(KW/M**2)=    0.585[illegible]5E+05
   A(CM)=        38.3447     Q(KW/M**2)=    0.58099E+05
   A(CM)=        57.5171     Q(KW/M**2)=    0.55361E+05
   A(CM)=        76.6895     Q(KW/M**2)=    0.52744E+05
   A(CM)=        95.8618     Q(KW/M**2)=    0.48[illegible]E+05
   A(CM)=       115.0342     Q(KW/M**2)=    0.45[illegible]
   A(CM)=       134.2065     Q(KW/M**2)=    0.399[illegible]0E+05

                                                                RUNNING

   A(CM)=       153.3789     Q(KW/M**2)=    0.33294E+05
   A(CM)=       172 5513     Q(KW/M**2)=    0.24172E+05
   A(CM)=       191.7236     Q(KW/M**2)=    0.144[illegible]E+05
K(ABSORBTION COFFICIENT)=0.0050(1/cm
   A(CM)=         0.0000     Q(KW/M**2)=    0.79[illegible]
   A(CM)=        19.1724     Q(KW/M**2)=    0.797[illegible]
   A(CM)=        38.3447     Q(KW/M**2)=    [illegible]
   A(CM)=        57.5171     Q(KW/M**2)=    [illegible]
   A(CM)=        76.6895     Q(KW/M**2)=    [illegible]
   A(CM)=        95.8618     Q(KW/M**2)=    [illegible]
   A(CM)=       115.0342     Q(KW/M**2)=    [illegible]
   A(CM)=       134.2065     Q(KW/M**2)=    [illegible]
   A(CM)=       153.3789     Q(KW/M**2)=    [illegible]
   A(CM)=       172.5513     Q(KW/M**2)=    [illegible]
   A(CM)=       191.7236     Q(KW/M**2)=    [illegible]
```

ISD=10
NT=18
DZ=15cm

```
EXECUTION BEGINS...
K(ABSORBTION COFFICIENT)=0.0010(1/CM
   A(CM)=         0.0000      Q(KW/M**2)=     0.20572E+05
   A(CM)=        19.1724      Q(KW/M**2)=     0.21371E+05
   A(CM)=        38.3447      Q(KW/M**2)=     0.20378E+05
   A(CM)=        57.5171      Q(KW/M**2)=     0.20513E+05
   A(CM)=        76.6895      Q(KW/M**2)=     0.19109E+05
   A(CM)=        95.8618      Q(KW/M**2)=     0.18674E+05
   A(CM)=       115.0342      Q(KW/M**2)=     0.16825E+05
   A(CM)=       134.2065      Q(KW/M**2)=     0.15794E+05
   A(CM)=       153.3789      Q(KW/M**2)=     0.13176E+05
   A(CM)=       172.5513      Q(KW/M**2)=     0.11115E+05
   A(CM)=       191.7236      Q(KW/M**2)=     0.67260E+04
K(ABSORBTION COFFICIENT)=0.0030(1/CM
   A(CM)=         0.0000      Q(KW/M**2)=     0.54034E+05
   A(CM)=        19.1724      Q(KW/M**2)=     0.56463E+05
   A(CM)=        38.3447      Q(KW/M**2)=     0.53770E+05
   A(CM)=        57.5171      Q(KW/M**2)=     0.54527E+05
   A(CM)=        76.6895      Q(KW/M**2)=     0.50912E+05
   A(CM)=        95.8618      Q(KW/M**2)=     0.50290E+05
   A(CM)=       115.0342      Q(KW/M**2)=     0.45662E+05
   A(CM)=       134.2065      Q(KW/M**2)=     0.43578E+05
                                                                     VM READ

   A(CM)=       153.3789      Q(KW/M**2)=     0.36972E+05
   A(CM)=       172.5513      Q(KW/M**2)=     0.32117E+05
   A(CM)=       191.7236      Q(KW/M**2)=     0.20471E+05
K(ABSORBTION COFFICIENT)=0.0050(1/CM
   A(CM)=         0.0000      Q(KW/M**2)=     0.72593E+05
   A(CM)=        19.1724      Q(KW/M**2)=     0.76662E+05
   A(CM)=        38.3447      Q(KW/M**2)=     0.72543E+05
   A(CM)=        57.5171      Q(KW/M**2)=     0.74224E+05
   A(CM)=        76.6895      Q(KW/M**2)=     0.68947E+05
   A(CM)=        95.8618      Q(KW/M**2)=     0.68773E+05
   A(CM)=       115.0342      Q(KW/M**2)=     0.62245E+05
   A(CM)=       134.2065      Q(KW/M**2)=     0.60061E+05
   A(CM)=       153.3789      Q(KW/M**2)=     0.50689E+05
   A(CM)=       172.5513      Q(KW/M**2)=     0.44345E+05
   A(CM)=       191.7236      Q(KW/M**2)=     0.26985E+05
R; T=[illegible].54 12:00.37
[illegible]
                                                                     RUNNIN
```

# NUCLEATE AND FILM POOL BOILING IN R11: THE EFFECTS OF INCLINATION ANGLE AND SURFACE ENHANCEMENT

D.S. Jung*, J.E.S. Venart*, A.C.M. Sousa*

Results are reported on the effects of heat flux, surface inclination and pressure on free convection, nucleate and film pool boiling with R11. An evaluation of the heat transfer capabilities with EXPLOSAFE was also performed.

## INTRODUCTION

As part of a program of studies towards understanding and modelling the behavior of LPG tanks under fire accident conditions (1) there is the necessity for the specification of the fluid side boundary conditions. Tank storage and transport normally utilize large horizontal cylinders or spheres and hence the interior fluid sees a variety of surface inclinations and heat fluxes under fire accident conditions. Fire engulfment tests have suggested that boiling in the tank interior can be either by nucleate (2,3) or film (4) boiling. Some fire tests in addition have utilized an interior tank protection consisting of an EXPLOSAFE+ mesh (3).

The purpose of this paper is to present results obtained in R11 as a function of heat flux (1-180 kW/m$^2$) and angle (0-180°) at pressures from 1 to 2 bars in the free convective, nucleate, and film boiling regions with and without EXPLOSAFE.

## EXPERIMENTAL

### Apparatus

The experimental apparatus consists of 5 components (Fig. 1): an electric heater (including a holder for EXPLOSAFE and a copper surface), a reflux condenser, auxiliary heaters, thermocouples, a T-vessel and rotating system, and an HP-85/3497 computer and data acquisition system.

*Department of Mechanical Engineering, The University of New Brunswick, Fredericton, N.B., Canada, E3B 5A3.

---

+Vulcan Industrial Packaging Ltd., Rexdale, Ontario, Canada

Electric heaters: There have been very few boiling experiments with large surface area. In order to model large systems similar to railway tank cars with reasonable confidence, a careful study with reasonably large surface areas must be undertaken. To meet this purpose an 8 cm diameter copper plate was used. A coil heater, located behind the plate, permitted an evenly distributed temperature field. A cross sectional view of the test section is shown in Fig. 2. To limit the heat transfer to one side of the heating plate, an insulation block made of lava was used. Thermal compound between the copper plate and the ground surface of the encapsulated heating element allowed good thermal contact so that the heat loss through the bottom was minimized.

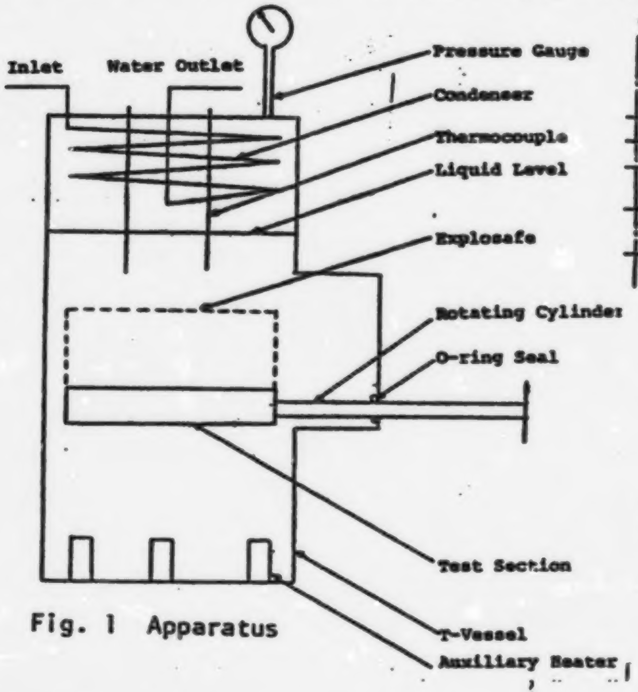

Inlet
Water Outlet
Pressure Gauge
Condenser
Thermocouple
Liquid Level
Explosafe
Rotating Cylinder
O-ring Seal
Test Section
T-Vessel
Auxiliary Heater

Fig. 1 Apparatus

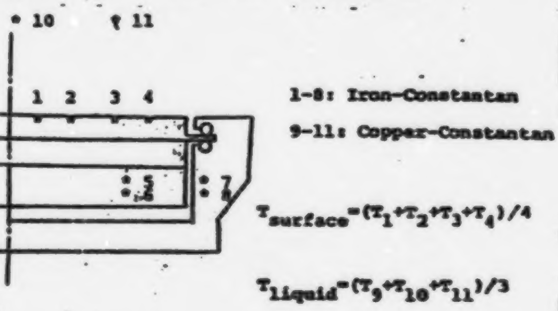

10
11
1
2
3
4
5
6
7
8
1-8: Iron-Constantan
9-11: Copper-Constantan
$T_{surface}=(T_1+T_2+T_3+T_4)/4$
$T_{liquid}=(T_9+T_{10}+T_{11})/3$

Fig. 2(b) Thermocouple Details

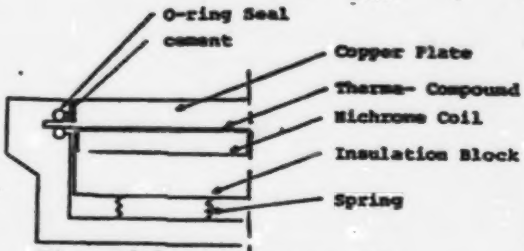

O-ring Seal
cement
Copper Plate
Therma- Compound
Nichrome Coil
Insulation Block
Spring

Fig. 2(a) Heater Details

## Experimental Procedure

The heat transfer surface was cleaned before testing with acetone. After assembly and charging of the system with R-11, the liquid was preheated to bring the system up to the desired pressure, and the power to the main surface heating element initiated for the desired orientation angle. After steady state was obtained, (15-20 min.), all readings were taken and the power increased to the next desired level. The pressure in the T-vessel was maintained constant throughout the test.

At each data point the following items were determined; surface temperature, liquid temperature, temperatures in the insulation block and stainless steel and two voltage drops across the heating element and a standard resistor in order to calculate the power input to the heater. The heat flux associated with boiling from the copper plate was obtained by subtracting the heat loss through the insulation block from the power delivered to the heater. The detailed heat loss calculation method is described elsewhere (5).

## Results and Discussion

The effect of orientation on nucleate boiling; The effect of orientation in boiling has been reported in reference (6). Here comparisons were made of boiling heat transfer for three different surface orientations of a strip heater in R11, facing upward, downward and vertical. Their results exhibit that for the orientations of facing upward and vertical, the boiling curves obtained are typical for nucleate boiling heat transfer; that is a pronounced increase of heat transfer rate with surface temperature after the onset of nucleation and the existence of a burnout point. For the case of facing downward, however, the curve differs very significantly from the other two with a very much reduced heat transfer capability but still with a burnout point. Li-Ting Chen (7) performed similar experiments and pointed out that the orientation effect is important in the region of inclination angle 150 degrees to 180 degrees (facing downward) from the horizontal. The test section areas used by the previous authors are however very small (9.25 $cm^2$ and 3.17 $cm^2$ respectively) so that edge effects may dominate heat transfer performance from their surfaces. For very large surfaces there will be an absence of edge effects and the effects of bubble agglomerationed bubble acceleration/retardation may become apparent. A detailed study has been conducted in the region 150 - 180 degrees. Figures 3 and 4 show the effect of the orientation of the surface. As seen in Fig. 3, at low heat flux, below 30 $kW/m^2$, as the angle increases up to 170°, so the temperature difference decreases continuously. This means that heat transfer performance is increased by increasing the angle of inclination. At high heat fluxes however (above 45 $kW/m^2$ to 70 $kW/m^2$), even though the angle increases, the temperature difference does not change by a large amount. It is evident that at this range of heat flux heat transfer performance is not dependent upon the orientation of the surface. At higher heat fluxes, above 80 $kW/m^2$, as the angle increases, temperature differences increase slowly but steadily and near 170 degrees the temperature difference increases to a very large value resulting in burnout.

Heat transfer performance for the 180° (facing downward) case is, of course, the poorest except at very low heat fluxes (2 or 3 kW/m) in the natural convection region. As seen in Fig. 4, there is an inflexion point around 8 - 9 $kW/m^2$ for the downward facing case in nucleate boiling so that below this heat flux however, due possibly to edge effects, heat transfer performance continuously decreases so that at around 80 $kW/m^2$ it yields the poorest heat transfer performance.

It is observed that once the surface is inclined, there are strong convection currents promoted by bubble motion, that induce the surface heat transfer. When the heating surface is facing downward bubbles agglomerate and are apt to collect on the underside so that the gross convection currents are not sufficient to sweep the bubbles away. As a consequence, the bubble motion does not add to the convection mechanism as it does when the surface is in any other position.

The effect of orientation in film boiling: The ordinary technique of obtaining boiling, i.e., traversing up the nucleate boiling curve and over the peak, would require complex, high capacity equipment, whereas the region of interest requires only a small fraction of the peak heat flux. E.R. Hosler et al (8) proposed another technique of heating the dry surface to a temperature above that required to obtain film boiling and then charging the liquid into the container. The advantage of this technique is that film boiling can be established directly without having to go over the peak of the boiling curve. In the present study it is observed that for facing downward case peak heat flux is less than half of that for the facing upward case. Thus we first generate film boiling for the facing downward case and then turn the rotating cylinder to the desired angle maintaining a heat flux necessary to maintain film boiling. The effect of the orientation in film boiling is very similar to that in nucleate boiling. In film boiling (Fig. 4), the facing downward case has the poorest heat transfer performance without exception. One thing to be pointed out here is that facing upward case in film boiling has the highest heat transfer performance, while inclination angle around 160 degrees has the highest one in nucleate boiling region. Photographic studies reveal that the vapor motion is a strong function of the orientation such that for facing downward case, vapor flows out in a radial direction along the heated surface, while the vapor escapes very easily to the bulk liquid for any other orientation. It is also observed that there is temperature gradient on the surface in radial direction such that center region attains the highest temperature which then decreases towards the edge. From inclination angles 0° to 150°, heat transfer curves are very close together but from 150° to 180° (facing downward) there is a large difference in terms of heat transfer. This also proves that once the surface is inclined, there is a convection current to sweep the heat away from the surface. Although the present technique did not permit a precise determination of the minimum temperature difference it can be seen that as the angle of inclination is increased the minimum temperature difference decreases.

## Effect of EXPLOSAFE

To improve the heat transfer in railway tank cars under accident conditions EXPLOSAFE, which is a honeycomb type expanded aluminum mesh, has been proposed as an internal protection device. In order to study this, six small studs and wire were used to hold down the 19, 25, and 50 mm thick EXPLOSAFE samples in good contact with the surface. Fig. 5 shows that EXPLOSAFE does not cause any appreciable enhancement in nucleate boiling. As the thickness increases, the heat transfer is retarded. This can be explained by introducing a thermal contact resistance theory. At first it was thought that this material will work as a fin to take the heat away from the surface. However, it is deduced from these results that even though EXPLOSAFE is in good contact, there is a micro layer between the EXPLOSAFE and the surface. Therefore, this layer acts as a thermal resistance to prevent the liquid from having a good access to the surface, wetting the surface and taking the heat away as a result. Dhir and Catton (9) analyzed boiling in porous media. As they pointed out, in a deep bed, the vapor channels extended only part way into the bed while in shallow beds the channels were well formed throughout the bed. That is why as the thickness of EXPLOSAFE increases, it forms a deep bed and accordingly retards the heat transfer.

## Effect of Pressure

W. Nakayama et al (10) observed that as the pressure is increased the required wall superheat decreases. This experimental study also shows the same trend in nucleate and film boiling regions (Fig. 6). This may be explained by the fact that as a particular surface has a given cavity size distribution, the superheat required must activate a particular size of cavity. With increasing pressure less superheat will be required.

## Effect of Fouling

The effect of heating surface fouling on saturated pool boiling was reported first by Akagawa et al(9). Boiled organic fluids such as Freon-11 contaminate the heating surface with deposits formed by their thermal decomposition upon being subjected to high surface temperatures. In this experiment the clean surface was not initially contaminated by nucleate boiling, but easily built up deposits under film boiling. Under these conditions the color of the Freon-11 changes to light yellow from clear and the boiling curve shifts to the right with larger temperature differences.

## CONCLUSIONS

Free convection, nucleate, and film boiling results are reported for heat fluxes to 180 $kW/m^2$ at angles of inclination from horizontal vertically upwards (0°) to 180°, horizontal facing downwards, at pressures from 1 to 2 bar in R-11.

Minimum film boiling temperature differences decrease with increasing angle of inclination.

Tests performed using a variety of thickness of EXPLOSAFE (19, 25, 50 mm) in the nucleate boiling region indicate that there is no pronounced enhancement with this material.

Film boiling causes severe surface fouling due to R-11 decomposition.

## ACKNOWLEDGMENTS

Funding for this work was provided by the Natural Sciences and Engineering Research Council of Canada and Transport Canada, Transportation Development Centre.

## REFERENCES

1. J.E.S. Venart, A.C. Mendes de Sousa, F.R. Steward, J.G. Lenard, "Tank Car Thermal Modeling," a Proposal to Supply and Services Canada: DSS File No. 09SDT8200-1-1540, October 23, 1981, 52 pages.
2. "The effects of a Fire Environment on a Rail Tank Car filled with LPG," FRA-OR&D 75-31, C. Anderson, W. Townsend, J. Zook, G. Cowgill, September 1974.
3. "Testing and Evaluation of the EXPLOSAFE System as a method of controlling the Boiling Liquid Expanding Vapour Explosion (BLEVE)," TP 2740, R.D. Appleyard, Dept. of Res. & Dev. EXPLOSAFE Div. of Vulcan Ind. Packaging Ltd., August 1980.
4. A.F. Roberts, D.P. Cutler, and K. Billings, Proc. 4th Int. Symposium Loss Prevention and Safety Promotion in the Process Industries, Vol. 3, pp. D1-D10, I. Chem. E. Symposium Series 82 (1983).
5. D.S. Jung, "Nucleate and Film Pool Boiling," MScE Thesis UNB (1984) to be published.
6. Githinji, P.M. and Sakersby, R.H., ASME Journal of Heat Transfer, 1963, Vol. 85, p. 379.
7. Li-Ting Chen, Letters in Heat and Mass Transfer, Vol. 5, 1978, pp. 111-120.
8. E.R. Hosler and J.W. Westwater, Journal of American Rocket Society, Vol. 32, 1962, pp. 553-558.
9. V.K. Dhir and I. Catton, Applied Scientific Research, Vol. 38, 1982, p. 69.
10. Rohsenow, W.M. and Choi, H.Y., "Heat, Mass and Momentum Transfer," Prentice-Hall, Inc., Englewood Cliffs, New Jersey, 1961, p. 217.
11. K. Akagawa, T. Sakaguchi and T. Fkujii, Paper B1.6, Proc. Fifth Int. Heat Transfer Conference, Sept. 3-7, 1974, Tokyo, pp. 25-29.

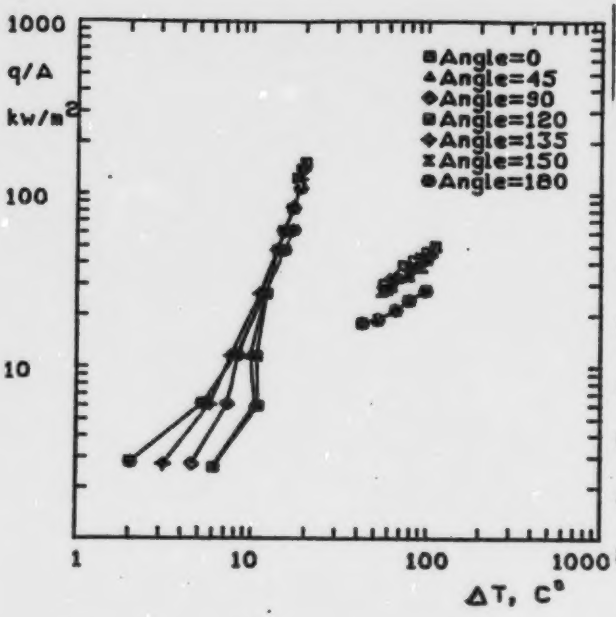

Fig. 3. Pool Boiling Heat Transfer with Freon-11 At 2 Bar

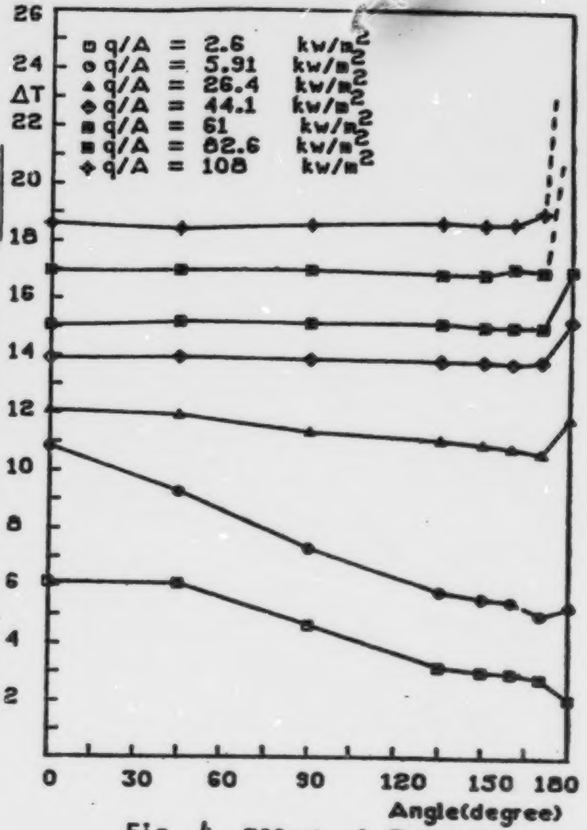

Fig. 4. Effect of Orientation

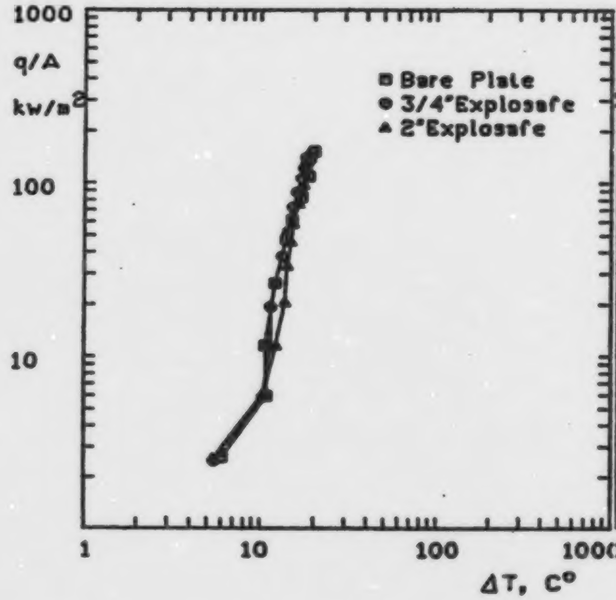

Fig.5. Pool Boiling Heat Transfer with Freon-11(Effect of Explosafe)

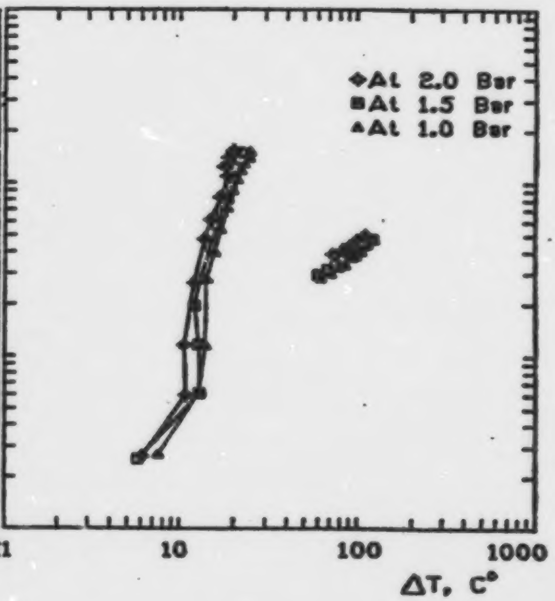

Fig. 6 Pool Boiling Heat Transfer with Freon-11(Effect of Pressure)

# RAIL TANK CAR GEOMETRY

By

Paul Callaghan

The attached program analyzes the geometry of a cylindrical rail tank car. Eventually the program will be incorporated with other software to develop a computer model which simulates a rail tank car subject to a fire environment. Specifically the program determines the wetted surface area (WSA) and the fire surface area (FSA), for the cars. Both of these quantities are necessary in analyzing the heat transfer to the tank car's lading.

The objective of this report is to summarize the development of the attached program, as well as discuss its limitations.

In an accident situation a rail tank car may end up with any angle of pitch with respect to the horizontal. Also, when subject to a fire environment, the liquid/vapour ratio of the contents will vary with time. The variation will depend on the boiling action caused by heating, as well as upon the dissipation of the contents through the pressure release valve. Thus the attached program computes the free and wetted surface areas for a car with any angle of pitch and any liquid/vapour ratio.

As input the program requires the angle of pitch, as well as the liquid and vapour volumes. The angle of pitch is an assumed value which can vary from $0-\pi/2$ radians. The volumes are supplied by software developed which determines the state of the tank's contents.

The first task in developing the program was to recognize all possible shapes the liquid (vapour) could assume. It turns out that only three distinct shapes need be considered. These shapes, referred to as a truncated cylinder, a wedge, and a truncated wedge are illustrated in figures 1-3 inclusive. Figure 4 illustrates possible tank configurations for the occurence of each of the shapes. Figure 5 illustrates the free surfaces associated with each of the shapes. As noted these surfaces are ellipses, or a portion thereof, for all possible tank configurations.

Having recognized the necessary shapes to consider, the chief task of solving for the wetted and free surface areas could be approached more clearly. The manner in which this task was approached is summarized in the five steps listed below;

1. General formulae for the volume, FSA, and WSA were obtained or developed for each of the three shapes [Ref. 1].

2. The formulae for volume were then expressed such that each involved only one unknown dimension. That is, the number of unknowns in the equation

was reduced to one by noting the interdependence of the various dimensions. The various dimensions are related in terms of the angle of pitch and the known tank dimensions.

3. Using the known volume this one unknown dimension can now be determined either explicitly or by employing an iterative scheme.

4. Having solved for one dimension, the others necessary to solve for WSA and FSA were easily determined.

5. As a final step the various dimensions were funneled into the appropriate equations for WSA and FSA.

Presently the values for the liquid and vapour volumes are initialized by arithmetic assignment statements. By incrementing the vapour volume and decrementing the liquid volume after each run of the program a number of vapour/liquid ratios were easily tested for each angle of pitch. Later the program will be defined as a subroutine and will be accessed by means of a CALL statement. Input parameters will include VLIQ, VVAP, and the angle of pitch.

In conclusion it should be emphasized that the values for the WSA and the FSA calculated by the attached program are ideal values only. Ideal in the sense that it is assumed that the liquid and vapour phases are entirely distinct. The effect of boiling makes this assumption invalid. Thus further work will attempt to appropriately modify the inputs, and/or outputs, of the program.

## Reference

[1] Esbach, O.W., "Handbook of Engineering Fundamentals", John Wiley & Sons Inc., New York, 1936.

```
*****************************************************************************************************************
      $JOB WATFIV CALLAGHAN/U
      C      THE FOLLOWING PROGRAM COMPUTES THE FREE SURFACE AREA (FSA),
      C      AS WELL AS THE WETTED SURFACE (WS), FOR A RAIL TANK CAR WITH
      C      ANY ANGLE OF TILT (PHI).AS INPUT THE PROGRAM REQUIRES VLIQ,
      C      VVAP,TANK DIMENSIONS, AND THE ANGLE OF TILT PHI, IN RADIANS.
      C      MAIN PROGRAM ***************************************************
             REAL MA,L
             VLIQ=123.7
             VVAP=10.0
             PHI=0.1396
             PI=3.141596
             L=18.3
             D=3.05
             R=D/2
         05  IF(PHI.GE.0.165)GO TO 40
             THETC=ARCOS((R-L*TAN(PHI))/R)
             CV=(R**3/TAN(PHI))*(SIN(THETC)-(SIN(THETC)**3)/3-THETC*COS(THETC))
             CV1=PI*R*R*L-CV
             IF(VLIQ.GE.CV.AND.VLIQ.LE.CV1)GO TO 10
             GO TO 40
      C TRUNCATED WEDGE
         10  A=(R-L*TAN(PHI))/R
             B=SQRT(2*R*L*TAN(PHI)-L*L*TAN(PHI)**2)/R
             V=VLIQ
             C=V*TAN(PHI)/R**3
             XMAX=D
      C BISECTION ALGORITHM TO SOLVE FOR X
             I=1
             EA=L*TAN(PHI)
             EB=XMAX-0.001
         15  CALL VFUNC(EA,FX,DFX,A,B,C,R)
             FXEA=FX
             EP=EA+(EB-EA)/2
             CALL VFUNC(EP,FX,DFX,A,B,C,R)
             FXEP=FX
             IF((EB-EA).LT.0.05) GO TO 17
             IF(I.GT.15)GO TO 17
             PROD=FXEA*FXEP
             IF(PROD.GT.0.0)EA=EP
             IF(PROD.LT.0.0)EB=EP
             I=I+1
             GO TO 15
         17  X=EP
             PRINT, 'ESTIMATE FROM BINARY SEARCH',X,'FX(EP)=',FXEP
      C NOW KNOW X AND CAN THEREFORE COMPUTE FSA & WS
         25  MA=R/SIN(PHI)
             THETA=ARCOS((R-X)/R)
             THETB=THETA-ARCOS(A)
             D1=R-R*COS(THETB)
             XB=MA-D1/SIN(PHI)
             XA=X/SIN(PHI)-MA
             YA=R*SIN(THETA)
             YB=R*SIN(THETB)
             FSA=PI*MA*R-(-XA*YA+MA*R*ARCOS(XA/MA))-(-XB*YB+MA*R*ARCOS(XB/MA))
             TCS=2*R/TAN(PHI)*(YA+(X-R)*THETA)
             SCS=2*R/TAN(PHI)*(YB+(D1-R)*THETB)
             A1=PI*R**2-R**2*(THETA-SIN(THETA))/2
             IF(THETA.LT.(PI/2)) A1=R**2*(THETA-SIN(THETA))/2
             A2=R**2*(THETB-SIN(THETB))/2
      IF(THETB.GT.(PI/2))A2=PI*R**2-R**2*(THETB-SIN(THETB))/2
      WS=TCS-SCS+A1+A2
      GO TO 100
C ANGLE OF TILT (PHI) > 0.165 RADS.
   30 CV=(PI*R**3)/TAN(PHI)
      CV1=PI*R**2*(L-R/TAN(PHI))
      IF(VLIQ.GE.CV1.OR.VLIQ.LE.CV)GO TO 40
      D1=D/TAN(PHI)
      S1=2*VLIQ/(PI*R**2)
      H2=(D1+S1)/2
      H1=H2-D1
      A=SQRT(D**2+D1**2)
      FSA=PI*A*R
      WS=PI*R*(H1+H2)+PI*R**2
      GO TO 100
C WEDGE: REGARDLESS OF ANGLE OF TILT.
   40 PMAX=PI
      POLD=PI/2
      FLAG=0
      ITCHK=1
      IF(VVAP.GT.VLIQ)FLAG=1
      IF(FLAG.EQ.1)GO TO 45
      V=VVAP
      GO TO 48
   45 V=VLIQ
   48 C=V*TAN(PHI)/(R**3)
      P=POLD
      ITER=1
C NEWTON-RALPHSON ITERATION SCHEME TO SOLVE FOR P
   50 FP=SIN(P)-(SIN(P)**3)/3-P*COS(P)-C
      DFP=SIN(P)*(P-SIN(P)*COS(P))
      PNEW=P-FP/DFP
      IF(ABS(P-PNEW).LT.0.035)GO TO 60
      IF (ITER.GT.8)GO TO 110
      IF(PNEW.GT.PMAX)P=(P+PMAX)/2
      IF(PNEW.GT.0.0.AND.PNEW.LT.PMAX)P=PNEW
      ITER=ITER+1
      GO TO 50
C NOW KNOW P AND CAN THEREFORE SOLVE FOR WS AND FSA
   60 POLD=PNEW
      P=PNEW
      MA=R/SIN(PHI)
      A=R*SIN(P)
      B=R-R*COS(P)
      BA1=R**2*(2*P-SIN(2*P))/2
      IF(P.GT.(PI/2))GO TO 70
      X=MA-B/SIN(PHI)
      FSA=-X*A+MA*R*ARCOS(X/MA)
      GO TO 80
   70 X=B/SIN(PHI)-MA
      FSA=PI*MA*R-(-X*A+MA*R*ARCOS(X/MA))
C     WETTED SURFACE
   80 CONVA=(2*R/TAN(PHI))*(A+(B-R)*P)
      IF(FLAG.EQ.1)GO TO 90
      WS=2*PI*R*(R+L)-BA1-CONVA
      GO TO 100
   90 WS=BA1+CONVA
C OUTPUT OF RESULTS
  100 WRITE(6,120) PHI,WS,FSA
  120 FORMAT(' ','PHI=',F9.6,2X,'WS=',F9.4,2X,'FSA=',F9.4)
```

```
          VLIQ=VLIQ-5.0
          VVAP=VVAP+5.0
          IF(VLIQ.GT.CV) GO TO 05
          GO TO 130
     110  PRINT, 'FAILURE DUE TO ITERATION SCHEME'
          IF(ITCHK.EQ.1) PRINT, ITCHK,P,PNEW,VLIQ,VVAP
     130  STOP
          END

          SUBROUTINE VFUNC(X,FX,DFX,A,B,C,R)
          F1X=SQRT(2*R*X-X**2)/R
          F2X=(R-X)/R
          FX=F1X-(F1X**3)/3-F2X*ARCOS(F2X)-A*F1X+B*F2X+((A*F1X-B*F2X)**3)/3
         $+(ARCOS(F2X)-ARCOS(A))*(A*F2X+B*F1X)-C
          DFX=(F2X/F1X-F1X*F2X+ARCOS(F2X)-1)/R+((A*F1X-B*F2X)**2)*(A*F2X/F1X
         $+B)/R+(B*F2X/F1X-A)/R*(ARCOS(F2X)-ARCOS(A))
          RETURN
          END

      $ENTRY
HI= 0.139600  WS=163.6737  FSA= 19.7381
HI= 0.139600  WS=155.9595  FSA= 24.6658
HI= 0.139600  WS=148.7852  FSA= 28.8027
HI= 0.139600  WS=142.1917  FSA= 32.3320
HI= 0.139600  WS=135.9247  FSA= 35.5528
HI= 0.139600  WS=129.8982  FSA= 38.3806
HI= 0.139600  WS=124.0162  FSA= 40.9206
HI= 0.139600  WS=118.2589  FSA= 43.2061
HI= 0.139600  WS=112.5769  FSA= 45.2581
HI= 0.139600  WS=106.9400  FSA= 47.0870
STIMATE FROM BINARY SEARCH              2.9445240 FX(EP)=             0.0031805
HI= 0.139600  WS=100.9737  FSA= 51.0235
STIMATE FROM BINARY SEARCH              2.8549750 FX(EP)=             0.0219774
HI= 0.139600  WS= 96.6455  FSA= 50.7982
STIMATE FROM BINARY SEARCH              2.7355760 FX(EP)=            -0.0155708
HI= 0.139600  WS= 90.5793  FSA= 49.6032
STIMATE FROM BINARY SEARCH              2.6460270 FX(EP)=             0.0101643
HI= 0.139600  WS= 86.0624  FSA= 48.3812

TATEMENTS EXECUTED=      1094

ORE USAGE       OBJECT CODE=    8928 BYTES,ARRAY AREA=       0 BYTES,TOTAL AREA AVAILABLE=  131072  BYTE

IAGNOSTICS        NUMBER OF ERRORS=        0, NUMBER OF WARNINGS=        0, NUMBER OF EXTENSIONS=        0

OMPILE TIME=    0.16 SEC,EXECUTION TIME=     0.07 SEC,      14.06.33     THURSDAY      10 JUN 82     WATFIV

        C$STOP
```

## WEDGE.

$$V = \frac{hr^3}{b}\left[\sin\theta - \frac{\sin^3\theta}{3} - \theta\cos\theta\right]$$

$$CA = \frac{2rh}{b}\left[a + (b-r)\theta\right]$$

$$DS = CA + \frown, \quad WS = TSA - DS$$

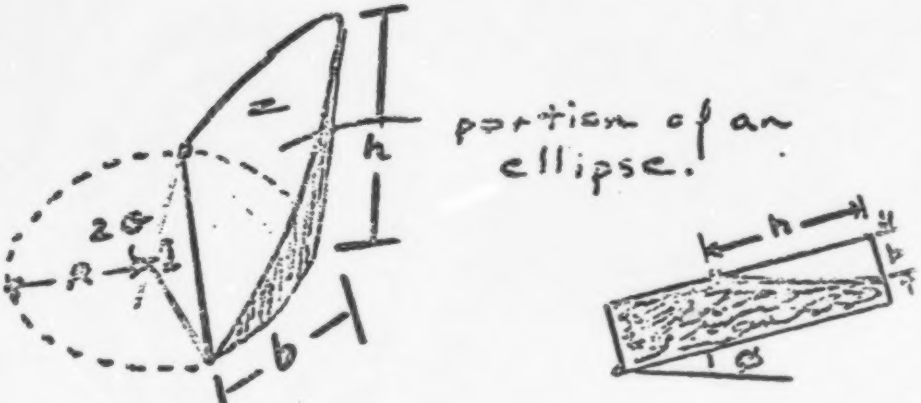
a
h
portion of an ellipse.
2θ
r
b
h
b
φ

Figure 1.

$$\tan\phi = \frac{b}{h}$$

## TRUNCATED CYLINDER.

$$V = \frac{\pi r^2}{2}(h_1 + h_2)$$

$$CA = \pi r(h_1 + h_2)$$

$$W.S = CA + \pi r^2.$$

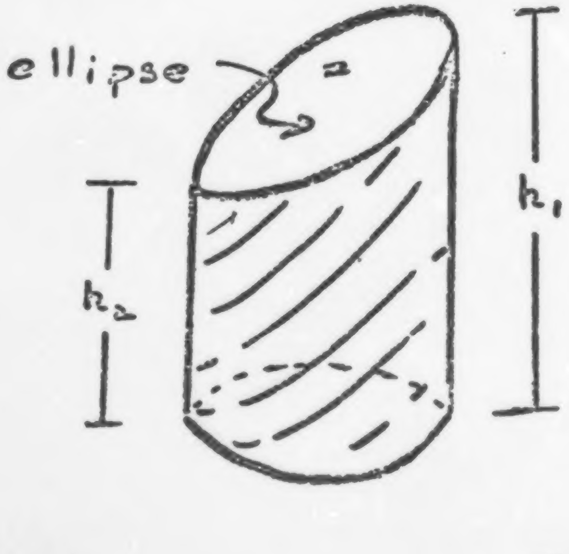
ellipse
a
$h_1$
$h_2$
r

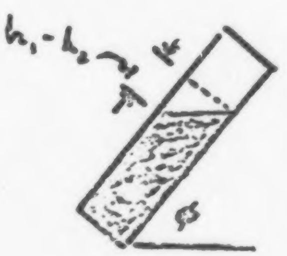

$$h_1 - h_2 = \frac{D}{\tan(\phi)}.$$

Figure 2

## TRUNCATED WEDGE

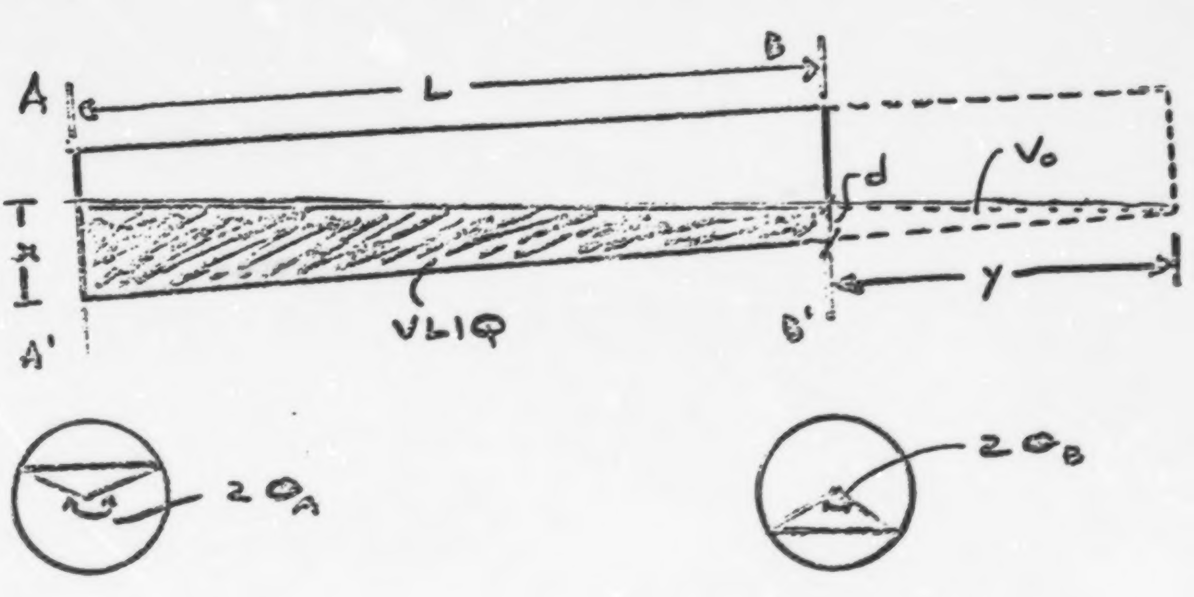

$$V_{LIQ} = V - V_0$$

$$V = \frac{(L+y)r^3}{x}\left[\sin\Theta_A - \frac{\sin^3\Theta_A}{3} - \Theta_A\cos\Theta_A\right]$$

$$V_0 = \frac{y r^3}{d}\left[\sin\Theta_B - \frac{\sin^3\Theta_B}{3} - \Theta_B\cos\Theta_B\right]$$

BUT, $\tan\phi = \frac{x}{L+y} = \frac{d}{y}$

$$\therefore V_{LIQ} = \frac{r^3}{\tan\phi}\left[\left(\sin\Theta_A - \frac{\sin^3\Theta_A}{3} - \Theta_A\cos\Theta_A\right) - \left(\sin\Theta_B - \frac{\sin^3\Theta_B}{3} - \right.\right.$$

HOWEVER, $\Theta_A = \cos^{-1}\left(\frac{r-x}{r}\right)$

$$\Theta_B = \Theta_A - \Theta_A^{\bullet}$$

$$= \cos^{-1}\left(\frac{r-x}{r}\right) - \cos^{-1}\left(\frac{r-L\tan\phi}{r}\right)$$

→ SUBST. THESE EXPRESSIONS INTO VLIQ WE OBTAIN

$$VLIQ = f(x).$$

→ USING BISECTION ALGORITM SOLVED FOR X.

Figure 3

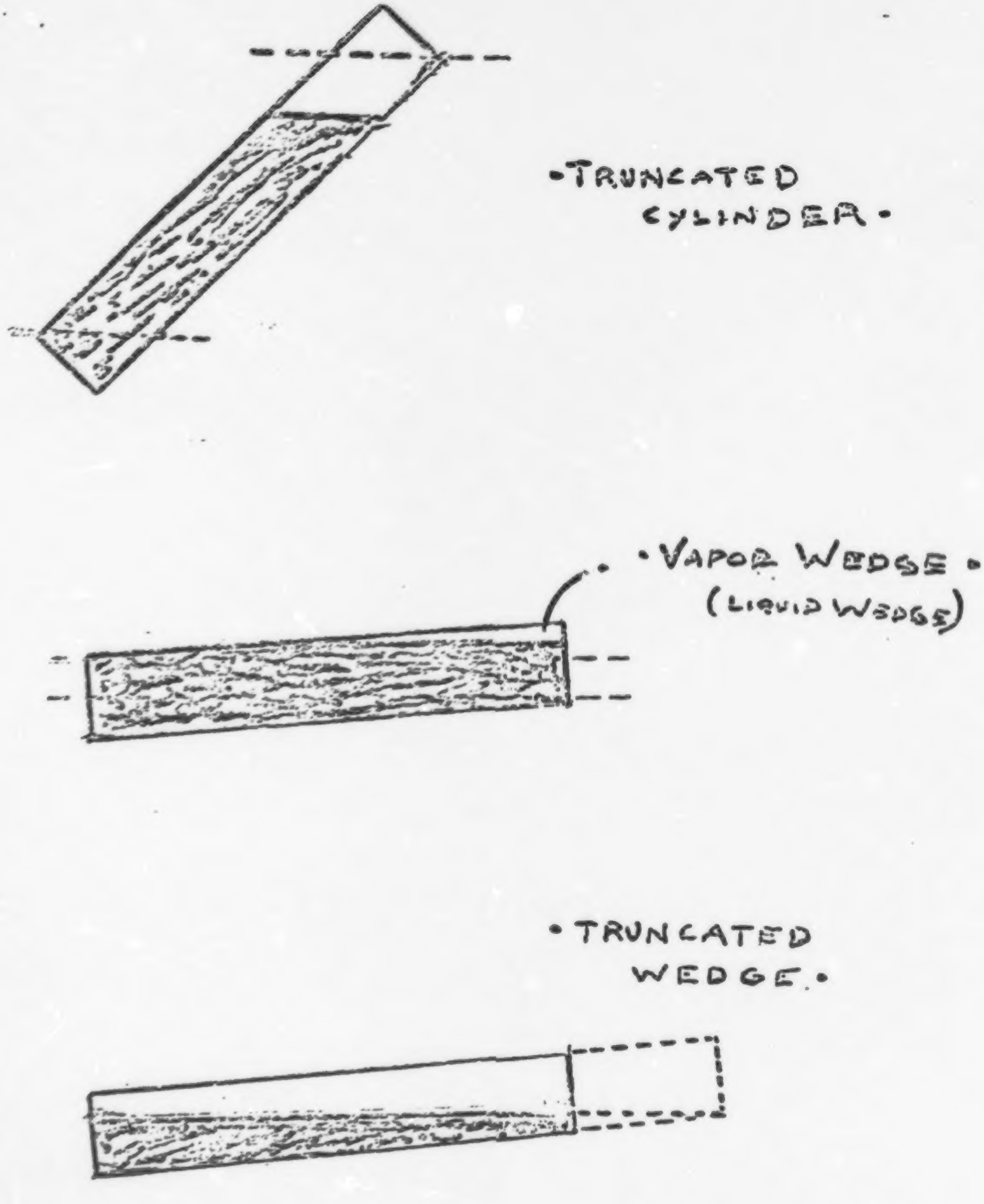
•TRUNCATED CYLINDER•
•VAPOR WEDGE•
(LIQUID WEDGE)
•TRUNCATED WEDGE•

Figure 4

# FREE SURFACE AREA.

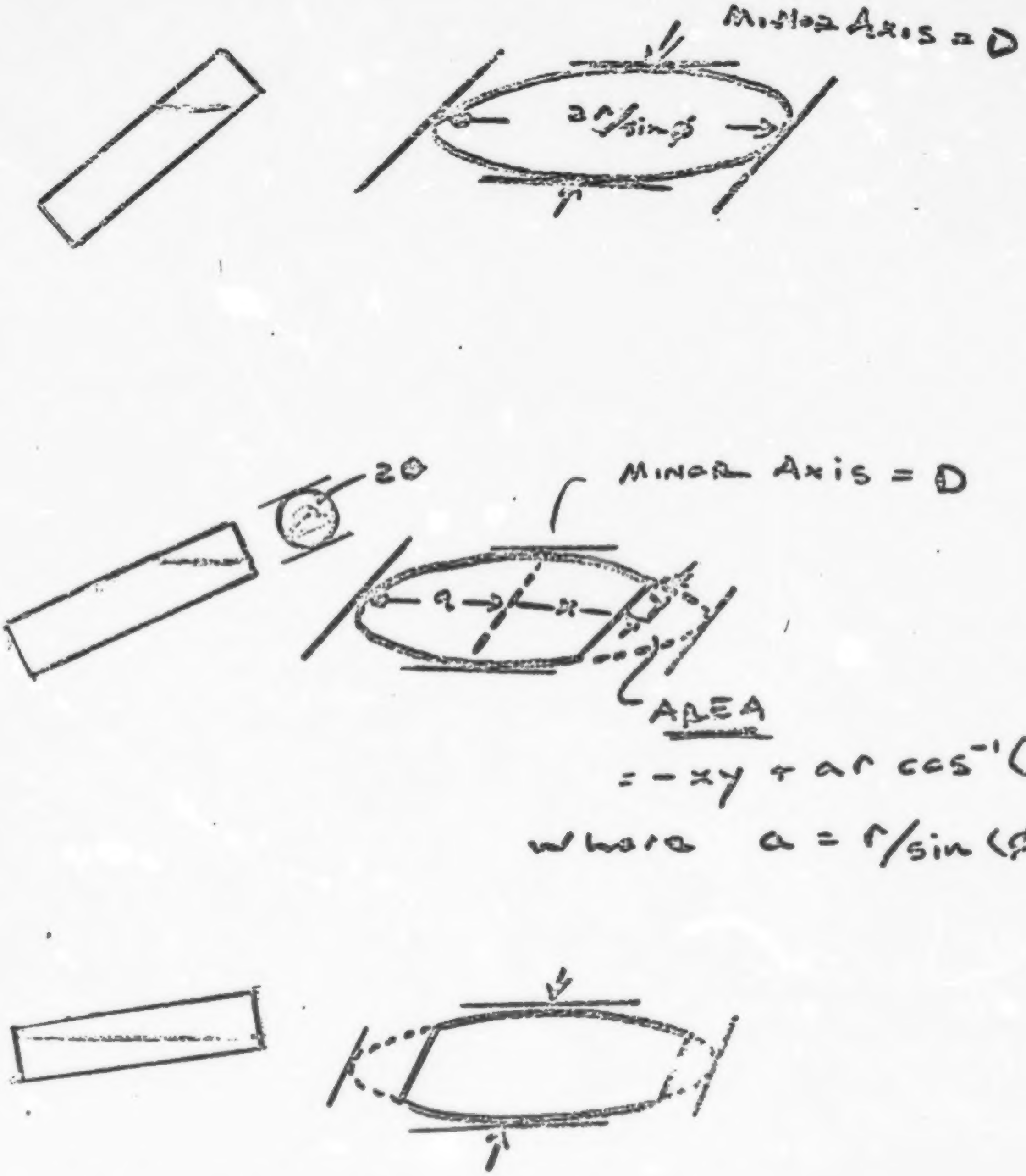
MINOR AXIS = D
2r/sin φ
2r
MINOR AXIS = D
a
x
AREA

$$= -xy + ar\cos^{-1}\left(\frac{x}{a}\right),$$

where $a = r/\sin(\phi)$

Figure 5

# THE
# DESIGN, CONSTRUCTION
# AND
# TESTING
# OF A
# CYLINDRICALLY SURFACED
# CALORIMETER

by

KEN F. SOLLOWS

prepared for

ME 6003

MEASUREMENTS IN HEAT TRANSFER

MAY 1983

DR. J.E.S. VENART

# TABLE OF CONTENTS

INTRODUCTION 1

DESIGN 4

  CALCULATION OF AREA 5

  HEATERS 6

  CALORIMETER 7

  POWER DENSITY 8

  TEMPERATURE PROBE 9

FABRICATION 9

TESTING 11

CONCLUSIONS 12

TABLE AND FIGURES 13

PHOTOGRAPHS 16

APPENDICES 24

## INTRODUCTION

This paper was motivated by an ongoing investigation into the mechanisms of heat transfer in liquified petroleum gas (LPG) tank cars. The investigation is funded by Transport Canada, and the ultimate objective is increased safety in transportation of these fuels (principally propane transported by rail).

The direction in which the investigation proceeds has been deliniated by experience with actual accidents and scale model tests. This experience has led to consideration of 3 different situations that result in heat tansfer to the lading.

One situation is when the tank (or a portion of same) is subjected to a pool fire. This may be typified by an accident where an LPG tank car remains intact after derailment and is subsequently engulfed in flames.

Another is the radiant heat transfer from the flare of LPG which vents through the pressure relief valve (PRV). The heat from a pool fire will increase the temperature and pressure of the lading. When this pressure exceeds the PRV set-point the PRV will open and vent to reduce pressure. This is intended to reduce the chances of a catastrophic rupture occuring. If the rate of heat transfer to the tank is great enough the PRV will remain open, otherwise it will cycle. Upon ignition, this gas forms a high temperature flare above the valve. The geometry of the flare can be distorted by surface winds. If the wind should blow so as to increase the view factor between the flare and the tank, then that area of the pressure vessel will be subjected to higher heat fluxes.

The third situation is similar to the second in its results. In this case, a portion of the tank is subjected to direct impingment of a torch or flare. This will likely result in the highest heat fluxes. The flare may issue from a PRV on another car, or from a hole created by the impact of an LPG tank car with another car or coupler. These high local heat fluxes can force the metal temperature above safe limits and result in weakening and failure.

Such a localized failure can have catastrophic consequences. The sudden reduction in pressure within the tank may trigger a rapid and extensive phase change in the lading, from liquid to vapor. Such an event has the outward appearance of an explosion and has been termed a Boiling Liquid Expanding Vapor Explosion (BLEVE). THis event can transform an expensive nusance into a virtual disaster.

It shoyld not be suprising that some work has been done to mitigate against these accidents. In particular, attention has been paid to the sizing of the PRV and the use of fire protective coatings on the outer surface of the tank. Recently, treatments for the interior of the tank have been given consideration. This research was initiated to evaluate on such treatment, Explosafe. This material is constructed of expanded metal foil and it appears to augment heat transfer from the tank to the lading, at least in some circumstances.

It should be apparent that, because the mechanism of heat transfer to the tank and lading can be different from one situation to another, any treatment may have benificial and detrimental effects upon safety. For example, a treatment which is particularly effective in mitigating against the effects of a pool fire could actually augment the effects of a torch or radiative load. In this way one may reduce the effects of a relatively high probability accident at the expense of increasing the probability of a more severe accident. This implies that an optimal manner and degree of protection may be attained, in the sense of a maximum overall safety.

It is hoped that the basic research into the heat transfer and failure mechanisms which is being conducted will aid in such an optimization. Certainly it will not be possible to so optimize the thermal protection sustem unless these mechanisms are well understood.

The project described in this paper is a cylindrically surfaced calorimeter. It has been developed to permit investigation of high and localized flux heat transfer to a liquid. Physically, it is thought that this apparatus will approximate the behavior of a torch impinging upon the tank (third situation above).

## DESIGN

The basic design of the calorimeter was conceptualized in the summer of 1982 by Mr. Paul Wentzell (Appendix #1), then an undergraduate research assistant. It would be constructed so as to fit a Pyrex glass "T" pipe section which had been procured from the Chem. Engr. Dept.. The through pipe on this section was 6 inches (nom.) in diameter and the branch pipe was 4 inches (nom.) in diameter. It was anticipated that the calorimeter would be mounted to a flange which could be coupled to the branch (4") pipe. The ends of the through (6") pipe would be sealed with sheet acrylic plates. Thus one would achieve maximal visibility of the calorimeter surface and the fluid.

## CALCULATION OF SURFACE AREA

The first step in the detailed design of the calorimeter was the derivation of an expression for the area of the curved surface. This was approached from the integration of an infinitesimal, as follows:

From Figure #1 we can see (by symmetry) that the surface area will be given by:

$$As = 4\int_{0}^{Rs} da \text{ ---------------------- } [1]$$

Also,

$$da = L \; dx$$

$$= R1\,\Theta \; dx \text{ ----------------------- } [2]$$

But

$$\sin\Theta = y/R1$$

$$\Theta = \arcsin(y/R1) \text{ -------------- } [3]$$

Substituting [3] into [2] we see

$$da = R1 \arcsin(y/R1)\; dx \text{ ----------- } [4]$$

Since y is a point on a circle of radius Rs

$$Rs^2 = x^2 + y^2$$

$$y = \sqrt{Rs^2 - x^2} \text{ --------------- } [5]$$

Finally substituting [5] into [4] we get

$$da = R1 \arcsin\left(\frac{\sqrt{Rs^2 - x^2}}{R1}\right) dx \text{ --- } [6]$$

which is an integrand in terms of x only.

Thus we need to solve the integral equation

$$As = 4\ R1 \int_{0}^{Rs} \arcsin\left(\frac{\sqrt{Rs^{\wedge}2 - x^{\wedge}2}}{R1}\right) dx \text{ --- } [7]$$

Numerical integration of this formula was carried out using the Fortran subroutine QANC8S (Appendix #2). The value obtained for R1=3" & Rs=2" is presented in Table #1. Also included is the area of a circle with radius 2" and the area of an ellipse with a minor axis of 4" and a major axis of 4.38". The estimate of error for the numerical solution, provided by the subroutine was e=0.000

## HEATERS

The heaters to be used had been acquired previously. They are 450-W 120-V cartridge type units, approximately 1-1/2" long and 3/8" diameter. Initial calculations suggested the use of 12 elements, 8 in the guard section and 4 in the main section. The number of cartridges was subsequently increased to 5 in the main heater section, making 13 overall.

## CALORIMETER

The calorimeter itself consists of a brass rod with one end machined to form a concave cylinder (Photographs #1,#2). The guard and main heater sections are deliniated by a groove cut from the back of the unit to within 1/8" of the concave surface at its innermost point (Photograph #3). This gap should limit radial heat conduction. It was not possible to maintain a fixed distance between the bottom of the groove and the concave surface due to machining limitations.

The cartridge heaters are mounted in holes drilled from the back to within 1/8" of the concave surface (Photograph #3). Holes are also provided which will permit insertion of thermocouples to measure the temperature on both sides of the gap as well as at different points near the surface of the main heater.

The main body of the calorimeter is affixed to a bronze tube which is attached to a brass flange. This flange incorporates an 8 bolt-hole circle to permit the attachment of the complete unit to the glass "T".

## POWER DENSITY

Superficially, the maximum heat flux available from the main heater can be determined by dividing the maximum input power (5*450=2250W.) by the surface area of the main heater (6.12 sq.in. = 0.00395 sq.m.). This calculation yeilds a value of 570,000 W/sq.m.. In reality the power input must be set lower than the maximum value. The guard heater has a larger surface area and this is only partially compensated for by the greater number of heater elements in the guard section. Since the maximum power input to the guard is limited the main heater input may have to be reduced to minimize heat loss from the main section in the radial direction. Some of the energy input to the heaters is also lost out the back of the unit. As long as the liquid side heat transfer coefficient is substantially greater than the air side convection coefficient this loss should remain small. If the critical heat flux, on the liquid side, is exceeded this condition may be violated and damage to the unit may result.

## TEMPERATURE PROBE

Information on the temperature profile within the fluid was to be sought in subsequent experiments, and a temperature probe was fabricated to facilitate this.

The probe consists of a 3/8" dia. stainless steel tube with a bar affixed to one end. Thermocouples can be attached to the bar, their leads run through the centre of the tube and an epoxy seal. The tube is passed through a sealing gland in the acrylic plate. This gland is located on the axis of the pipe. It is constructed so as to permit rotation and translation of the tube without violating the seal. Thus one can position the tcpls. anywhere in the tank at any time during the test (Photograph #4).

Previous experience suggested that the acrylic sheet was prone to early failure when subjected to stress by tapered (pipe) threads. For this reason, the sealing gland incorporates straight threads and an "O"-ring seal to the acrylic sheet. This design was found to work well.

The epoxy seal in the S.S. tube was found to leak during tests with water (@ 130 C.). Metal filled epoxy was subsequently used on another apparatus (guarded hot plate) with good success. This material may give better results in subsequent work with the temperature probe.

## FABRICATION

Working drawings were prepared and the calorimeter was fabricated in the U.N.B. Engineering Faculty Shop. The calorimeter body, tube and flange were affixed to one another using silver solder.

The heaters were installed, in the heat transfer laboratory, using a soft solder paste. No tcpls. were installed.

The temperature probe and seal were fabricated by the author in the Mech. Engrg. Machine Shop.

## TESTING

The completed unit was assembled. Only one tcpl. was installed on the temperature probe and this was connected to a Fluke digital tcpl. meter. The 5 main heater elements were wired in parallel and connected to 2 - 120V. autotransformers (Photograph #5). The unit was filled with water for the tests, to reduce the hazard of exposure to toxic chemicals. The apparatus was situated so that the axis of the calorimeter was approximately 25 deg. below horizontal. The power was applied to the main heater and observations were made.

Flow inside the tank was made visible by the refractions introduced by the density gradients. This indicated the presence of a stratified layer, and the tcpl. readings confirmed that this layer was substantially warmer than the fluid below (approx. 11 C. temp. diff., Photograph #6,#7). This layer gradually grew in thickness until the entire contents of the tank demonstrated a profound anticlockwise motion (Fig. #2).

The high temperature stratified layer is also indicated by rapid venting of the tank through the relief valve. Once the pressure is lowered boiling occurs throughout the high temperature region, while the cool region remains relatively undisturbed (Photographs #8-#13).

The acrylic sheet which had the temperature probe installed in it eventually failed. A crack developed on the cold side of the sheet extending from the centre to the outside edge. If subsequent tests are to be done at similar temperatures some measures will have to be taken to re-enforce the plate (Photographs #14,15).

## CONCLUSIONS

The curved surface calorimeter was designed, constructed and initial testing was performed. These tests indicate that the apparatus should perform adequately.

| SURFACE | FORMULA | PARAMETERS | RESULT | ERROR |
|---|---|---|---|---|
| INTEGRAL | [7] | Rs=2",R1=3" | 13.41 | 0 |
| CIRCLE | $\pi$ Rs^2 | Rs=2" | 12.57 | -6.3 |
| ELLIPSE | $\frac{\pi \text{S1 Ss}}{4}$ | S1=4.38",Ss=4" | 13.76 | 2.6 |
| | | inches | sq. in. | % |

TABLE # 1

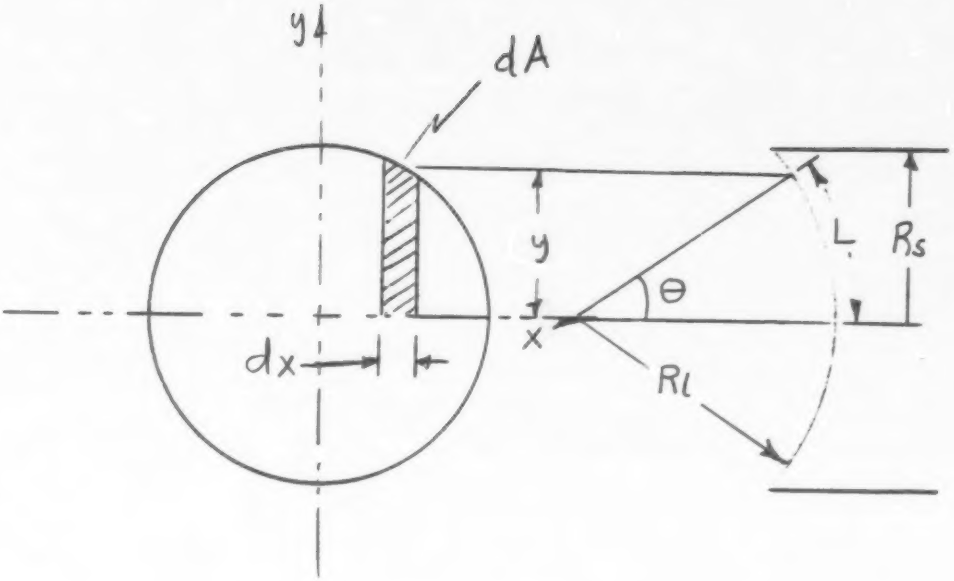
y
dA
y
θ
x
L
$R_s$
$R_l$
dx

FIGURE #1

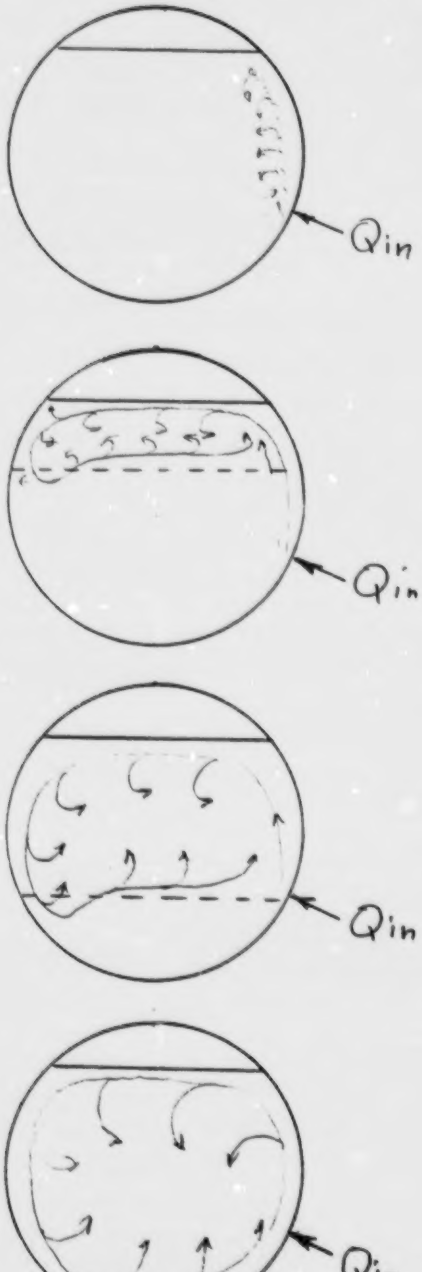
Qin
Qin
Qin
Qin

FIGURE #2

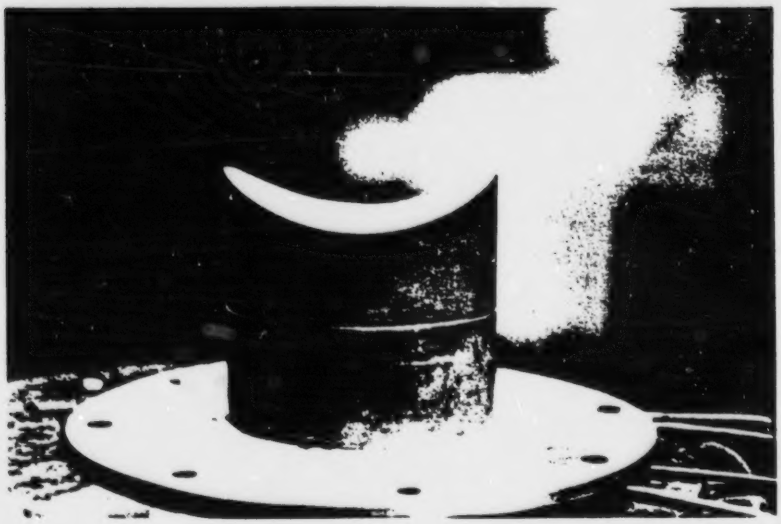

PHOTOGRAPH # 1

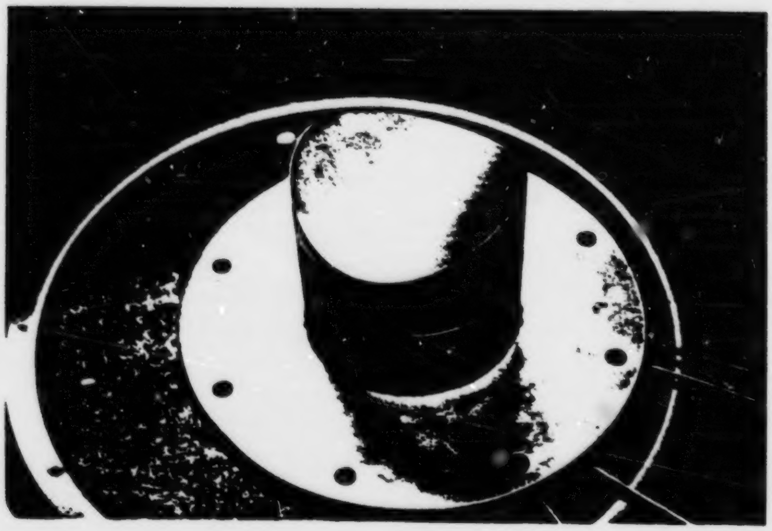

PHOTOGRAPH # 2

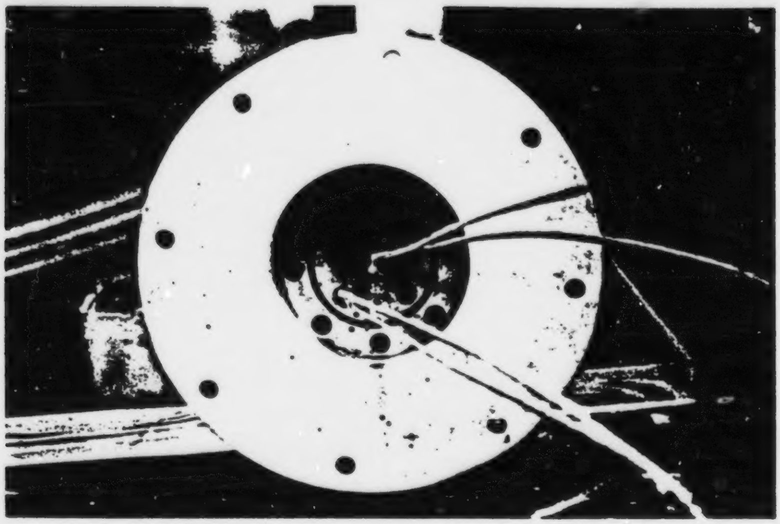

PHOTOGRAPH # 3

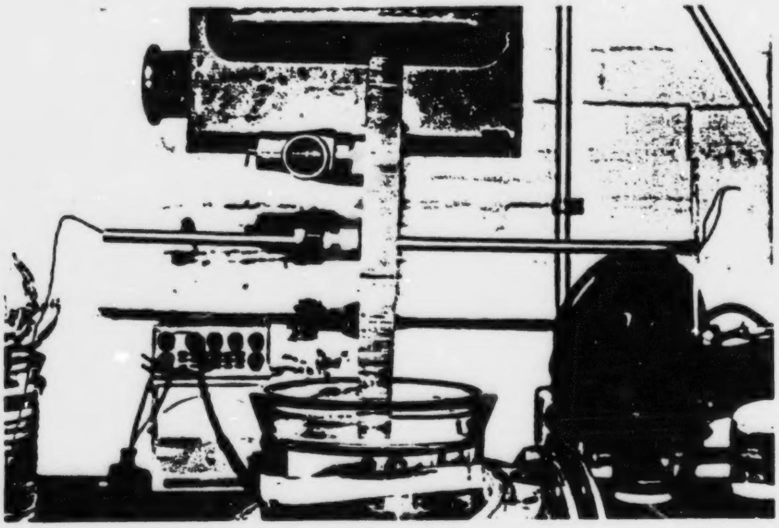

PHOTOGRAPH # 4

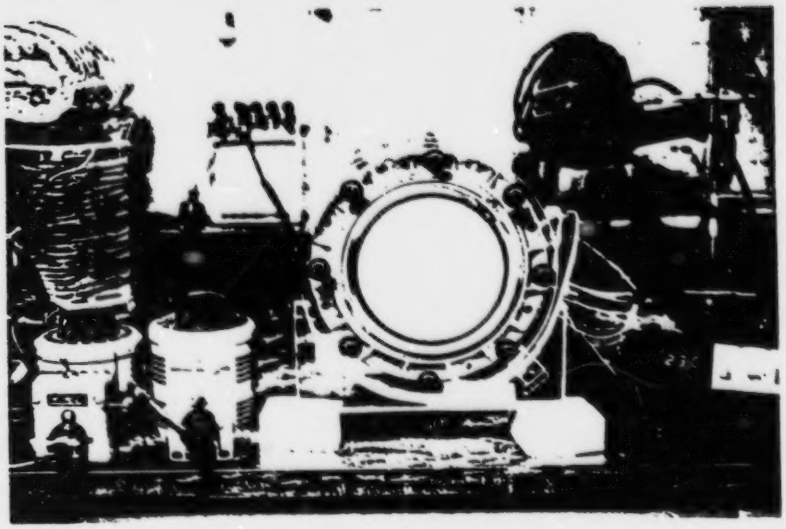

PHOTOGRAPH # 5

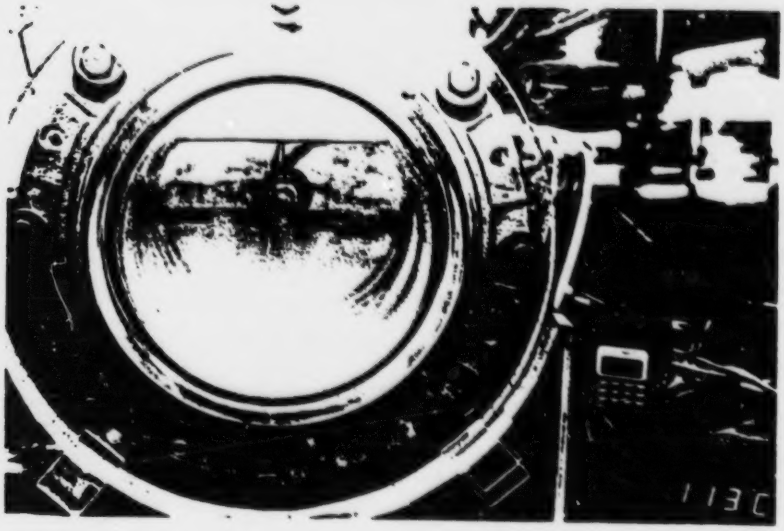

PHOTOGRAPH # 6

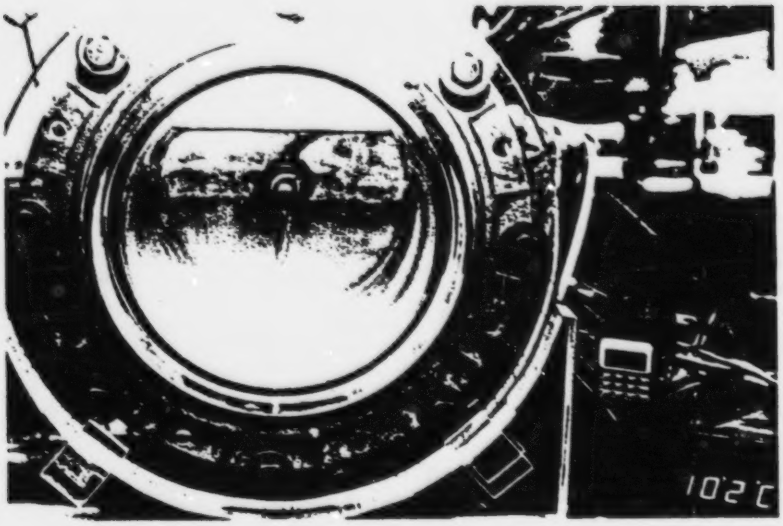

PHOTOGRAPH # 7

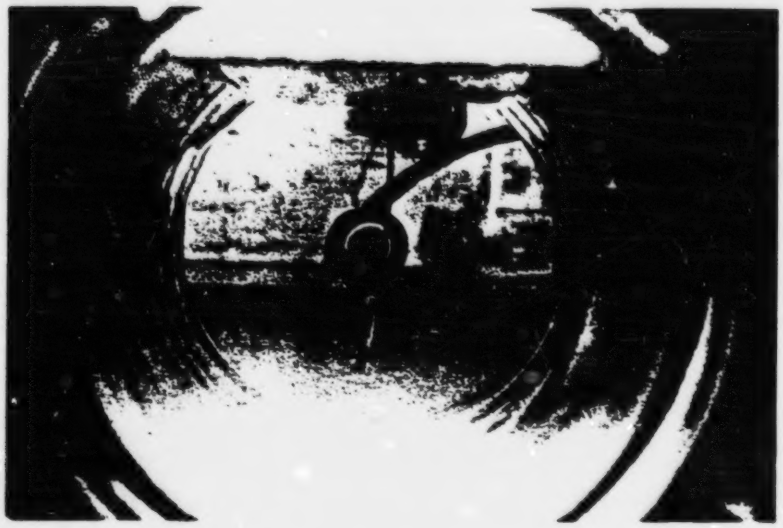

PHOTOGRAPH # 8

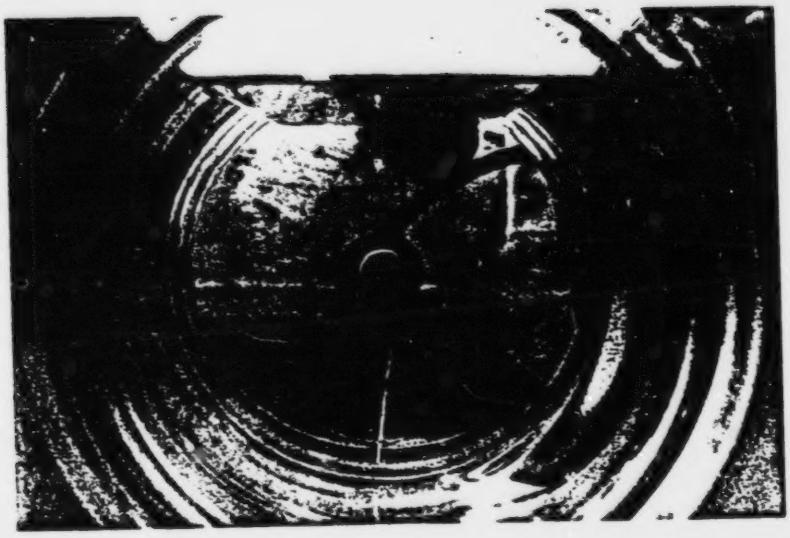

PHOTOGRAPH # 9

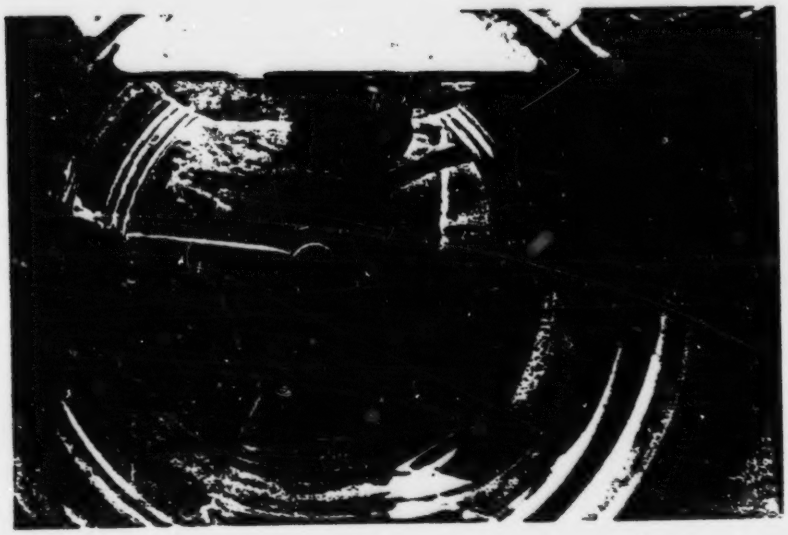

PHOTOGRAPH # 10

PHOTOGRAPH # 11

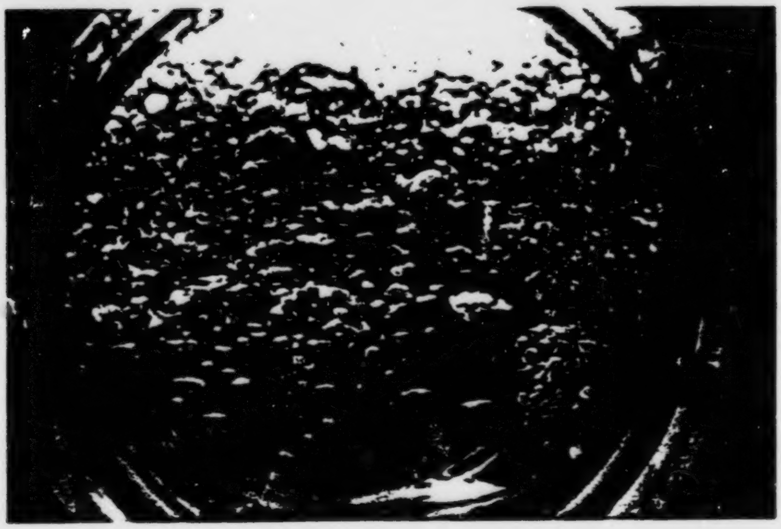

PHOTOGRAPH # 12

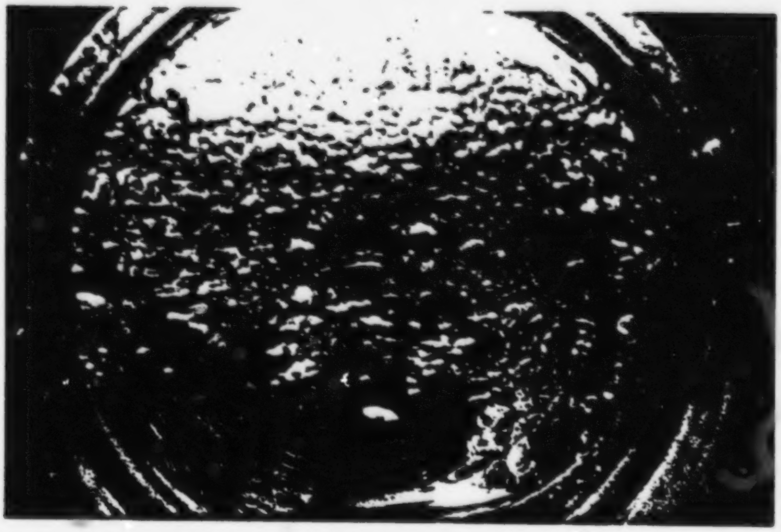

PHOTOGRAPH # 13

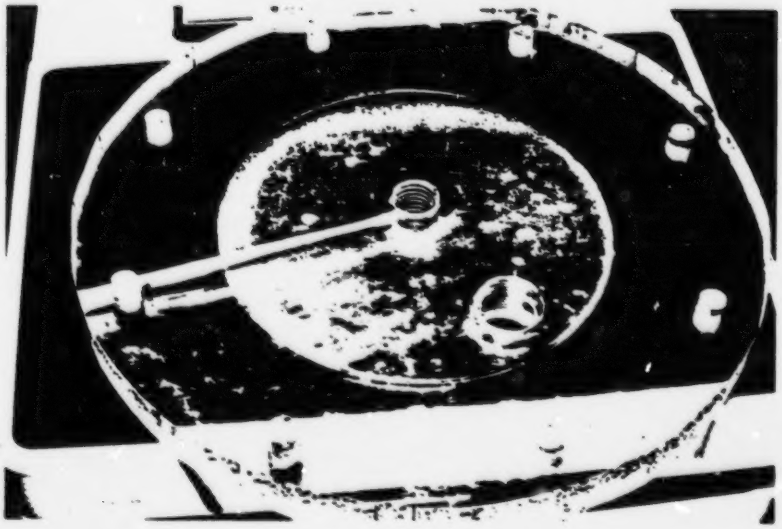

PHOTOGRAPH # 14

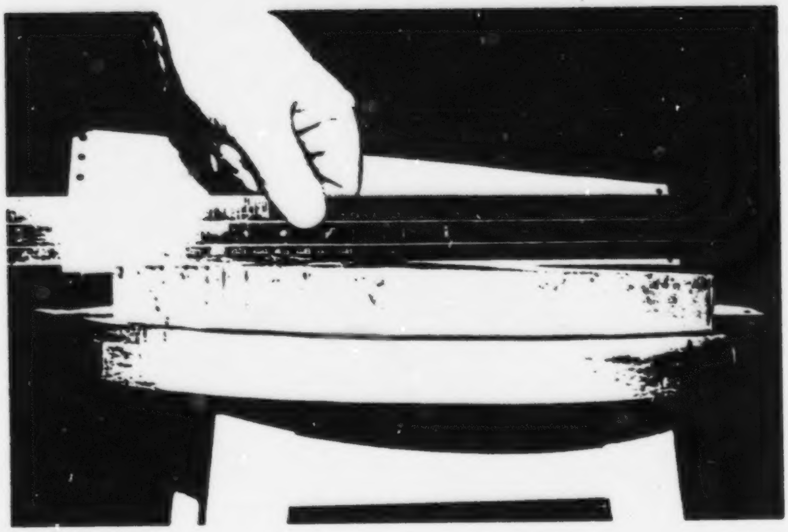

PHOTOGRAPH # 15

# APPENDIX # 1

Paul Wentzell
Aug. 26/82.

# Flare Vessel
## (Some considerations)

## Flare Vessel:

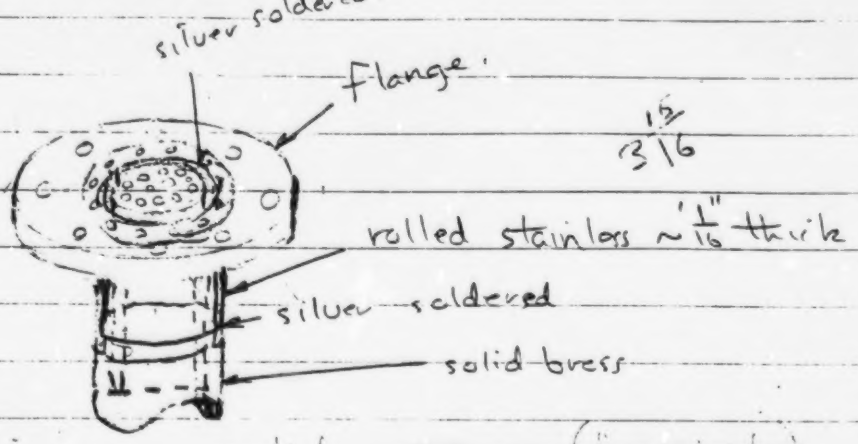
silver soldered.
flange.
3 15/16
rolled stainless ~1/16" thick
silver soldered
solid brass

~~Inner cylinder = solid copper~~ [illegible]

~~Outer cylinder [illegible] copper~~ [illegible]

~~Flange = disc of copper.~~

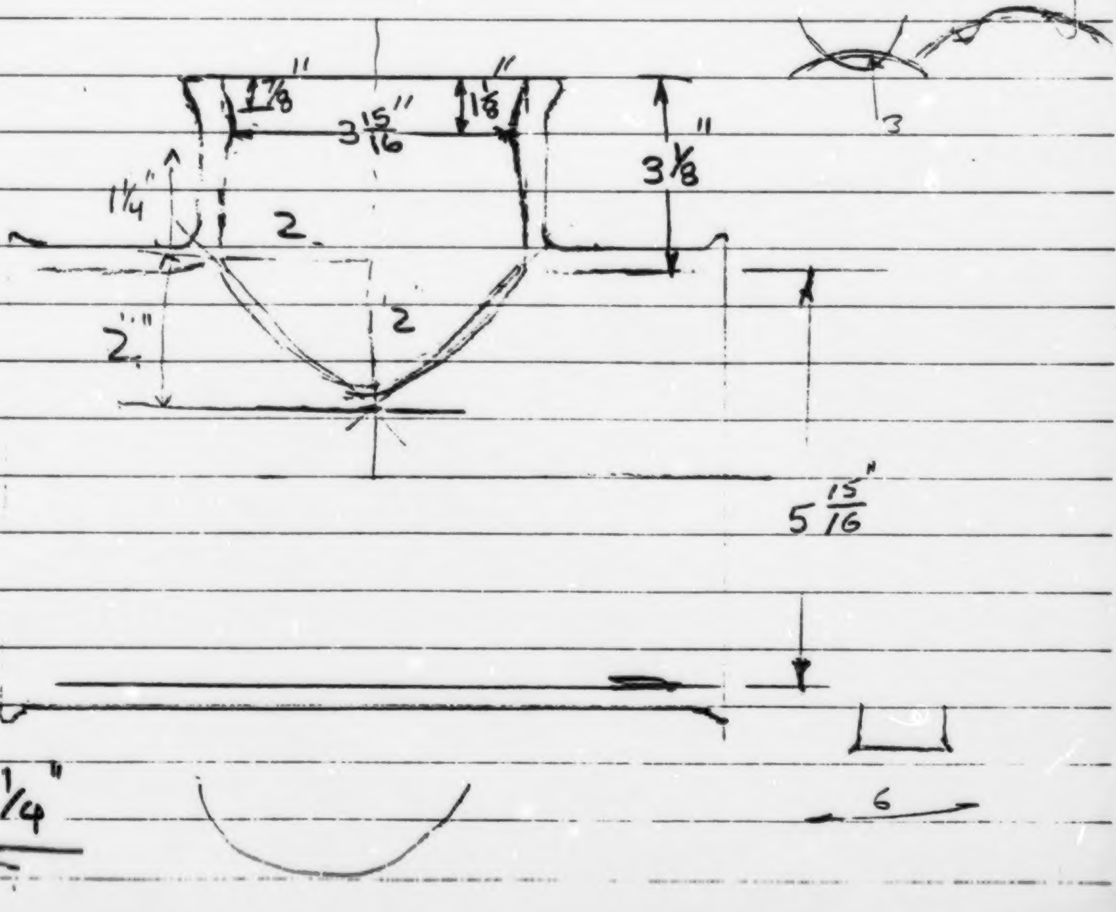
1/8"
1 1/8"
3 15/16"
3 1/8"
1 1/4"
2
2
2"
3
5 15/16"
6

4"φ x 3 1/4"

# Area of the Saddle on 'Tee' Section

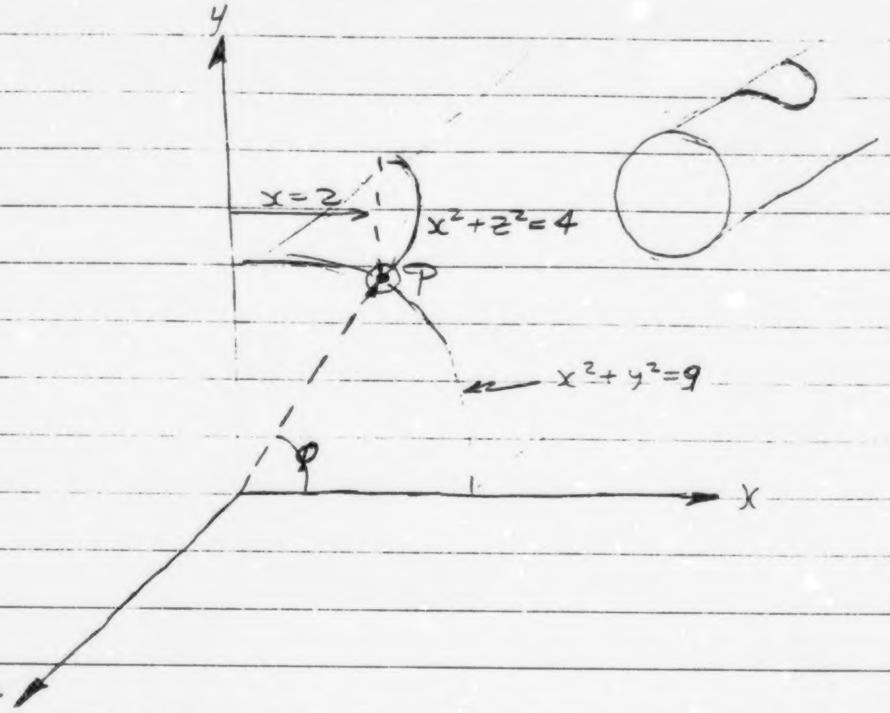

P: $x^2 = 4 - z^2$

$@ z=0 \qquad x^2 + 0 = 4 \Rightarrow x = 2$

$\therefore x^2+y^2=9 \Rightarrow y^2 = 5 \rightarrow y = \sqrt{5}$

$\boxed{P\ (2, \sqrt{5})}$

$\Phi = \tan^{-1}\left(\frac{\sqrt{5}}{2}\right) = 0.8411$ rad.

Circumference of $x^2+y^2=9 = 2\pi(3'') = 18.85$ in.

Ellipse major axis $= \frac{0.841}{\cancel{2}\pi}(18.85) \times \cancel{2} = 5.046$

Ellipse minor axis $= 4$

$\therefore$ Area of saddle $= \frac{\pi}{4} a b = \frac{\pi}{\cancel{4}}(5.046)\cancel{4} = \boxed{15.85 \text{ in}^2}$

Flange - Yellow brass plate - $8\frac{1}{2} \times 8\frac{1}{2} \times \frac{1}{4}$
- in Heat transfer lab.

Neck leading to heaters - Stainless Steel rolled sheet metal (lapped

Heating plate - solid brass to be acquired from L+A

Must acquire more heating elements (24) ie 2 dozen.

Very little work has been done on this vessel but the machining can be done either in the machine shop or the Faculty shop.

→ Faculty shop has a 6" diam milling tool for 3-D cutting.

One O-ring will be used ~~&~~ on the flange of the heater.

# APPENDIX # 2

```
****************************************************************************************************************FABLE***
       $JOB WATFIV SOLLOWS/U,PAGES=10
       C
       C   PROGRAM TO EVALUATE AREA OF CYLINDERICAL SURFACE CALORIMETER
       C
             EXTERNAL FUNC
             REAL A,B,TOL,ABSERR,ERREST,FLAG,AREA
             INTEGER NOFUN
             COMMON B
       C
             TOL=0.001
             A=0.0
       C
             DO 99 I=1,20
       C
       C   CALCULATE UPER LIMIT
       C
                B=FLOAT(I)/10.
       C
             ABSERR=0.0
             AREA=0.0
             CALL QANC8S(FUNC,A,B,ABSERR,TOL,AREA,ERREST,NOFUN,FLAG)
       C
             AREA = 12*AREA
       C
       C
             PRINT 1,B,AREA,ERREST
       1     FORMAT(' ',' B= ',F4.1,10X,'AREA= ',F7.2,10X,'ERREST= ',F5.3)
       C
             IF(FLAG.NE.0.0) PRINT,'**** ERROR **** FLAG = ',FLAG
       C
       99    CONTINUE
             STOP
             END
       C
       C
             REAL FUNCTION FUNC(X)
             REAL X,Y
             COMMON B
             Y=(SQRT(B*B-X*X))/3.
             FUNC=ARSIN(Y)
             RETURN
             END
       $ENTRY
=  0.1          AREA=     0.03          ERREST= 0.000
=  0.2          AREA=     0.13          ERREST= 0.000
=  0.3          AREA=     0.28          ERREST= 0.000
=  0.4          AREA=     0.50          ERREST= 0.000
=  0.5          AREA=     0.79          ERREST= 0.000
=  0.6          AREA=     1.14          ERREST= 0.000
=  0.7          AREA=     1.55          ERREST= 0.000
=  0.8          AREA=     2.03          ERREST= 0.000
=  0.9          AREA=     2.57          ERREST= 0.000
=  1.0          AREA=     3.19          ERREST= 0.000
=  1.1          AREA=     3.87          ERREST= 0.000
=  1.2          AREA=     4.62          ERREST= 0.000
=  1.3          AREA=     5.44          ERREST= 0.000
=  1.4          AREA=     6.34          ERREST= 0.000
```

```
 1.5          AREA=     7.31        ERREST= 0.000
 1.6          AREA=     8.36        ERREST= 0.000
 1.7          AREA=     9.49        ERREST= 0.000
 1.8          AREA=    10.71        ERREST= 0.000
 1.9          AREA=    12.01        ERREST= 0.000
 2.0          AREA=    13.41        ERREST= 0.000
TEMENTS EXECUTED=     7583
E USAGE       OBJECT CODE=     5184 BYTES,ARRAY AREA=    2184 BYTES,TOTAL AREA AVAILABLE=   102400  BYTES
GNOSTICS        NUMBER OF ERRORS=       0, NUMBER OF WARNINGS=        0, NUMBER OF EXTENSIONS=        0
PILE TIME=      0.09 SEC,EXECUTION TIME=      0.20 SEC,      8.47.41    FRIDAY       15 OCT 82    WATFIV - MA
```

THE UNIVERSITY OF NEW BRUNSWICK

# REPORT ON SIGNIFICANCE OF FLARE RADIATION ON RAILWAY CAR CONTINING LPG

J.W. Reid and R. Prasad

The basic equation to be used in calculating the radiation effect of the flare is $q = \frac{fQ}{4\pi x^2}$ [1] [2] [3]

f = factor of heat from a flame which is dissipated as radiation

Q = heat released in combustion, which is the lower heating value multiplied by the mass flowrate.
Lower heating value for propane is 46353 $\frac{kJ}{kg}$ [4]

x = the distance from the radiation center of the flame to the point of interest.

For all the following calculations, the results will be based on a tank contents pressure of 2000 kPa, tank contents temperature of 350 K, and pure vapour flow through a 1/5 scale model of the rail car (unless otherwise specified). The PRV used on the 1/5 scale tests was the REGO 75836 valve.

The value of the factor f is shown to be approximately 0.15 by Brzustowski [13], [14].
Note that this vlaue for the factor also appears accurate for crosswinds [13], [14].

For the above analysis, the height of the flame is required to locate the radiation center. This can be obtained by methods outlined by Steward [6] or Brzustowski [7], [8].

From Steward, $\frac{H}{R} \times \left[\frac{1-\omega}{(r + \omega/\rho_0')\rho_0'^{\frac{1}{2}}}\right] = 27.4$ [6]

H = height of flare
R = radius of base of flare
r = mass ratio of air to fuel in combustion
$\rho_0' = \frac{\rho_0}{\rho_a}$ where $\rho_a$ is atmosphere density, and $\rho_0$ is density of propane at beginning of flare.
$\omega$ = inverse volumetric expansion ratio due to combustion
27.4 is an experimentally developed constant for propane.

To evaluate these variables:

for r,

$$C_3H_8 + 5(O_2 + 3.79 N_2) \Rightarrow 3CO_2 + 4H_2O + 18.95 N_2$$

$$r = \frac{m_a}{m_f} = \frac{5(32 + 3.79 \times 28)}{3(12) + 8} = 15.695 \frac{g\ \text{AIR}}{g\ \text{FUEL}}$$

$\omega$ can be expressed as

$$\omega = \frac{1}{1 + \left(\frac{Q_c}{r C_p T_a}\right)}$$

$C_p$ = specific heat of air = 1.0035 $\frac{kJ}{kgK}$ [4]

$T_a$ = ambient temperature = 300K

$Q_c$ = lower heating value for propane = 46353 $\frac{kJ}{kg}$ [4]

r = mass ratio of air to fuel = 15.695 as shown above.

Hence $$\omega = \frac{1}{1 + \frac{46353}{15.695 \times 1.0035 \times 300}} = 0.0925$$

for $\rho_o'$, $\rho_o' = \frac{\rho_o}{\rho_a}$

For $\rho_a$, the density of air was evaluated at 1 atm and 300K as 1.2 kg/$m^3$. [9]

For $\rho_o$, the density of fuel, this is to be evaluated at the beginning of the flare (or exit of nozzle), at atmospheric density (e.g. after the crash). This is shown in Figure 2.

Figure 2: Sketch of nozzle pressure vs distance variation.

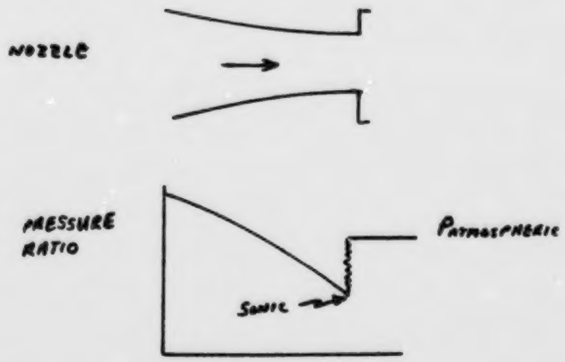

The density $\rho_o$ may be evaluated by considering the expansion through the nozzle to be a constant enthalpy process, as shown in Figure 3.

Figure 3: Sketch of a pressure enthalpy diagram for propane

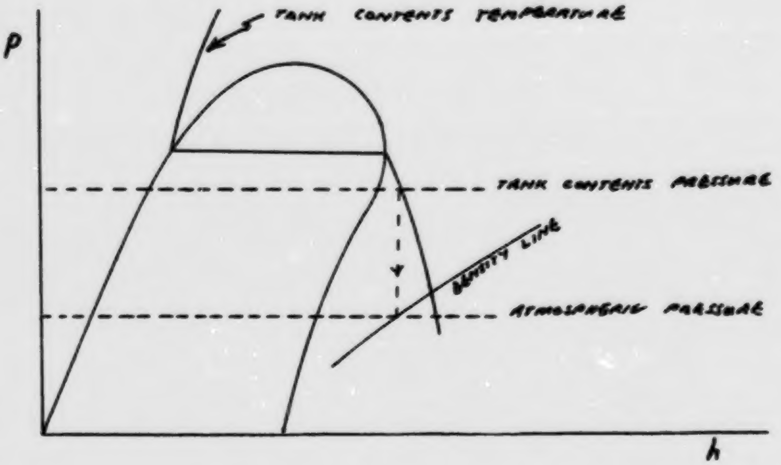

With tank conditions of T = 350 K and P = 2000 kPa, a constant enthalpy expansion to 0.1 MPa yields a fuel density of 1.76 kg/m$^3$. The pressure enthalpy chart used was from reference [10].

Hence $\rho_o' = \frac{\rho_o}{\rho_a} = \frac{1.76}{1.2} = 1.47$

Therefore $\frac{H}{R} \times \frac{1-\omega}{(r+\omega/\rho_o')\rho_o'^{\frac{1}{2}}} = 27.4$

$$\frac{H}{R} \times \frac{1-0.0925}{(15.695+\frac{0.0925}{1.47})1.47^{\frac{1}{2}}} = 27.4$$

$\therefore \frac{H}{R} = 576.85$

For the 1/5 scale model tests, the value used had an effective diameter at the tip of approximately 4 cm, yielding a calculated flame height of 11.54 m. Note however that the proposed model assumes turbulent mixing instantaneously, and consequently neglects the blow off distance associated with high speed fuel jets. This blows off distance is formed when the speed of the existing fluid is greater than 0.2 M. This is caused because the fluid is flowing too fast to allow stable combustion. [1], [2], [3].

Kent proposes the following method of calculating the blow off distance, "$a$".

$$\frac{U_m}{U_0} \times \frac{a}{D} = 6.4$$ [1],[3],[17]

and $\frac{\pi}{4} U_m = U_a = 0.2M$ ; where $U_m$ is maximum velocity at "$a$" and $U_a$ is average velocity at "$a$". Hence with $U_0$ = sonic velocity, and D = diameter = 0.04 m for the 1/5 scale model tests;

$$\frac{4}{\pi} \times \frac{U_a}{U_0} \times \frac{a}{D} = 6.4$$

$$\frac{4}{\pi} \times \frac{0.2}{1} \times \frac{a}{0.04} = 6.4$$

$$\therefore \quad a = 1.0\ m$$

Hence for the total height of flame, the flare length should be added to the separation distance.

Total height = $H + a = 11.54 + 1.0 = 12.54\ m$

Brzustowski proposes several methods for calculating the flame height.

From reference [8],[16]

Hawthorne Method

For a turbulent diffusion flame.

$$\frac{L}{d_j} = \frac{5.3}{C_T}\left\{\frac{T_F}{\alpha_T T_j}\left[C_T + (1-C_T)\frac{M_a}{M_f}\right]\right\}^{\frac{1}{2}}$$ [8], [16]

For $C_3H_8$

$C_T = 0.038$ [8]

$d_T = 0.96$ [8]

$T_F/T_S = 7.6$ [8]

$M = 28.9$ [8]

$M_f = 44.1$ [8]

$$\therefore \quad \frac{L}{d_j} = \frac{5.3}{0.038}\left\{\frac{7.6}{0.96}\left[0.038 + (1-0.038)\frac{28.9}{44.1}\right]\right\}^{\frac{1}{2}}$$

$$\therefore \frac{L}{d_j} = 325$$

∴ for a jet diameter of 0.04 m,
length of flare = 13.0 m

Brzustowski Method I

In the same paper, a simplified equation is given for hydro carbon gases as

$$\frac{L}{d_j} = \frac{15}{C_r}\left(\frac{M_c}{M_f}\right)^{\frac{1}{2}} = \frac{15}{0.038}\left(\frac{28.9}{44.1}\right)^{\frac{1}{2}} = 319.5 \qquad [8]$$

hence for jet diameter of 0.04m, flare length is 12.8 m.

Brzustowski Method II

An alternate solution is also given in reference [8]

as $$\frac{L}{d_j} = \frac{10.5}{C_L}\left(\frac{M_a}{M_f}\right)^{\frac{1}{2}} \qquad [8]$$

and $$\frac{1}{C_L} = 45.5 \qquad [8]$$

hence $$\frac{L}{d_j} = 10.5 \times 45.5\left(\frac{28.9}{44.1}\right)^{\frac{1}{2}} = 386.75$$

Therefore, for a jet diameter of 0.04m,

length of flare = 15.48 m.

Brzustowski Method III

From reference [7], Brzustowski proposes the following model, which includes the effect of a wind.

Using an arbitrary wind velocity of 10 $\frac{\text{km}}{\text{Hr}}$

Calculate $\bar{C_L}$

$$\bar{C_L} = C_L\left(\frac{u_j}{u_\infty}\right)\left(\frac{\bar{m}_j}{\bar{m}_\infty}\right) \qquad [7]$$

$\frac{\bar{m}_j}{\bar{m}_\infty}$ = ratio of molecular weight fuel to molecular weight air
$u_j$ = jet velocity. For sonic condition of tank

contents at 2000 kPa and 350K, $u_j = 220 \text{ m/s}$

From reference [8] $\frac{1}{C_L} = 45.5$

Therefore $\frac{u_j}{u_\infty} = \frac{220}{2.8}$

Hence $\bar{C}_L = \frac{1}{45.5}\left(\frac{220}{2.8}\right)\left(\frac{44.1}{28.9}\right) = 2.64 > 0.5$

Since $\bar{C}_L > 0.5$,

Calculate $\bar{S}_L$ using

$$\bar{S}_L = 2.51\,(\bar{C}_L)^{-0.625} = 1.37 \qquad [7]$$

From Figure 9 on page 136 of reference [7], $\bar{X}_L = 0.20$

Calculate $\bar{Z}_L$

$$\bar{Z}_L = 2.05\,\bar{X}_L^{\,0.28} = 2.05(0.20)^{0.28} = 1.31$$

Calculate R

$$R = \frac{\rho_j u_j^2}{\rho_\infty u_\infty^2} = \frac{5.75(220)^2}{1.2\,(2.8)^2} = 29.58 \times 10^3$$

Now, using a jet diameter of 0.04 m, calculate $X_L$ and $Z_L$ as

$$Z_L = \bar{Z}_L \times d_j \times R^{\frac{1}{2}} = 1.39 \times 0.04 \times (29.58 \times 10^3)^{\frac{1}{2}} = 9.02 \text{ m} \qquad [7]$$

$$X_L = \bar{X}_L \times d_j \times R^{\frac{1}{2}} = 0.20 \times 0.04 \times (29.58 \times 10^3)^{\frac{1}{2}} = 1.38 \text{ m} \qquad [7]$$

The physical significance of $X_l$ and $Z_l$ is shown below.

Figure 4: Sketch defining the quantities $X_l$ and $Z_l$

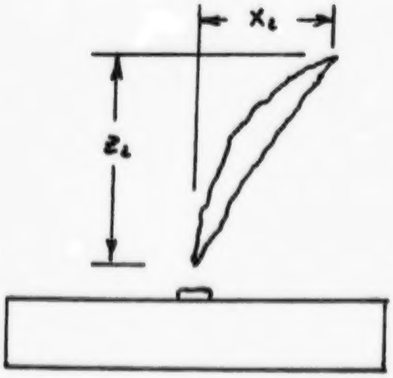

In all the models proposed by Brzustowski, the separation distance as calculated by Kent should be added to the flame length to get the total flame height.

The radiation from the flame may now be calculated for the various calculated lengths by the following procedure.

For the calculation of heat radiating on point of interest, the distance from the radiation center to the point of interest must be calculated. This can be easily done if we assume radiation center of flame is at half its length, as shown in Figure 5.

Figure 5: Geometry of flame with respect to tank surface.

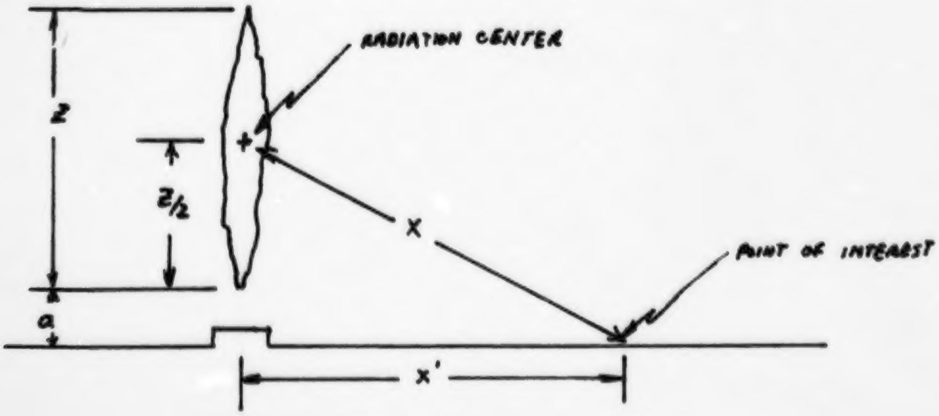

$$\therefore \; x = \sqrt{(x')^2 + (Z/2 + a)^2}$$

The heat flux calculated at a distance $x'$ from the center is expressed per unit area, where the area is normal to the line from the radiation center to the point of interest. Hence the heat flux must be corrected since the rail car surface is not normal to the radiating ray. This can be done as illustrated in Figure 6.

Figure 6: Geometry consideration on Radiation from Flame

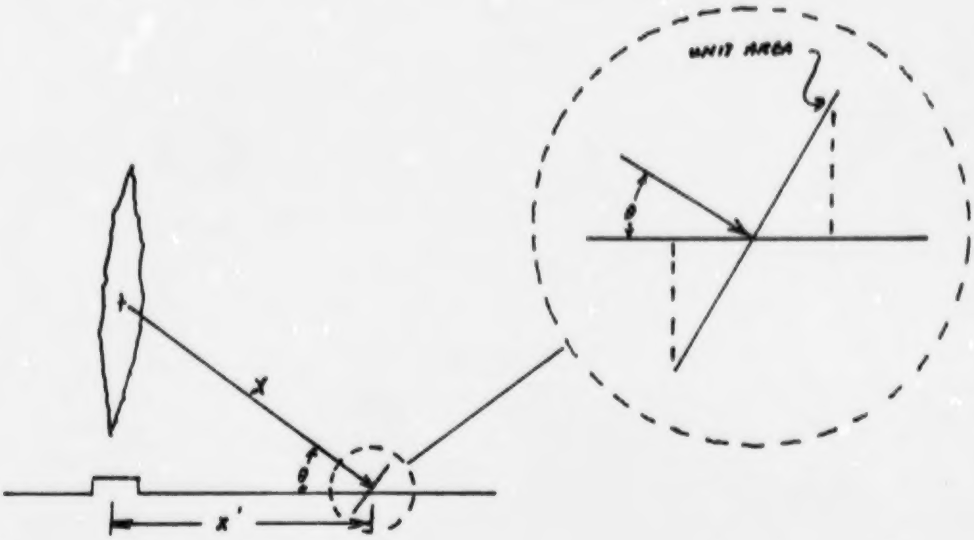

The correction is a multiflication factor of $\sin\theta$

Using Stewards result of flame length of 10.54 m and a separation distance of 1 m, for the area directly beneath the flame, $x' = 0$

$$\therefore x = \frac{Z}{2} + a = \frac{11.54}{2} + 1.0 = 6.77\,m$$

For the area at the far end of the tank car, $x' = 2.2\,m$

$$\therefore x = \sqrt{2.2^2 + 6.77^2} = 7.12\,m \text{ AND } \sin\theta = 0.95$$

For a mess flowrate of 1 kg/sec in the 1/5 scale test, at center

$$q_{MAX} = \frac{fQ}{4\pi x^2} = \frac{0.15 \times 46353 \times 1}{4\pi \times 6.77^2} = 12.07\ KW/m^2$$

at the end

$$q_{MIN} = \frac{fQ}{4\pi x^2} \times \frac{1}{\sin\theta} = \frac{0.15 \times 46353 \times 1}{4\pi \times 7.12^2} \times 0.75 = 10.36\ KW/m^2$$

For the other four flame lengths, the results are tabulated in Table 1.

Table 1: Results of Radiation analysis

| Method | Ref. | Flame Length* (m) | Heat Flux $(KW/M^2)$ | |
|---|---|---|---|---|
| | | | $q^{MAX}_{CENTER}$ | $q^{MIN}_{END}$ |
| Steward | 5 | 11.54 | 12.07 | 10.36 |
| Hawthorne | 8 | 13.0 | 9.84 | 8.60 |
| Brzustowski I | 8 | 12.8 | 10.10 | 8.81 |
| Brzustowski II | 8 | 15.48 | 7.24 | 6.50 |
| Brzustowski III | 7 | 9.02 | 18.22 | 14.93 |

*This does not include the separation blow off distance of 1m.

The result of the flame length appears to be fairly good as the observed length in the actual testing was in the order of 15 m.[6]

The pool heat flux in the 1/5 scale tests was an average of intensity 50 kw/m$^2$[6]. This indicates that the radiation from the flame was from 15% to 35% (depending upon the flame height) of the radiation from the pool fire. The effect of the flame radiation was also evident from the final results of the 1/5 scale tests. The analysis of Brzustowski (7) predicts only a small deflection of the tip of the flame for wind velocities of 10-30 $\frac{KM}{HR}$ which does not affect the intensity of the maximum flame radiation, however the wind does affect the location of the flame radiation.

The tank surface directly under the flame and extending slightly in the east will be subjected to the maximum radiation in test #1, 2, and 3 for the prevailing cross-wind direction (Figure 7).

In test #1 (BASELINE), it was observed (Figure 26 of Ref. (6)) that the failure began with a thermal rupture at the top dead centre. Also, in Test #3 (HOWLER) (Figure 28A, 28B of Ref. (6)), the tank bulged on the upper portion of the far east end. These are apparently due to increased radiation from the flare. This is further substantiated by Figure-44A in Ref. (6) which shows the melting of the EXPLOSAFE in this region.

In test #4 (NOVA), it was reported (6) that the temperature of the surface facing north was higher than that facing south (6) evidently due to the radiation from the flare deflected towards north by the cross-wind (Fig. 7). The failure of the EXPLOSAFEin the region (Figure 45A of Ref. (6)) can also be seen.

Figure 7: Direction of cross wind in 1/5 scale tests (6)

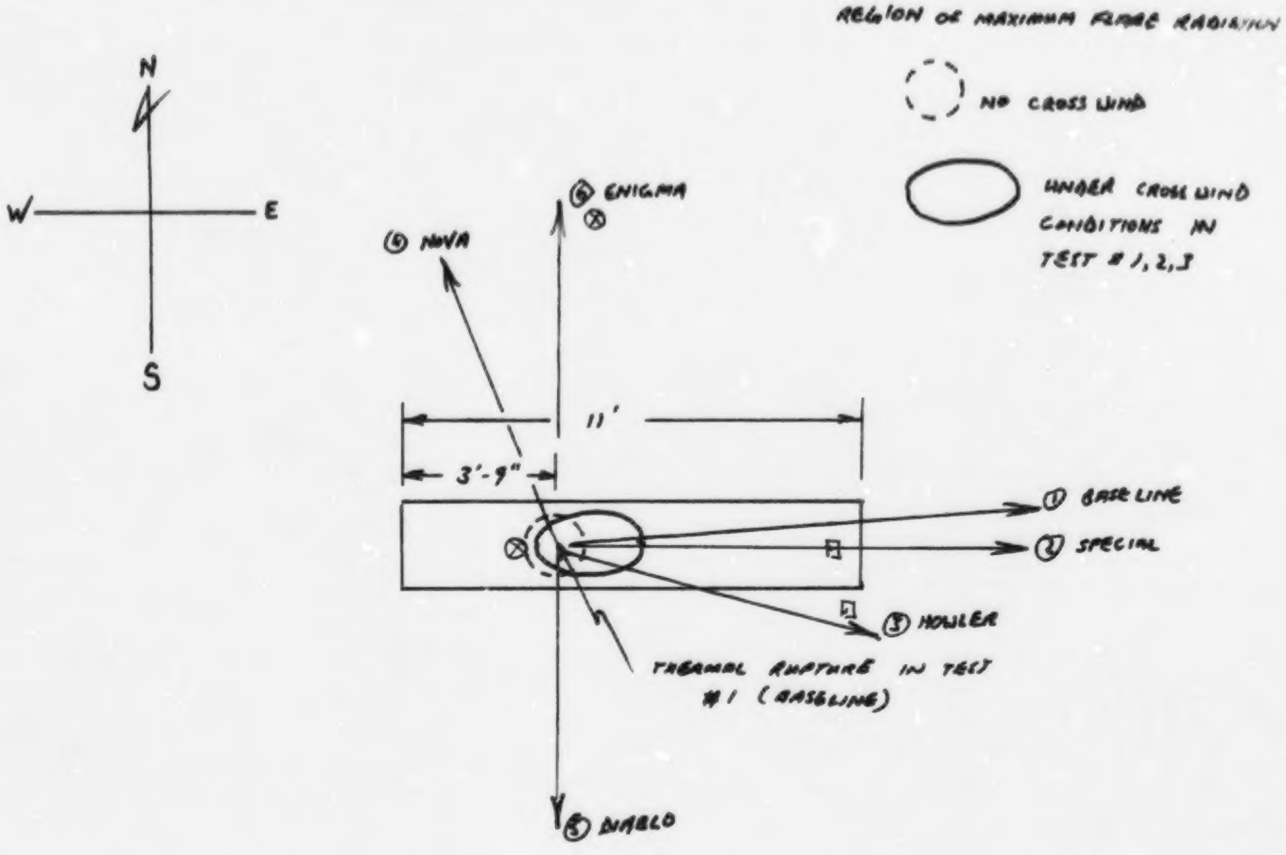
REGION OF MAXIMUM FLARE RADIATION
NO CROSS WIND
UNDER CROSS WIND CONDITIONS IN TEST # 1,2,3
N
W
E
S
⑥ ENIGMA
④ NOVA
11'
3'-9"
① BASE LINE
② SPECIAL
③ HOWLER
THERMAL RUPTURE IN TEST #1 (BASELINE)
⑤ DIABLO

| Test # | Wind direction CLKW from North, Towards the centre | Wind Velocity | | Outside Amb. Temperature | Code Names of Tests |
|---|---|---|---|---|---|
| | degrees | KM/Hr | m/SEC | °C | |
| 1 | 260-270 | 12.0 | 3.33 | 0 | BASELINE |
| 2 | 270 | 9.7 | 2.69 | -22 | DRES SPECIAL |
| 3 | 300 | 11.3 | 3.14 | -7 | HOWLER |
| 4 | 150 | 4.0 | 1.11 | -2 | NOVA |
| 5 | 360 | 14.0 | 3.89 | -3 | DIABLO |
| 6 | 170 | 3.22 | 0.89 | 0 | ENIGMA |

In test #6 (ENIGMA), the tank ruptured at the top surface to the left of the valve location. This is the region subjected to the maximum flare radiation under the cross-wind conditions (Figure 7).

Conclusion:

The present calculations indicate a maximum flare radiation of about 15 KW/M$^2$ in case of the 1/5 scale tests (6). This is over 30 percent of the heat flux form of the pool fire employed in these tests. It is suspected that the flare radiation will be significantly higher due to a higher mass flow rate of propane in case of liquid flowing through the PRV.

The exit area of the PRV in the full scale rail cars is approximately four times that of the 1/5 scale model cars. This means that a flare four times longer than that observed on the 1/5 scale tests could be expected. This flare would therefore be 40 to 50 meters in length. Using the distance to the flare radiation center from the center of the car as 25m, and the mass flowrate as 40 kg/sec (15), the heat radiation from the flare can be shown to be 35.5 kW/m$^2$. On full scale tests, the heat flux from a pool fire has been measured as 105 kW/m$^2$ on average (15), indicating the radiation from the flare as 34% of the radiation from the pool fire.

As reported in the tests (6), the failure has consistently resulted at the top surface of the tank and in a region which is subjected to the maximum radiation from flare under the prevailing cross-wind direction.

# REFERENCES

(1) KENT, G.R., "Find Radiation Effect of Flares," Hydrocarbon Processing and Petrolium Refiner, Vol. 47, No. 6, June 1968.

(2) KENT, G.R., "Practical Design of Flare Stacks" Hydrocarbon Processing and Petrolium Refiner, Vol. 43, No. 8, August 1964.

(3) KOVACS, F., HONTI, G., "Secondary Heat Effect on LPG Storage Spheres in Cases of Fire," AICHE Symposium Series, No. 198, 1980.

(4) SONNTAG, R.E., VAN WYLEN, G., "Fundamentals of Classical Thermodynamics, 2nd Ed." John Wiley & Sons, New York, 1978.

(5) STEWARD, F.R., "Prediction of the Height of Turbulent Diffusion Boyant Flames," Combustion Science and Technology, Vol. 2, pp. 203-212, 1970.

(6) APPLEYARD, R.D., " Testing and Evaluation of the Explosafe System as a method of controlling the Boiling Liquid Expanding Vapour Explosion (BLEVE)," Vulcan Industrial Packaging Ltd., 1980.

(7) BRZUSTOWSKI, T.A., "Flaring in the Energy Industry," Prog. Energy Combust. Science Vol. 2, pp. 127-141, Pergaman Press, Great Britain, 1976.

(8) BRZUSTOWSKI, T.A., "A New Criterion for the Length of a Gaseous Turbulent Diffusion Flame," Combustion Science and Techology, Vol. 6, pp. 313-319, 1973.

(9) CRC Handbook, Appl. Eng. Science Table 1.18 p. 42.

(10) "LNG Materials and Fluids," Cryogenics Division, Institute for Basic Standards, National Bureau of Standards, Boulder, Colerado, 80302, 1977.

(11) STEWARD, F.R., "The Distribution of Radiation in a Horizontal Surface Surrounding a Uniformly Emitting Gray Gas Cone," 57 Annual Meeting, American Institute of Chemical Engineers, Boston, Mass. Dec. 6-10, 1966.

(12) SALLET, P.E. et al., "The Flow of Liquids and Gases Through Pressure Relief Valves," ASME PVP-33, presented at the Third National Congress on Pressure Vessels and Piping, Francisco, California, June 24-29, 1979.

(13) BRZUSTOWSKI, T.A., "Flares, Some Fundamentals and Design Considerations," from notes prepared for the seminar "Flare Systems," arranged by the Norwegian Society of Chartered Engineers, Stevanger, Norway, December 19-21, 1980.

(14) BRZUSTOWSKI, T.A., et al, "Radiant Heating from Flares," ASME Paper 75-HT-4, 1976.

(15) ANDERSON, C. et al., "The Effects of a Fire Environment on a Rail Car Filled with LPG," Ballistic Research Laboratories, prepared for Federal Railroad Administration, September 1974.

(16) VAN ELBE, L., "Combustion, Flames and Explosions of Gases 2nd Ed.", P. 486, Academic Press Inc., New York, 1961.

(17) FORSTALL, W., et al., "Momentum and Mass Transfer in a Submerged Water Jet," A.S.M.E. Transactions, Vol. 77, 1955.

# REPORT ON POOL FIRE EXPERIMENTS RELATED TO TANK CAR MODELLING

J.W. Reid

## TABLE OF CONTENTS

Page

ABSTRACT . . . . . . . . . . . . . . . . . . . . . . . . ii

LIST OF TABLES, FIGURES AND GRAPHS . . . . . . . . . . . 1

APPERATUS LIST . . . . . . . . . . . . . . . . . . . . . 1

PROCEDURE . . . . . . . . . . . . . . . . . . . . . . . 2

RESULTS . . . . . . . . . . . . . . . . . . . . . . . . 4

REFERENCES . . . . . . . . . . . . . . . . . . . . . . . 12

APPENDIX . . . . . . . . . . . . . . . . . . . . . . . . 13

CALCULATIONS . . . . . . . . . . . . . . . . . . . . . . 21

## ABSTRACT

The objective of these experiments was to obtain an estimate of the heat flux from a pool fire, find the dependance of diameter of the engulfed object on surface heat flux, and the axial temperature distribution of the pool fire. These results can be used to verify the heat flux in the 1/5 scale tests (1), which was deduced from the quantity of propane which was vented from the tank car over an interval of time, and the heat of vaperization for propane.

Page

## List of Tables

Table 1A: Results of 1" Diameter Calorimeter Test 1 4
Table 1B: Results of 1" Diameter Calorimeter Test 2 4
Table 2 : Results of 1/4" Diameter Calorimeter Test 2 5
Table 3 : Results of Suction Pyrometer Test 6

## List of Figures

Figure 1: Calorimeter used to determine heat flux, 1" diameter. 14
Figure 2: Calorimeter used to determine heat flux, 1/4" diameter. 15
Figure 3A: Diagram of Suction Pyrometer 16
Figure 3B: Photograph of Suction Pyrometer 17
Figure 4: Calibration curve for Matheson 604 Rotameter 18
Figure 5: Characteristic Axial Temperature Profiles in the Flame for Pure Substances. 19
Figure 6: Diagram of experimental apperatus 20
Figure 7: Diagram of Typical Boiling Liquid Level in a cylinder 9

## List of Graphs

Graph 1: Heat flux as a function of height 7
Graph 2: Flame axial temperature distribution 8

1" Diameter calorimeter strip chart recorder outputs 22
1/4" diameter calorimeter strip chart recorder output
Suction pyrometer strip chart recorder output

## Apperatus

HP 7100B strip chart recorder #1148A06048
Matheson 604 rotameter
Suction pyrometer
1" diameter calorimeter
1/4" diameter calorimeter
Gast suction pump (0522-V3-G180X) #1078

Fuel Used: N Propyl Alcohol

The experiments were conducted at the University of New Brunswick using the facilities of the Fire Science Center.

Using a 30.5 cm. diameter by 5.7 cm. deep pan, with an propyl alcohol as the fuel, the heat flux around a cylinder and the flames axial temperature distribution were found.

The measurements were made 1 1/2 hours after ignition, at which time the pool fire was considered to have reached steady state (2). Note that the fire from the 30.5 cm. diameter pan was fully turbulent, displaying a random motion. According to Mitsoulis, the flame is fully turbulent for source dimeters above 15 cm. (2).

To determine the heat flux, two experiments were made, one with a one inch diameter calorimeter and the other with a 1/4 inch diameter calorimeter (see Figures 1 and 2 respectively). The heat flux was calculated from the mass flowrate and temperature rise of the cooling water, by;

$$q = m\ C_p\ \Delta T$$

where $C_p$ is the specific heat of water, taken to be 4.18 $\frac{kJ}{KgK}$. To evaluate the mass flowrate, a Matheson 604 rotameter was used to get the volumeteric flowrate, and converted to mass flowrate by multiplying by the density, taken to be 1000 $^{Kg}/_{m^3}$. The calibration curve for the rotameter (shown as Figure 4) was verified experimentally.

To get the temperature difference, the thermocouple leads in the calorimeter were connected to a HP 7100 B strip chart recorder, and the resulting output in $m^V$ was converted using the appropriate conversion chart (3). Note that for both the calorimeter experiments, the heights of 3, 6, 9, 12 and 15 inches above the pool fire were tested. The resulting heat flux as a function of height for both the calorimeters is shown in Graph 1. The outputs from the strip chart recorder are shown in the appendix.

To determine the axial temperature distribution, a suction pyrometer was used (see Figures 3A and 3B).

From the strip chart recorder output, the dependance of suction pressure on the readings can be seen, (see output at beginning of pyrometer test shown in Appendix). By varying the suction pressure form 540 mm Hg to 640 mm Hg, there was a drop in the reading of approximately 5%. This drop increased to a maximum of approximately 10%, at which point there was no air flow through the suction hose as it was clamped shut. This indicated the readings have little dependance on suction pressure. Note that the pressure used in the test was 540 mm Hg. The temperature was evaluated at 3 inch increments from 3" to 36". The resulting temperature distribution as a function of height is shown in Graph 2. The results of Mitsoulis (2) also shown on Graph 2 are based on an ethanal fire in a 30.5 by 5.7 cm. circular pan.

Mitsoulis measured the flame temperature by using a bare thermocouple. The temperatures indicated by the thermocouple were generally lower than the actual gas temperatures due to heat loss by radiation from the thermocouple edge to the surroundings.$^{(2)}$ Consequently the readings were corrected by balancing the radiation loss by the convection from the gas. Neglecting the heat loss by conduction along the wires and assuming no radiative interchange between the thermocouple and the gas, the gas temperatures could be calculated by writing an energy balance for the thermocouple, as in;

$$hA\ (T_g - T_{th}) = \varepsilon_{rw}\ A\ (T_{th}^4 - T_o^4) \qquad (2)$$

From this, the gas temperature Tq could be solved. Note however, that the parameters in the above equation are difficult to obtain accurately, hence the results of Mitsoulis are subject to speculation.

Mitsoulis also presents a comparison of flame temperatures for propanol and ethanol, shown in Figure 5, indicating ethanol burns slightly hotter than propanol. From this, it is evident that the flame temperature of a propanol fire evaluated using Mitsoulis method would be in the order of 20% lower than that obtained using the suction pyrometer.

## Results

Table 1A: Large Calorimeter test results (Test 1)

| Height (inches) | Diff (mV) | Temp (°C) | $\dot{m}$ (kg/sec) | q (KW/$m^2$) |
|---|---|---|---|---|
| 3 | 0.10 | 2.6 | 0.00643 | 8.11 |
| 6 | 0.19 | 4.9 | " | 16.59 |
| 9 | 0.19 | 4.9 | " | 16.59 |
| 12 | 0.17 | 4.5 | " | 14.04 |
| 15 | 0.13 | 3.3 | " | 10.45 |

Table 1B: Large Calorimeter test results (Test 2)

| Height (inches) | Diff (mV) | Temp ($o_C$) | $\dot{m}$ (kg/sec) | q (KW/$m^2$) |
|---|---|---|---|---|
| 3 | 0.17 | 4.5 | 0.0062 | 13.54 |
| 6 | 0.34 | 8.7 | " | 26.29 |
| 9 | 0.25 | 6.5 | " | 19.56 |
| 12 | 0.30 | 7.8 | " | 23.45 |
| 15 | 0.22 | 5.7 | " | 17.14 |
| 18 | 0.16 | 4.2 | " | 12.62 |
| 21 | 0.12 | 3.1 | " | 9.32 |

Table 2: Small Calorimeter test results

| Height (inches) | Diff (mV) | Temp ($o_C$) | $\dot{m}$ (kg/sec) | q (KW/$m^2$) |
|---|---|---|---|---|
| 3 | 0.07 | 1.8 | 0.003166 | 11.58 |
| 6 | 0.10 | 2.6 | " | 16.72 |
| 9 | 0.10 | 2.6 | " | 16.72 |
| 12 | 0.08 | 2.1 | " | 13.50 |
| 15 | 0.05 | 1.3 | " | 8.36 |
| 18 | 0.07 | 1.6 | " | 11.58 |
| 21 | 0.03 | 0.8 | " | 5.14 |

Table 3: Results from Pyrometer experiment (Thermecouple: Platinum 13% Rh i.e., type R)

| Height | mV | Temp (°C) - Based on 0°c REF. |
|---|---|---|
| 3 | 6.6 | 700 |
| 6 | 9.2 | 920 |
| 9 | 9.6 | 961 |
| 12 | 9.3 | 910 |
| 15 | 8.6 | 855 |
| 18 | 8.2 | 822 |
| 21 | 7.8 | 791 |
| 24 | 5.0 | 550 |
| 27 | 4.0 | 457 |
| 30 | 4.0 | 457 |
| 33 | 3.3 | 391 |
| 36 | 2.4 | 320 |

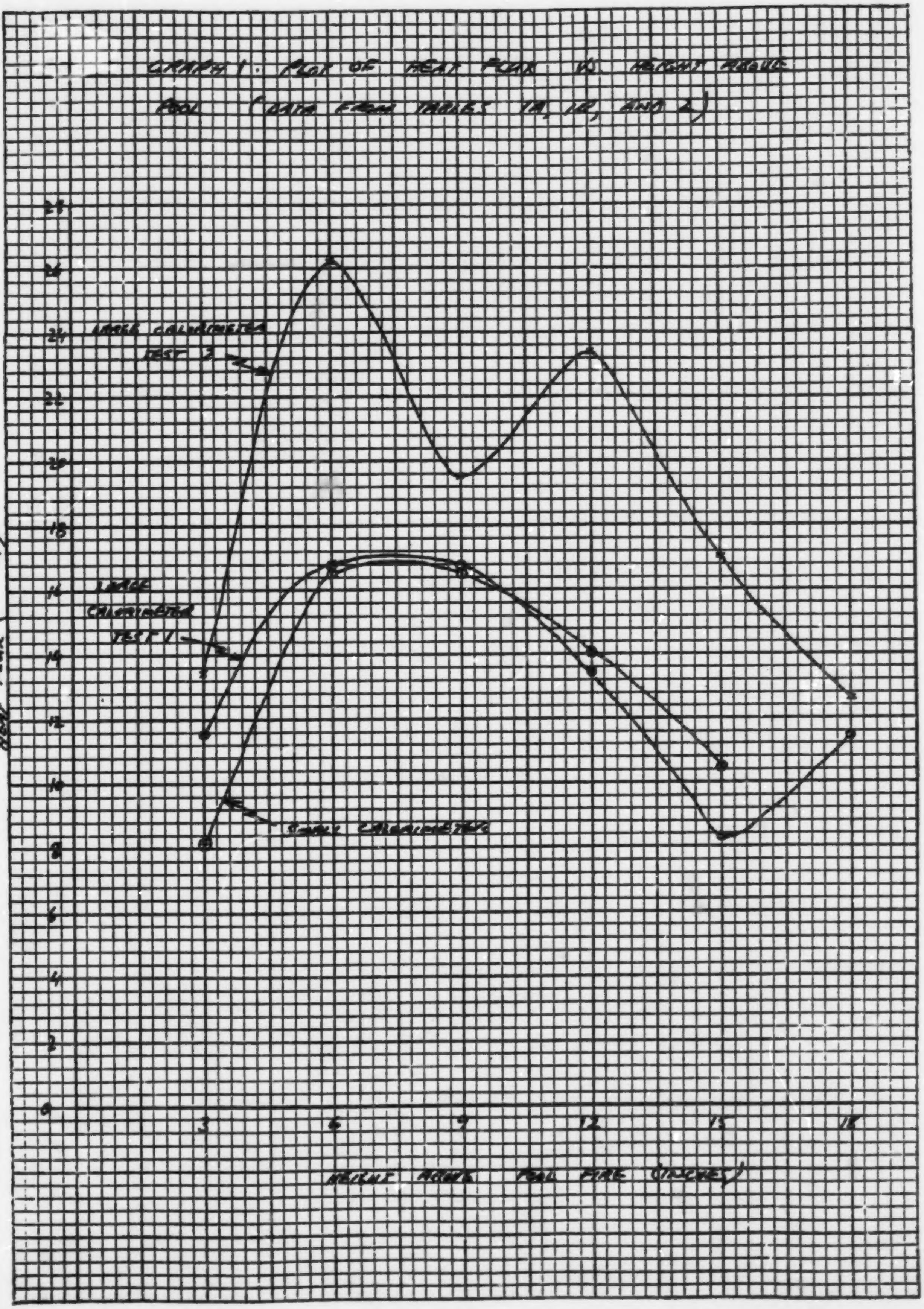

GRAPH 1: PLOT OF HEAT FLUX VS. HEIGHT ABOVE POOL (DATA FROM TABLES 1A, 1B, AND 2)

GRAPH 2 : PLOT OF AXIAL FLAME TEMPERATURE VS DISTANCE ABOVE POOL FIRE

(DATA FROM TABLE 3)

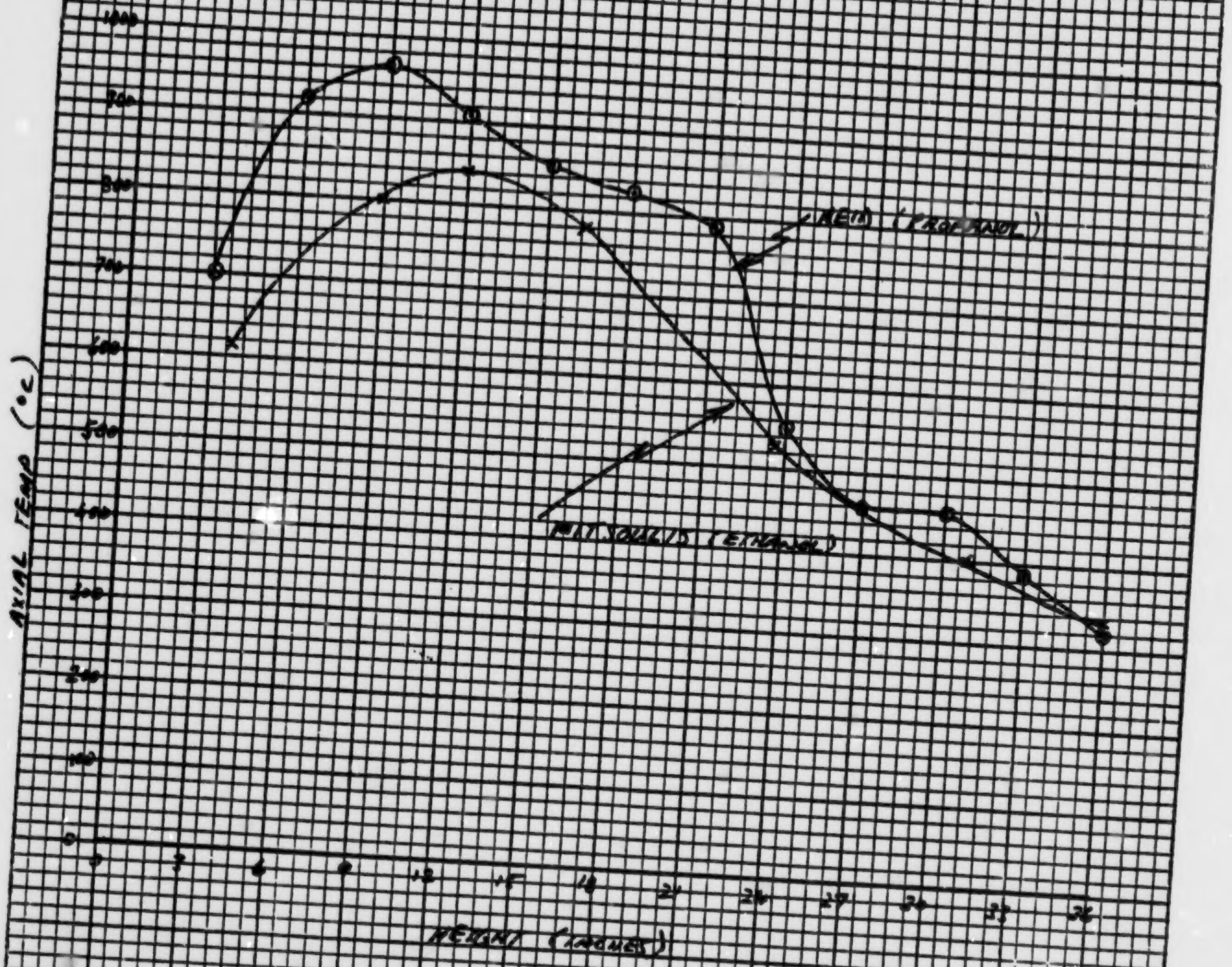

From Graph 1, we can see that the heat flux for the two calorimeters with respect to height are similar. The maximum for both was approximately 17 to 26 kW/m$^2$, occuring in both cases in the region from 6 to 9 inches above the pool fire. In both cases, the heat flux increased to the maximum and then decreased.

In comparison with the heat flux calculated to exist in the 1/5 scale tests, the result of 26 kw/m$^2$ is quite low. In the 1/5 scale tests, the heat flux was deduced by estimating the fluid level in the car over a certain time increment, the corresponding quantity of propane which existed from the car, and from the heat of vapourization, the heat flux can be found.

The average heat flux on the 1/5 scale tests was found to be approximately 53 kw/m$^2$ (1).

Note that there may be a small error in the analysis used in reference (1), since the liquid level was determined by checking the thermocouple output at the walls, and assuming a horizontal liquid level at the level on the walls. However, when looking at the thermocouple readings towards the center of the car, it can be seen that in many cases (particularly when the fluid level is low) that the actual level is more like that shown in Figure 7.

Figure 7: Diagram of typical boiling liquid level in a cylinder

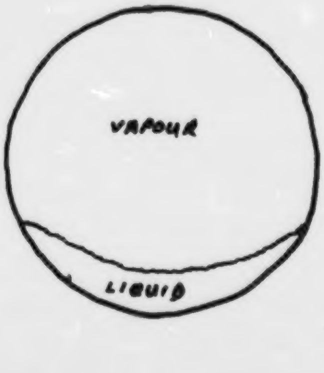

Consequently, the heat flux is underpredicted when the liquid level in the car is getting low. In the full scale tests, the heat flux on the cars was an average 104 kw/m$^2$. (4)

Although the heat flux measured by the calorimeter is low compared to that in the 1/5 and full scale tests, the results are considered to be in the correct range for our test conditions. Note however that there was quite a lot of trouble in the calorimeter experiments concerning reproducability. As seen in Tables 1A and 1B there were two tests done with the large calorimeter. Although the results are of the same magnitude, at times one set is close to twice as large as the other. This is probably due to the difficulty in obtaining two fires of the same characteristics, and the nature of the fire itself. As seen on the strip chart recorder output, there was a large fluctuation in the "hot" water output. Although an attempt was made to use an average, the possibility of error is still large. Note also that due to the availability of equipment, the "cold" water was measured at a sensitivity of 5mV compared to the "hot" water at 1mV. Hence the accuracy of the cold reading was also reduced.

The applicability of the results when considering a full size tank car is also subject to speculation since the apperatus used (i.e. the 1/4" and 1" diameter calorimeter) are not very similar to a tank car. Note also that the fuel used in the calorimeter tests was n propyl alcohol, whereas that used in the 1/5 scale test was JP-4 fuel. (1)

The results of the axial flame temperature distribution were in fairly good agreement with those of Mitsoulis (2) as seen in Graph 2. The flame didn't appear to be significantly disturbed by the suction pyrometer. The results of Mitsoulis indicate a maximum difference in the order of 20% between the suction pyrometer and Mitsoulis bare thermocouple tests (see page 4 of this report). This difference is probably due to an inaccurate determination of h, the convective heat transfer coefficient, which was vital in Mitsoulis analysis (2), or fluctuations in gas concentration in the pyrometer tests. The interesting point to note when compairing the results is the similarity in shape of the distribution. Both analysis yielded a maximum temperature in the range of 9 to 12 inches above the pool fire, and both appeared to show a similar decay in temperature as the height increased.

At the height of 21" and greater, the pyrometer readings were slightly lower than what would be expected, as they were almost the same as those of Mitsoulis for these heights. This was probably due to the increased turbulence of the flame at the larger heights, and the consequent increase in fluctuation of gas density due to the turbulence.

# REFERENCES

(1) APPLEYARD, R. D., "Testing and Evaluation of the Explosafe System as a Method of Controlling the Boiling Liquid Expanding Vapour Explosion (BLEVE)," Vulcan Industrial Packaging Ltd., 1980.

(2) MITSOULIS, E. C., "Liquid Pool Fires," Thesis for M.Sc. (Chem. Eng.), University of New Brunswick, June 1979.

(3) KNAPPE, A. A., "Guide to the Selection of Thermocouples in Temperature Measurement," Department of Chemical Engineering, University of New Brunswick (Reference tables for the various calibrations in above manual are based on the "International Practical Temperature Scale of 1948")

(4) ANDERSON, C. et al., "The Effects of a Fire Environment on a Rail Tank Car Filled with LPG," Ballistic Research Laborateries, Distributed by NTIS, Sept. 1974.

# APPENDIX

Contains all calculations, Figures 1 to 6, and strip chart recorder output.

FIGURE 1 : CALORIMETER USED TO DETERMINE HEAT FLUX

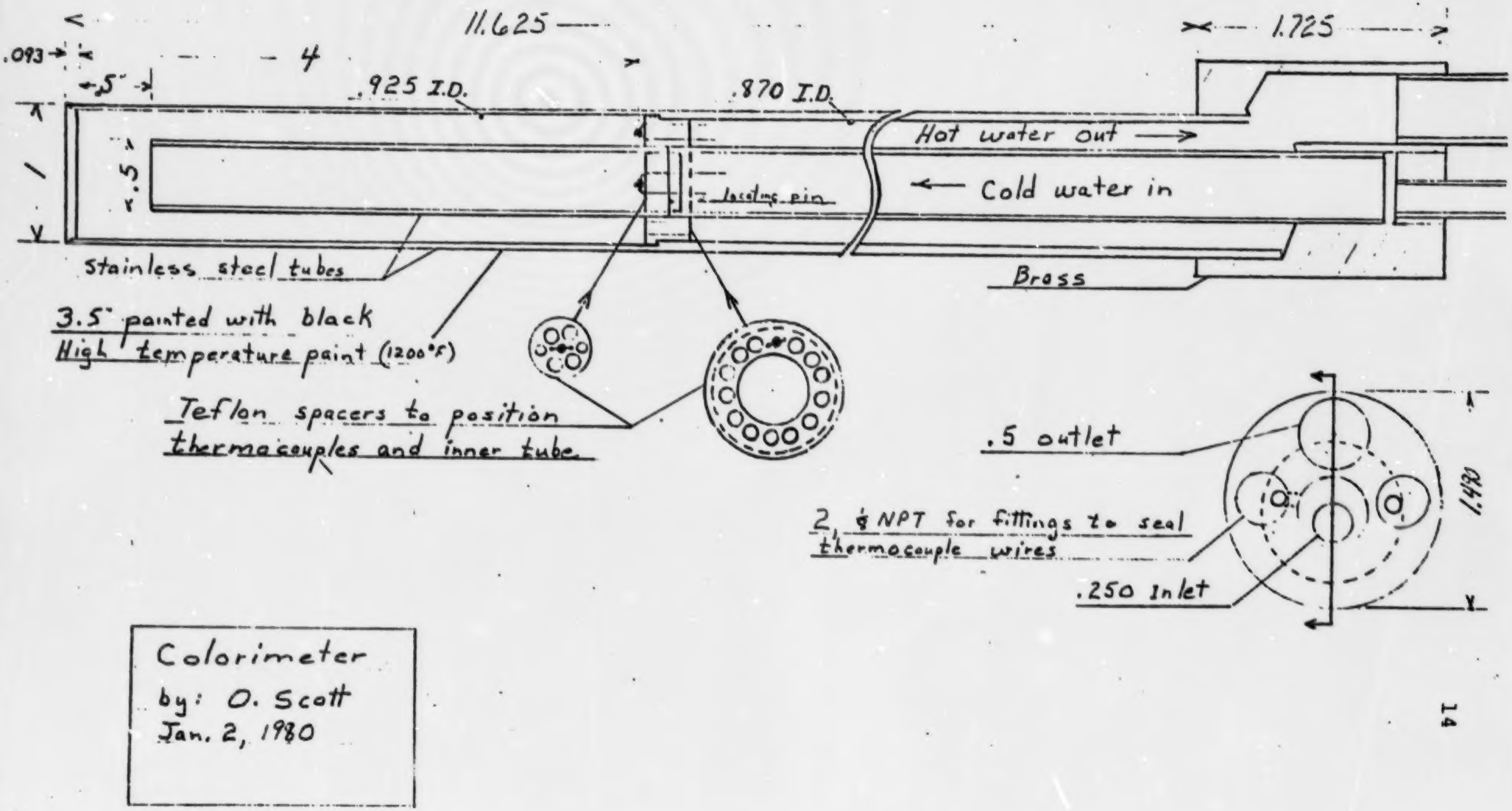
11.625
1.725
.093
4
.5"
.925 I.D.
.870 I.D.
1
.5
2 locating pin
Hot water out
Cold water in
Stainless steel tubes
Brass
3.5" painted with black High temperature paint (1200°F)
Teflon spacers to position thermocouples and inner tube
.5 outlet
2, ⅛ NPT for fittings to seal thermocouple wires
.250 Inlet
1.490
Colorimeter
by: O. Scott
Jan. 2, 1980

FIGURE 2: CALORIMETER USED TO DETERMINE HEAT FLUX

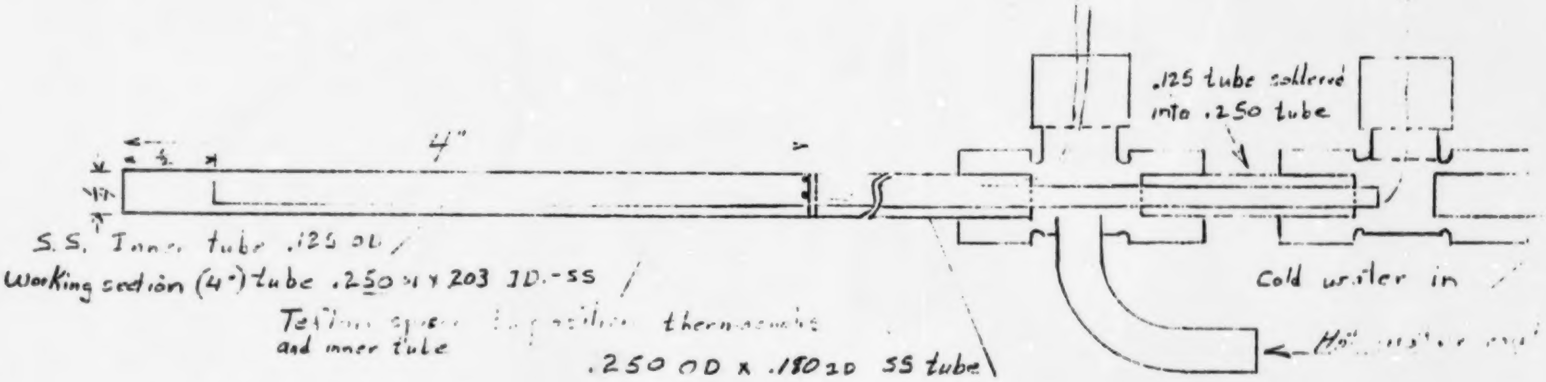
4"
.125 tube soldered into .250 tube
S.S. Inner tube .125 OD
Working section (4") tube .250 x .203 ID.-SS
Teflon spacer [illegible] thermocouple and inner tube
.250 OD x .180 ID SS tube
Cold water in
Hot water out
.250 ss tube painted with High temp (1200°F) black paint for first 3.5"

Colorimeter
by: O. Scott
1979

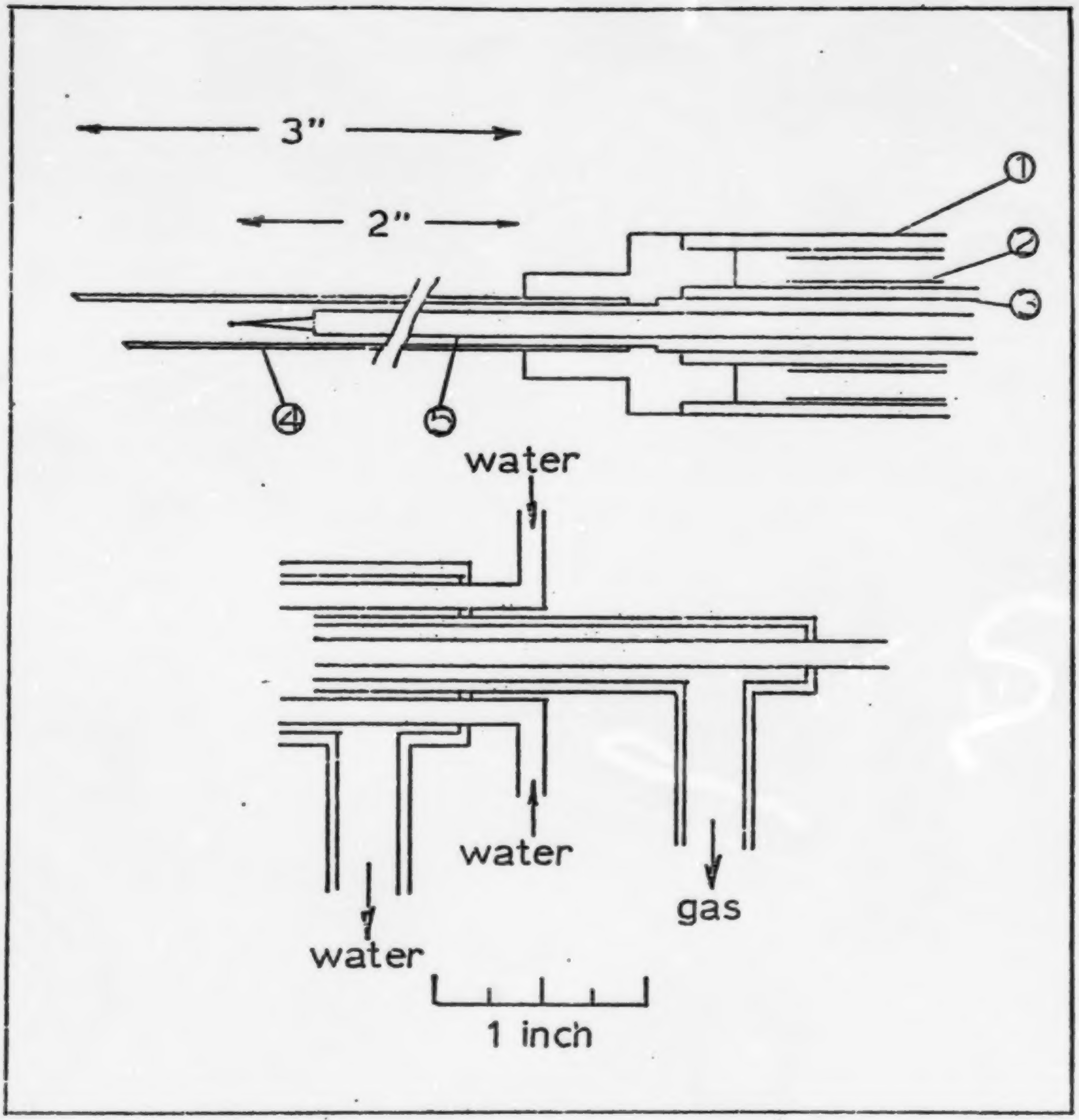
3"
2"
①
②
③
④
⑤
water
water
gas
water
1 inch

Figure 3A Water cooled suction pyrometer.
1) 3/4" ID copper tube;
2) 1/8" OD stainless steel tube;
3) 3/8" OD copper tube;
4) Ceramic tube;
5) Thermocouple sheath

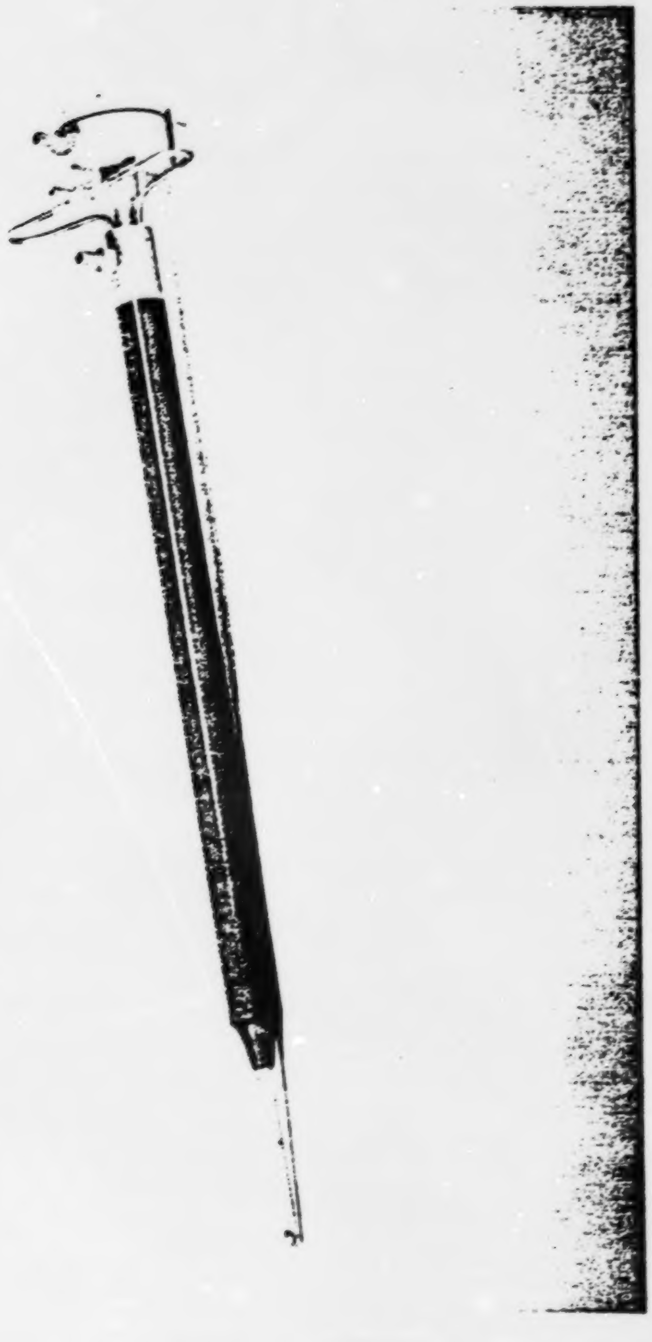

Figure 38 Water cooled suction pyrometer.

FIGURE 4 : CALIBRATION CURVE FOR 604 ROTAMETER

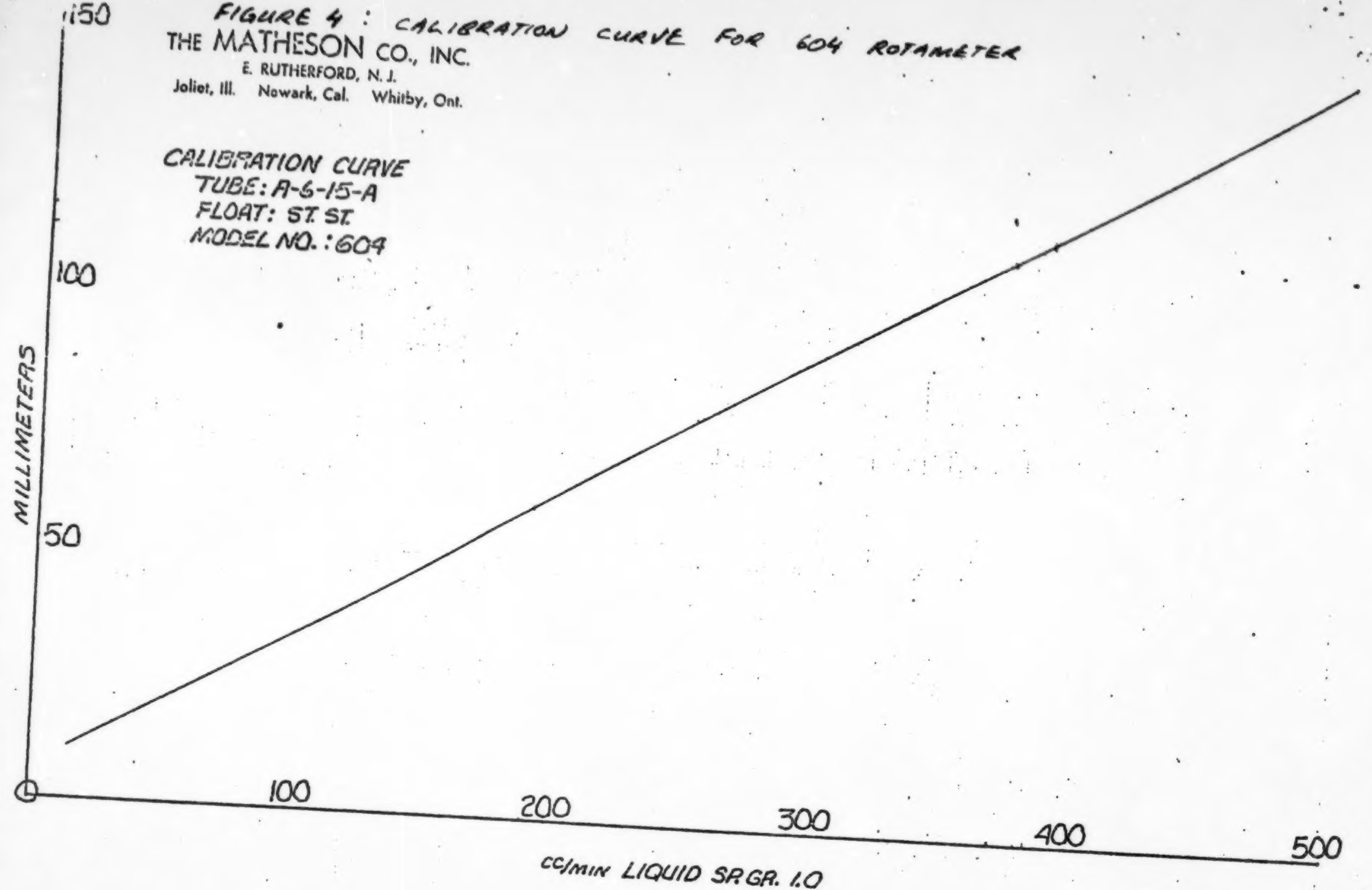

FOR DUAL FLOAT UNIT, USE ONLY WITH GLASS & ST. ST. TOGETHER

2-20-63

M604-2W

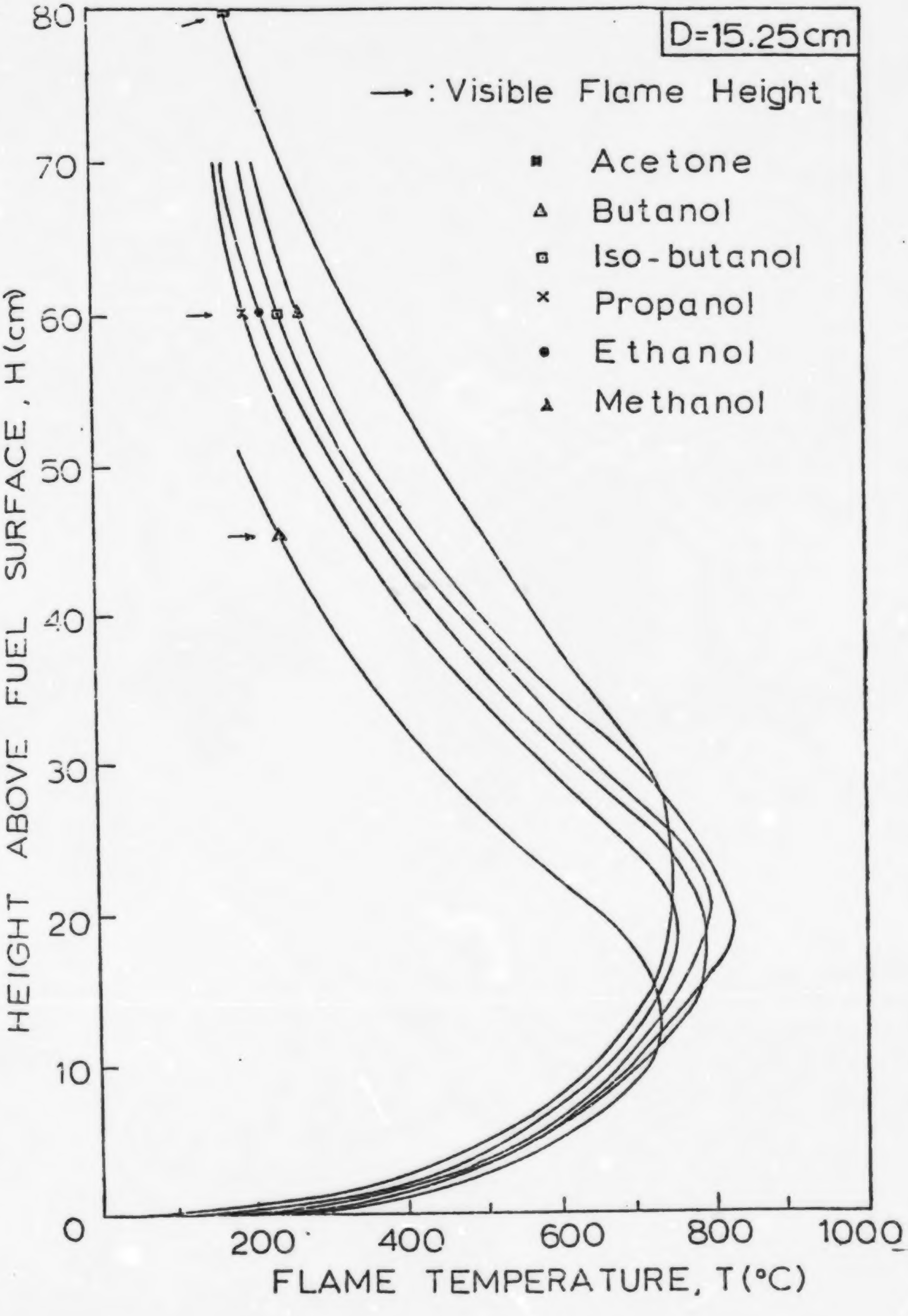

Figure *5* Characteristic Axial Temperature Profiles in the Flame for Pure Substances. [2]

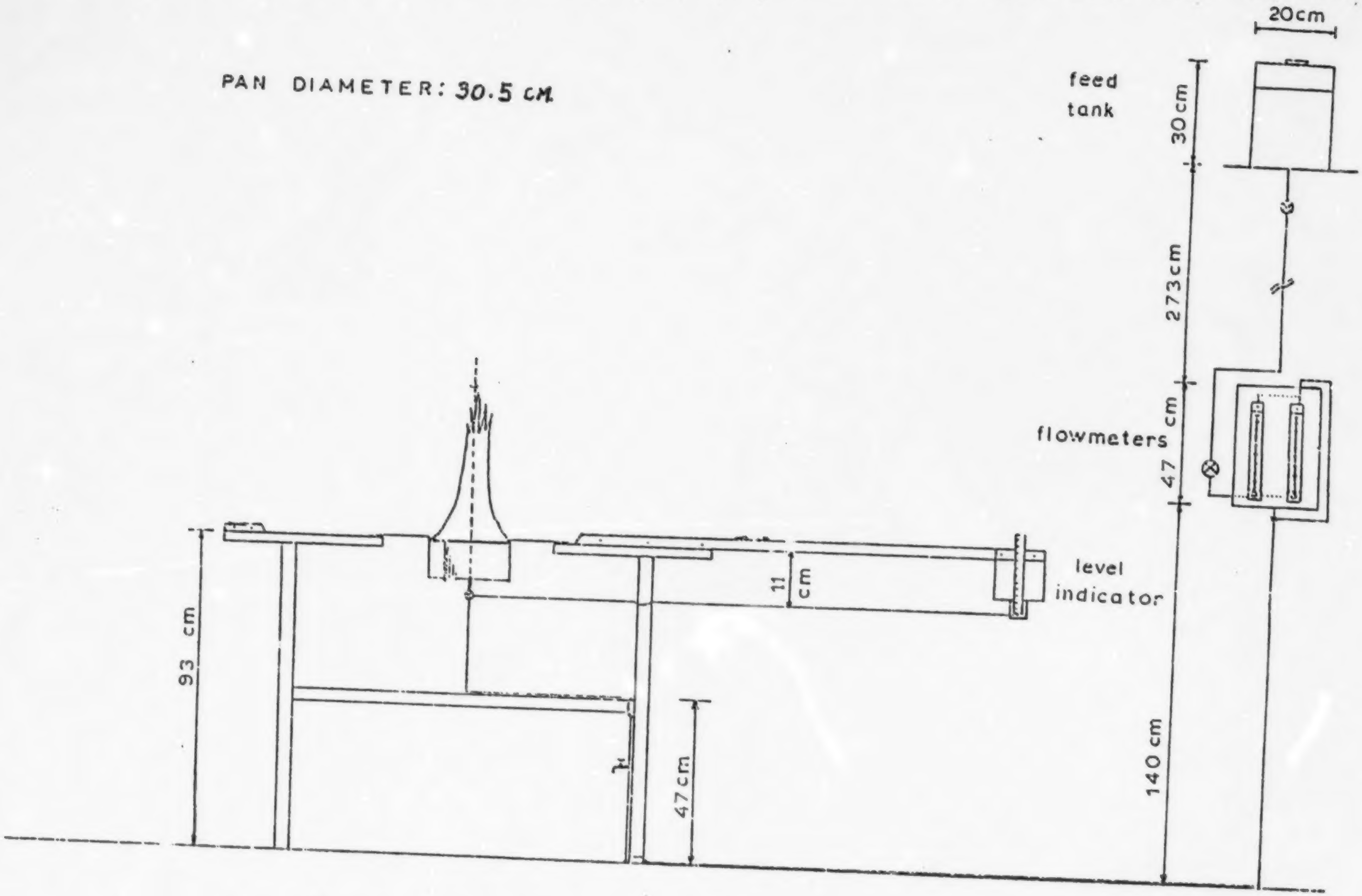
PAN DIAMETER: 30.5 cm
20cm
feed
tank
30cm
273cm
flowmeters
47 cm
level
indicator
11 cm
93 cm
47cm
140 cm

Figure 6 : Schematic Diagram of Apparatus.

# Development of Computer Code to Determine the Thermodynamics and Transport Properties of Propane

R.C. Prasad, Robert Doyle & John Reid

## 1. Thermodynamic Properties

A subroutine "TDPROP' has been written (in Fortran) which calculates various thermodynamic properties of propane under the following four conditions within a tank:

1) Compressed liquid, IFLAG=4
2) Saturated liquid and saturated vapor IFLAG=1
3) Saturated liquid and superheated vapor IFLAG=2
4) Only vapor (saturated or superheated) IFLAG=3

The input to the subroutine are

1) Total mass of propane = XMTOT
2) Total volume of the tank = VTOT
3) Temperature of vapor = TVAP
4) Temperature of liquid = TLIQ

In case of single phase state within the tank, the temperature of vapor and liquid must be assigned an identical value.

From the input data, the program determines the state of the fluid within the tank and sets the IFLAG. The properties such as, tank pressure, fluid density, enthalpy, internal energy, entropy, $dP/dT$, $dP/d\rho$, velocity of sound, and the latent heat (for liquids) are calculated for vapor and/or liquid as the case may be. The subroutines employed for computation are those from [1] with minor modification in some segments. The computational range of TDPROP is as follows:

$$231.07\ \text{K} < \text{TLIQ} < 369.8\ \text{K}$$

$$231.07\ \text{K} < \text{TVAP} < 700\ \text{K}$$

$$1.013\ \text{bar} < P < 42.42\ \text{bar}$$

and it is considered adequate for the present application. Should the need arise, these ranges can be extended.

The subroutine 'TDPROP' has been extensively tested and found to reproduce the result reported by Goodwin [1].

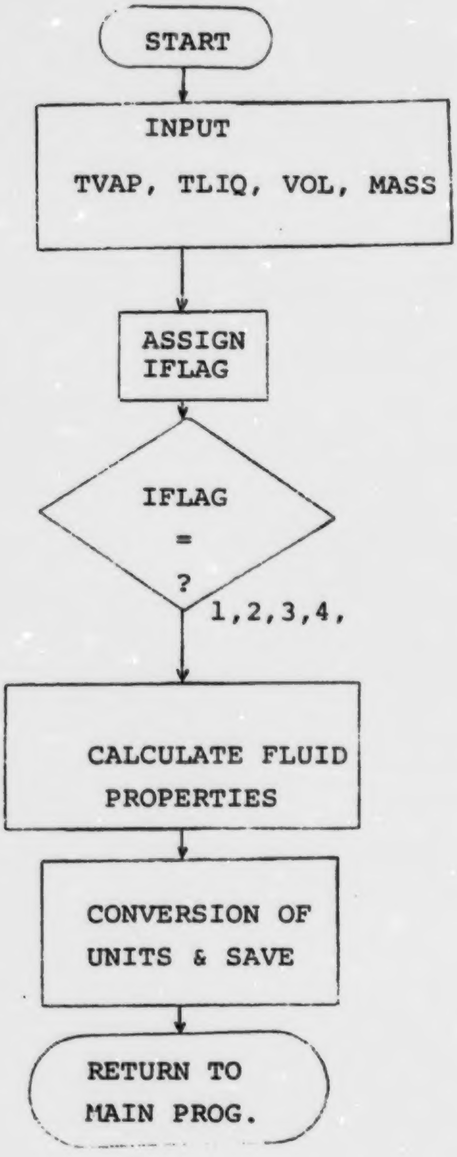
START
INPUT
TVAP, TLIQ, VOL, MASS
ASSIGN IFLAG
IFLAG = ?
1,2,3,4,
CALCULATE FLUID PROPERTIES
CONVERSION OF UNITS & SAVE
RETURN TO MAIN PROG.

IFLAG=1 : SAT LIQ + SAT VAP
=2 : SAT LIQ + SUP. VAP
=3 : ONLY VAP
=4 : ONLY LIQUID

Figure 1: Flow Diagram of Subroutine TDPROP

## 2. Transport Properties

### 2.1 Surface Tension of Propane - A Correlation

The surface tension data [2] for propane in the range -90°C to 10°C were correlated using the model [3]

$$\sigma = \sigma_o \left(1 - \frac{T}{T_c}\right)^{\mu} \left[1 + b \left(1 - \frac{T}{T_c}\right)\right] \tag{1}$$

In order to obtain convergence, the first estimates of $\sigma_o = \sigma_o^1$ and $\mu = \mu^1$ were obtained from the correlation model

$$\sigma = \sigma_o^1 \left(1 - \frac{T}{T_c}\right)^{\mu^1} . \tag{2}$$

Equation (2) was transformed first to

$$\ln \sigma = A + B \ln (T_c - T) \tag{3}$$

$$\text{where } A = \ln \sigma_o^1 - \mu^1 \ln T_c \qquad \text{and} \quad B = \mu^1 \tag{4}$$

The least square estimates of A and B and the calculated values of $\sigma_o^1$ and $\mu^1$ from equation (4) were determined as

$$\begin{aligned} A &= -2.0502358 \\ B &= 0.9343741 \\ \sigma_o^1 &= 32.28759 \qquad \mu^1 = 0.9343731 \end{aligned} \tag{5}$$

The paramater $\sigma_o$, $\mu$ and b of equation (1) were then estimated to be

$$\begin{aligned} \sigma_o &= 27.87011215 \\ \mu &= 0.86459884 \\ b &= 0.21334518 \end{aligned} \tag{6}$$

with a residual sum of squares = 0.00010386 using the SAS statisitical package.

Summary:

Equation of surface tension of propane:

$$\sigma = \sigma_o (1 - \frac{T}{T_c})^{\mu} [1 + b (1 - \frac{T}{T_c})]$$

$\sigma_o$ = 27.87011215
$\mu$ = 0.8645988
b = 0.21334518

T = Temperature, K
$T_c$ = Critical Temperature = 369.8 K
$\sigma$ = Surface tension, dynes/cm.

Table 1 Surface Tension Data for Propane

| | | $\sigma$, dynes/cm | |
|---|---|---|---|
| T,C | T,K | Data Ref.[1] | Calculated Values |
| -90 | 183.15 | 17.09 | 17.09 |
| -80 | 193.15 | - | 16.21 |
| -70 | 203.15 | 15.34 | 15.34 |
| -60 | 213.15 | - | 14.46 |
| -50 | 223.15 | 13.59 | 13.59 |
| -40 | 233.15 | - | 12.71 |
| -30 | 243.15 | 11.84 | 11.84 |
| -20 | 253.15 | - | 10.97 |
| -10 | 263.15 | 10.09 | 10.10 |
| 0 | 273.15 | - | 9.21 |
| 10 | 283.15 | 8.35 | 8.35 |
| 20 | 293.15 | - | 7.46 |
| 30 | 303.15 | - | 6.58 |
| 40 | 313.15 | - | 5.68 |
| 50 | 323.15 | - | 4.77 |
| 60 | 333.15 | - | 3.86 |
| 70 | 343.15 | - | 2.91 |
| 80 | 353.15 | - | 1.93 |
| 90 | 363.15 | - | 0.867 |
| 95 | 368.15 | - | 0.259 |
| 96 | 369.8 | - | 0 |

$\sigma$ Values at $T >10$°C are extrapolated values. However, these values appear to be well behaved. The model (Equation 1), therefore, may be used at $T > 10$°C.

## 2.2 Thermal Conductivity and Viscosity of Propane

The thermal conductivity and viscosity of propane are computed in terms of T,k and $\rho$, gm/cc propane are computed using the following correlation [4].

$$X(\rho,T) = X_o(T) + X_1(T)\rho + \Delta X^1(\rho,T) + \Delta X_c(\rho,T)$$

$$X_1 = A + B[C - \ln(T/F)]^2$$

$$\Delta X^1 = D \exp[k_1 + k_4/T] \cdot \{\exp[\rho^{0.1}(k_2 + k_3/T^{3/2}$$

$$+ \theta\rho^{0.5}(k_5 + k_6/T + k_7/T^2)]-1\}$$

$$\theta = (\rho - \rho_c)/\rho_c, \ \rho_c = \text{critical point density}$$

$$X_o(T) = \alpha_1 k + \alpha_2/T^{2/3} + \alpha_3/T^{1/3}$$

$$+ \alpha_4 + \alpha_5 T^{1/3} + \alpha_6 T^{2/3}$$

$$+ \alpha_7 T + \alpha_8 T^{4/3} + \alpha_9 T^{5/3}$$

$$\Delta X_c = \text{critical region enhancement.}$$

Where x represents the property $\lambda$ or $\eta$. The coefficients A, B, C, D, F, $k_1,..k_7$, $\alpha_1,..\alpha_9$ for the cases $X = \lambda$ and $X = \eta$ are both listed in reference [4].

Function subprograms CONDUC $(T,\rho)$ and VISCOS $(T,\rho)$ are written to compute the thermal conductivity and viscosity values.

These routines do not include the critical region enhancement term, $\Delta X_c$ which are estimated to be within the acceptable limits in the range of usage in the present application.

Further, with the correlation and coefficients of [4] it was not possible to reproduce the values reported by the author. The difference is very large (40-50%) for liquids at low temperatures. It is suspected that there are some typographical errors either in the equation or the coefficients. In the absence of any clarification, two equations are utilized in the present form. In the region of interest for the thermal modelling of the rail tank cars, the deviation between calculated values and tabulated values are computed (Table 2). It considered adequate to use these equations in the present application.

Table 2 Summary of deviations of the calculated values from the tabulated values for the thermal conductivity and viscosity of propane [1].

| Summary: | % deviation* | |
|---|---|---|
| | λ | η |
| Saturated liquid at 1 bar | 8.2 | 17.3 |
| Saturated vapor at 1 bar | 7.0 | 1.4 |
| Saturated liquid 270-330 K | 2 to 5 | -1 to 11 |
| Saturated vapor 270-Tcr. | 1 to 5<br>(-11.6) | -1 to 3 |
| Superheated vapor 270-500 K | -3 to 0.3<br>(-8.0) | 0.1 |
| Compressed liquid | 2 to 5 | 6 to 11 |

$$* \ \% \text{ deviation of } X = \frac{X_{calculated} - X_{tabulated}}{X_{tabulated}} \times 100$$

References:

[1] Goodwin, R.D., "Provisional Thermodynamic Functions of Propane, from 85 to 700 k at Pressure to 700 Bars", Report No. NBS1R77-860, NBS, Washington, July, 1977.

✓ [2] Jasper, J.J., "The Surface Tension of Pure Liquid Compounds", J. Phys. Chem. Ref. Data, V1, N4, 1972, P. 841-1009.

[3] Rathjen, W. and Straub, J., "Temperature Dependence of Surface Tension, Coexistence Curve, and Vapor Pressure of $CO_2$, $COF_3$, $CBrF_3$ and $SF_6$", Chapter 18, Heat Transfer in Boiling, Hahne, E and Grigull, U. (Editors), Academic Press, 1977.

✓ [4] Holland, P.M., Hanley, H.J.M., Gubbins, K.E. and Hail, J.M., "A Correlation of the Viscosity and Thermal Conductivity Data of Gaseous and Liquid Propane", J. Phys. Chem., Ref. Data V8, N2, 1979, P. 559-575.

```
*****************************************************************************************************
C ********************************************************
C **                                                    **
C **        SIMULATED MAIN PROGRAM FOR TDPROP           **
C ** TO COMPUTE  THERMODYNAMIC PROPERTIES OF PROPANE    **
C **                                                    **
C ********************************************************
      COMMON/TANK/TLIQ,TVAP,XMTOT,VTOT,XMLIQ,VLIQ,XMVAP,VVAP,PTANK,IFLAG
      COMMON/LIQ/DENL,EL,HL,SL,CVL,CPL,WL,DPLDT,DPLDD,QVL,QV
      COMMON/VAP/DENV,EV,HV,SV,CVV,CPV,WV,DPVDT,DPVDD
      WM = 44.09721
      TA = 231.071
      TCRT = 369.8
      PCRT = 42.4204
      DCRT = 4.69
      XDCRT = DCRT*WM
      IFLAG = 0
C
C-----INPUT: TLIQ,TVAP,MASS,VOLUME OF TANK
C
C-----TLIQ  = TEMPERATURE OF LIQUID
C-----TVAP  = TEMPERATURE OF VAPOR
C-----XMTOT = TOTAL MASS OF PROPANE IN KILOGRAMS
C-----VTOT  = VOLUME OF TANK IN LITRES
C-----SET TLIQ = TVAP IF THE TANK CONTAINS ONLY VAPOR
C
C-----ASSIGN TLIQ, TVAP, XMTOT, VTOT  :  THESE ARE INPUT DATA
C
      TLIQ  = 300.00
      TVAP  = 700.00
      XMTOT = 10000.00
      VTOT  = 30.0
C
C-----CHECK LIQUID TEMPERATURE WRT CRITICAL TEMPERATURE
C-----CALCULATE SATURATED LIQUID DENSITY AND VAPOR DENSITY AT T = TLIQ
C
      IF (TLIQ-TCRT) 10,10,20
C-----CHECK IF THE TANK CONTAINS ONLY VAPOR. IF SO SET IFLAG = 3.
 20   IF (XDCRT*VTOT .GT. XMTOT) IFLAG = 3
      IF (IFLAG .EQ. 3) GO TO 15
      WRITE(6,110)
 110  FORMAT(1X,'T .GT. TCRT : TCRT = 369.8 K')
      STOP
C
 10   DENL=DENLQF(TLIQ)
      XDENL=DENL*WM
      DENV=DENGSF(TLIQ)
      XDENV=DENV*WM
C
C-----ESTABLISH THE STATE OF FLUID (SAT/SUP LIQUID , COMPR LIQUID)
C-----IFLAG = 1 : SAT LIQUID,SAT VAP.
C           = 2 : SAT LIQUID,SUPERHEATED VAP.
C           = 3 : ALL VAPOR (SUP)
C           = 4 : COMPRESSED LIQUID
C           = 5 : TLIQ > TVAP :  CASES NOT CONSIDERED
C           = 6 : T < TA (= 231.071 K) : CASES NOT CONSIDERED
C
      IF (ABS(TVAP-TLIQ) .LE. 0.1) IFLAG=1
      IF (TVAP-TLIQ .GT. 0.1) IFLAG=2
      IF (XDENV*VTOT .GT. XMTOT) IFLAG=3
      IF (XDENL*VTOT .LT. XMTOT) IFLAG=4
      IF ((TLIQ -TVAP) .GT. 0.1) IFLAG=5
      IF ((TA-TLIQ) .GT. 0.1 .OR. (TA-TVAP) .GT. 0.1) IFLAG=6
C
C-----CALL SUBROUTINE  'TDPROP'  TO COMPUTE FLUID PROPERTIES
C
   15 CALL TDPROP
      CALL PRINT
C
C ************************************************************
C        H E A T     T R A N S F E R       A N A L Y S I S
C          ( TLIQ, TVAP, XMTOT ARE ALL RECALCULATED)
C ************************************************************
C
C-----CHECK TANK PRESSURE WRT PCRT= 42.4204 BARS
C
      IF (PTANK-PCRT) 30,40,40
   30 STOP
C
C-----CASE (T .GE. TCR)
C
   40 WRITE(6,120)
  120 FORMAT(1X,'TANK PRESSURE > PCRT (PCRT = 42.4204 BAR',/)
      STOP
      END
C ************************************************************

      SUBROUTINE TDPROP
C
C-----SUBROUTINE TO COMPUTE THERMODYNAMIC PROPERTIES OF PROPANE
C-----COMPUTATIONAL RANGE OF TLIQ  : 230.071 <= TLIQ  <= 369.8 K
C-----COMPUTATIONAL RANGE OF TVAP  : 230.071 <= TVAP  <= 700.0 K
C-----COMPUTATIONAL RANGE OF PTANK:    1.013 <= PTANK <= 42.42 BAR
C
      COMMON GK,GKK,B1,B2,B3,B4,E1,ER
      COMMON/B01/AL,BE,GA,DE,DCRT,TCRT,PCRT,DGAT,DTRP,TTRP,PTRP
      COMMON/B03/DPDT,D2PDT2,DPSDT,DPMDT,DPDD,DPDR,DTSDR,DTHDR
      COMMON/B04/XB1,XB2,XE1,XE2,DXBDR,DXEDR
      COMMON/B05/DDSDT
      COMMON/B06/TSAT,THETA,PSAT
      COMMON/B07/TA,TB,PB,EA,HA,SA,HB,SB,TY1,TY2,DYH,DYS
      COMMON/B08/IN,IK,P,T,DEN,E,H,S,CV,CP,CSAT,W,WK
      COMMON/B09/DNG,EG,HG,SG,CVG,CPG,WG,DPGDT,DPGDD
      COMMON/B10/DY(40),HY(40),EY(40),SY(40),CPY(40),CVY(40)
      COMMON/B11/DK(40),EK(40),SK(40),CVK(40)
      COMMON/B12/DELS,DELCV
      COMMON/B20/B,BD,ED,XB,XE,F1
      COMMON/B99/TI,EZZ,EZ,SZ,CVZ,HZ,CPZ
      COMMON/TANK/TLIQ,TVAP,XMTOT,VTOT,XMLIQ,VLIQ,XMVAP,VVAP,PTANK,IFLAG
      COMMON/LIQ/DENL,EL,HL,SL,CVL,CPL,WL,DPLDT,DPLDD,QVL,QV
      COMMON/VAP/DENV,EV,HV,SV,CVV,CPV,WV,DPVDT,DPVDD
C
      Q=1.01325
      PB=103.42135
      WM=44.09721
      WK=100000./WM
      GKK=0.0831434
      TTRP=85.47
      DTRP=16.62
      PTRP=3.0E-9
      TCRT=369.8
      DCRT=4.960
      PCRT = 42.4204
      DGAT=PTRP/GKK/TTRP
      GK=GKK*DCRT
      EZZ=27452.0
      AL=1.0
      BE=0.0
      GA=0.06
      DE=0.75
      ER=2.0
      B1=0.22566372605
      B2=1.04646227554
      B3=-0.44491000068
      B4=0.12708270211
      E1=-0.59883339489
      M=1
      TA = 231.071
C
C-----CHECK IFLAG AND BRANCH TO APPROPRIATE PROGRAM SEGMENT
C
      GO TO (40,50,60,70,80,90),IFLAG
C
C-----IFLAG = 1 : SAT LIQUID,SAT VAP.
C            = 2 : SAT LIQUID,SUPERHEATED VAP.
C            = 3 : ALL VAPOR (SUP)
C            = 4 : COMPRESSED LIQUID
C            = 5 : TLIQ > TVAP  :  CASES NOT CONSIDERED
C            = 6 : TLIQ < TA  .OR.  TVAP < TA : CASES NOT CONSIDERED
C
C-----CALCULATE THERMODYNAMIC PROPERTIES
C
C-----IFLAG = 1, SATURATED LIQUID & SATURATED VAPOR
C
   40 T=TLIQ
      PTANK = P = VAPRES(T)
      CALL COEXST
      CALL SAVE(1)
      CALL SAVE(2)
      CALL VOLMAS
      RETURN
C
C-----IFLAG = 2, SATURATED LIQUID AND SUPERHEATED VAPOR
C
   50 T=TLIQ
      PTANK = P = VAPRES(T)
      CALL COEXST
      CALL SAVE(1)
      T=TVAP
      CALL GENOUS
      CALL SAVE(3)
      CALL VOLMAS
      RETURN
C
C-----IFLAG=3:ONLY VAPOR WITHIN THE TANK
C
   60 T=TVAP
      XDENV = XMTOT/VTOT
      DENV = XDENV/WM
      PTANK = P = PVTFUN(T,DENV,0)
      IF(P .GT. PCRT) GO TO 30
      CALL GENOUS
      CALL SAVE(3)
      CALL VOLMAS
      RETURN
C
C-----IFLAG=4: COMPRESSED LIQUID
C
 70   T=TLIQ
      XDENL=XMTOT/VTOT
      DENL=XDENL/WM
      PTANK = P = PVTFUN(T,DENL,1)
      IF(P.GT.PCRT) GO TO 30
      CALL REMSAT
C-----REDEFINE  T = TLIQ  (NOTE THAT 'REMSAT' MIGHT HAVE ALTERED T)
      T = TLIQ
      CALL COMPRL
      CALL SAVE(1)
      CALL VOLMAS
      RETURN
 30   WRITE(6,120)
 120  FORMAT(1X,'P.GE.PCRT: P IS OUT OF RANGE',/)
      STOP
 80   WRITE(6,130)
 130  FORMAT(1X,'TLIQ > TVAP :  CASES  NOT CONSIDERED')
      STOP
 90   WRITE(6,140)
 140  FORMAT(1X,'TLIQ < TA .OR. TVAP < TA  : CASES NOT CONSIDERED')
      STOP
      END
C  ****************************************

      SUBROUTINE PRINT
C
C-----SUBROUTINE TO PRINT ALL DATA (SUPPLIED/CALCULATED)
C
      COMMON/TANK/TLIQ,TVAP,XMTOT,VTOT,XMLIQ,VLIQ,XMVAP,VVAP,PTANK,IFLAG
      COMMON/LIQ/DENL,EL,HL,SL,CVL,CPL,WL,DPLDT,DPLDD,QVL,QV
      COMMON/VAP/DENV,EV,HV,SV,CVV,CPV,WV,DPVDT,DPVDD
      WRITE(6,100) PTANK,XMTOT,VTOT,IFLAG
 100  FORMAT(1X,'TANK PRESSURE           =',F10.3,' BARS',/,
     @1X,'MASS OF PROPANE (L+V)=',F10.3,' KG.',/,
     @1X,'VOL. OF PROPANE (L+V)=',F10.3,' CUBIC METERS',//,
     @1X,'IFLAG                  =',5X,I2,/)
C
C-----BRANCH TO APPROPRIATE SECTION (IFAG = 1,2,3,4)
C
      GO TO (10,20,30,40),IFLAG
C
C-----IFLAG=1: SATURATED LIQUID, SATURATEDVAPOR STATE
C
 10   WRITE(6,110)
 110  FORMAT(1X,'SATURATED LIQUID STATE',/)
      WRITE(6,120) TLIQ,DENL,DPLDT,DPLDD,EL,HL,SL,CVL,CPL,WL
 120  FORMAT(1X,'TEMPERATURE               =',F10.3,' K',/,
     @1X,'DENSITY                   =',F10.4,' KG/M**3',/,
     @1X,'DP/DT                     =',F10.6,' BAR/K',/,
     @1X,'DP/DD                     =',F10.4,' BAR-M**3/KG',/,
     @1X,'INTERNAL ENERGY(E)        =',F10.2,' KJ/KG',/,
     [illegible]
     @1X,'SPECIFIC ENTROPY(S)    =',F10.3,' KJ/(KG-K)',/,
     @1X,'SPECIFIC HEAT(CV)      =',F10.2,' KJ/(KG-K)',/,
     @1X,'SPECIFIC HEAT (CP)     =',F10.2,' KJ/(KG-K)',/,
     @1X,'VELOCITY OF SOUND      =',F10.1,' M/SEC',/)
      WRITE(6,130) QVL
  130 FORMAT(1X,'LATENT HEAT OF EVAP. =',F10.1,' KJ/KG',/)
      WRITE(6,140)XMLIQ,VLIQ
  140 FORMAT(1X,'MASS OF LIQUID          =',F10.2,' KG',/,
     @1X,'VOLUME OF LIQUID      =',F10.2,' M**3',/)
      WRITE(6,150)
  150 FORMAT(1X,'SATURATED VAPOR STATE',/)
      WRITE(6,120) TVAP,DENV,DPVDT,DPVDD,EV,HV,SV,CVV,CPV,WV
      WRITE(6,160) XMVAP,VVAP
  160 FORMAT(1X,'MASS OF VAPOR           =',F10.2,' KG',/,
     @1X,'VOLUME OF VAPOR       =',F10.2,' M**3',/)
      RETURN
C
C-----IFLAG=2: SATURATED LIQUID ,SUPER-HEATED VAPOR
C
   20 WRITE(6,110)
      WRITE(6,120) TLIQ,DENL,DPLDT,DPLDD,EL,HL,SL,CVL,CPL,WL
      WRITE(6,130)QVL
      WRITE(6,140)XMLIQ,VLIQ
      WRITE(6,170)
  170 FORMAT(1X,'SUPERHEATED VAPOR STATE',/)
      WRITE(6,120) TVAP,DENV,DPVDT,DPVDD,EV,HV,SV,CVV,CPV,WV
      WRITE(6,160)XMVAP,VVAP
      RETURN
C  IFLAG=3: ALL VAPOR
   30 WRITE(6,180)
  180 FORMAT(1X,'ONLY VAPOR IN THE TANK.NO LIQUID',/)
      WRITE(6,120) TVAP,DENV,DPVDT,DPVDD,EV,HV,SV,CVV,CPV,WV
      WRITE(6,140)XMLIQ,VLIQ
      WRITE(6,160)XMVAP,VVAP
      RETURN
C
C-----IFLAG=4: COMPRESSED LIQUID
C
   40 WRITE(6,190)
  190 FORMAT(1X,'COMPRESSED LIQUID STATE',/)
      WRITE(6,120) TLIQ,DENL,DPLDT,DPLDD,EL,HL,SL,CVL,CPL,WL
      WRITE(6,140)XMLIQ,VLIQ
      WRITE(6,160)XMVAP,VVAP
      RETURN
      END
C ****************************************************

      SUBROUTINE SAVE(ICODE)
      COMMON/TANK/TLIQ,TVAP,XMTOT,VTOT,XMLIQ,VLIQ,XMVAP,VVAP,PTANK,IFLAG
      COMMON/LIQ/DENL,EL,HL,SL,CVL,CPL,WL,DPLDT,DPLDD,QVL,QV
      COMMON/VAP/DENV,EV,HV,SV,CVV,CPV,WV,DPVDT,DPVDD
      COMMON/B03/DPDT,D2PDT2,DPSDT,DPMDT,DPDD,DPDR,DTSDR,DTHDR
      COMMON/B08/IN,IK,P,T,DEN,E,H,S,CV,CP,CSAT,W,WK
      COMMON/B09/DNG,EG,HG,SG,CVG,CPG,WG,DPGDT,DPGDD
C
C-----SUBROUTINE TO SAVE THE CALCULATED PROPERIES
C
C----- ICODE = 1 : LIQUID PROPERTIES SAVED AS LIQUID PROPERTIES
C              2 : VAPOR  PROPERTIES SAVED AS VAPOR  PROPERTIES
```

```
C             3 : LIQUID PROPERTIES SAVED AS VAPOR  PROPERTIES
C
      WM = 44.09721
      GO TO (10,20,30), ICODE
C
C-----LIQUID PROPERTIES SAVED AS LIQUID PROPERTIES (ICODE = 1)
C
10    DENL = DEN*WM
      EL = E/WM
      HL = H/WM
      SL = S/WM
      CVL = CV/WM
      CPL = CP/WM
      WL = W
      DPLDT = DPDT
      DPLDD = DPDD/WM
      QVL = QV/WM
      RETURN
C
C-----VAPOR PROPERTIES SAVED AS VAPOR PROPERTIES (ICODE = 2)
C
20    DENV = DNG*WM
      EV = EG/WM
      HV =HG/WM
      SV = SG/WM
      CVV =CVG/WM
      CPV = CPG/WM
      WV = WG
      DPVDT = DPGDT
      DPVDD = DPGDD/WM
      RETURN
C
C-----LIQUID PROPERTIES SAVED AS VAPOR PROPERTIES (ICODE = 3)
C
30    DENV = DEN*WM
      EV = E/WM
      HV = H/WM
      SV = S/WM
      CVV = CV/WM
      CPV = CP/WM
      WV = W
      DPVDT = DPDT
      DPVDD = DPDD/WM
      RETURN
      END
C *********************************************

      SUBROUTINE VOLMAS
C
C-----SUBROUTINE TO CALCULATE VOLUME ANS MASS OF PROPANE (LIQUID/VAP)
C
      COMMON/TANK/TLIQ,TVAP,XMTOT,VTOT,XMLIQ,VLIQ,XMVAP,VVAP,PTANK,IFLAG
      COMMON/LIQ/DENL,EL,HL,SL,CVL,CPL,WL,DPLDT,DPLDD,QVL,QV
      COMMON/VAP/DENV,EV,HV,SV,CVV,CPV,WV,DPVDT,DPVDD
C
C-----BRANCH TO APPROPRIATE SECTION
C
      GO TO (10,10,20,30), IFLAG
C
C--- IFLAG = 1 OR 2 : SATURATED LIQUID AND SAT/SUP VAPOR STATE
```

```
      C
      10    XMLIQ=(DENL/(DENL-DENV))*(XMTOT-DENV*VTOT)
            XMVAP=XMTOT-XMLIQ
            VLIQ=XMLIQ/DENL
            VVAP=VTOT - VLIQ
            RETURN
      C
      C-----IFLAG = 3 : ONLY VAPOR IN THE TANK
      C
      20    XMVAP = XMTOT
            VVAP = VTOT
            XMLIQ = 0.0
            VLIQ = 0.0
            RETURN
      C
      C-----IFLAG = 4 : COMPRESSED LIQUID IN THE TANK
      C
      30    XMLIQ = XMTOT
            VLIQ = VTOT
            XMVAP = 0.0
            VVAP = 0.0
            RETURN
            END
      C ***************************************************************
      C     SUBROUTINES AND FUNCTION PROGRAMS FROM "PROVISIONALTHERMO-
      C     DYNAMIC FUNCTIONS OF PROPANE, FROM 85 TO 700 K AT PRESSURES
      C     TO 700 BAR", ROBERT D. GOODWIN, REPORT # NBSIR 77-860,
      C     NATIONAL BUREAU OF STANDARS, COLORADO, JULY 1977.
      C         (WITH MINOR MODIFICATION TO SOME ROUTINES)
      C  ************************************************************
      C     FUNCTIONS AND SUBROUTINES ARE LISTED IN ALPHABETIC ORDER
      C  ************************************************************

            SUBROUTINE COEXST
      C
      C   GIVEN T AT COEXISTENCE ,GET BOTH VAPOUR AND LIQUID FUNCTIONS
      C   FOR VAPOR ,GET DNG,EG,HG,SG,CVG,CPG,WG,DPGDT,DPGDD
      C   FOR LIQUID, GET DEN,E,H,S,CV,CP,CSAT,W.
      C   COEXST CALLED BY COMPRLQ,P NOT USED,MUST NOT CHANGE.
            COMMON/B01/AL,BE,GA,DE,DCRT,TCRT,PCRT,DGAT,DTRP,TTRP,PTRP
            COMMON/B03/DPDT,D2PDT2,DPSDT,DPMDT,DPDD,DPDR,DTSDR,DTHDR
            COMMON/B05/DDSDT
            COMMON/B08/IN,IK,P,T,DEN,E,H,S,CV,CP,CSAT,W,WK
            COMMON/B09/DNG,EG,HG,SG,CVG,CPG,WG,DPGDT,DPGDD
            COMMON/B12/DELS,DELCV
            COMMON/B99/TI,EZZ,EZ,SZ,CVZ,HZ,CPZ
            COMMON/LIQ/DENL,EL,HL,SL,CVL,CPL,WL,DPLDT,DPLDD,QVL,QV
            Q=1.01325
            G=0.0831434
      1     FORMAT(1H0,9X,'T EXCEEDS TCRT IN COEXST',/)
            IF(T.LE.TCRT) GO TO 4
      3     WRITE(6,1)
            STOP
      4     PS=VAPRES(T)
            DNG=DB=DENGSF(T)
      5     TI=T
            CALL IDEAL
            N=DB*20+10
      6     EG=EZZ+EZ+EDELF(1,N,T,0.0,DB)
            HG=EG+100.0*PS/DB
      7     SG=SZ+DELS-100.0*G*ALOG(G*T*DB/Q)
      8     IF(T.NE.TCRT) GO TO 11
      9     PX=PVTFUN(T,DB,1)
            DPGDT=DPDT
            DPGDD=DPDD
     10     CPG=CVG=WG=0
            GO TO 15
     11     CVG=CVZ+DELCV
            PX=PVTFUN(T,DB,1)
     12     CPG=CVG+100.0*T/DPDD*(DPDT/DB)**2
            WG=SQRT(WK*CPG*DPDD/CVG)
     13     DPGDT=DPDT
            DPGDD=DPDD
C   NOW TRAVERSE THE DOME USING QVAP,DATA,.
     15     DEN=DL=DENLQF(T)
            DDLDT=DDSDT
            QV=QVAP(T)
     16     H=HG-QV
            S=SG-QV/T
            E=H-100.0*PS/DL
     17     IF(T.NE.TCRT) GO TO 19
     18     PX=PVTFUN(T,DL,1)
            CP=CV=CSAT=W=0
            RETURN
     19     CSAT=CPSL(T)
            PX=PVTFUN(T,DL,1)
     20     CV=CSAT+100.0*T*DPDT*DDLDT/DL/DL
     21     CP=CV+100.0*T/DPDD*(DPDT/DL)**2
     22     W=SQRT(WK*CP*DPDD/CV)
            RETURN
            END
C   ****************************************

              SUBROUTINE COMPRL
C
C   GIVEN P,T FOR COMPRESSED LIQUID AT T.LT.TC GET DEN FUNCTIONS
C   IF T=MULTIPLE.10 K,START WITH DK,EK,SK,CVK ON SATLIQ.,
C   OTHERWISE,USE COEXST FOR START ON THE SATDLIQ.,AND
C   FINALLY,INTEGRATE ALONG ISOTHERM T FROM SATLIQ. TO POINT (P,T)
            COMMON/B03/DPDT,D2PDT2,DPSDT,DPMDT,DPDD,DPDR,DTSDR,DTHDR
            COMMON/B05/DDSDT
            COMMON/B08/IN,IK,P,T,DEN,E,H,S,CV,CP,CSAT,W,WK
            COMMON/B11/DK(40),EK(40),SK(40),CVK(40)
            COMMON/B12/DELS,DELCV
            TCRT=369.8
      1     FORMAT(1H0,9X,'T NOT UNDER TCRT IN COMPRLQ.',/)
            IF(T.LT.TCRT) GO TO 4
      3     WRITE(6,1)
            STOP
      4     I=T/10
            IF((T-10.0*I).EQ.0.0) GO TO 6
      5     CALL COEXST
            DA=DEN
            GO TO 10
      6     DA=DK(I)
            E=EK(I)
            S=SK(I)
            CV=CVK(I)
C   NOW INTEGRATE ALONG ISOTHERM T UP TO POINT (T,P)
     10     DEN=DB=FINDEN(T,P)
```

```
      DX=DB-DA
      IF(DX) 13,13,11
   11 N=DX*10+5
      E=E+EDELF(0,N,T,DA,DB)
   12 S=S+DELS
      CV=CV+DELCV
   13 H=E+100.0*P/DB
      PX=PVTFUN(T,DB,1)
   14 CP=CV+100.0*T/DPDD*(DPDT/DB)**2
   15 W=SQRT(WK*CP*DPDD/CV)
      RETURN
      END
C   ****************************************

        REAL FUNCTION CPSL(T)
C
C   SPECIFIC HEAT OF SATURATED LIQUID(CPSL)
C    VIA PROGRAM CSAT-C3,DEC.15,1976,AT11.18,USING
C    DATA FROM PTHERM4,DEC.13,1976,AT 10.31.
C    CS=A*X/(1-X)**EP+B+C*X+D*X2+E*X3
C    X=T/TCRT
        REAL EP,TCRT,A,B,C,D,ET,X,X2
C
C    DECLARING THE CONSTANTS
C
        EP=0.8
        TCRT=369.80
        A=4.201410
        B=79.737878
        C=18.313347
        D=-36.564448
        E=67.003225
C
C    CALCULATING THE SPECIFIC HEAT
C
        IF(T.LT.TCRT) GO TO 30
         CPSL=0.0
         RETURN
   30    X=T/TCRT
         X2=X*X
         Q=(1.0-X)**EP
         CPSL=A*X/Q+B+C*X+D*X2+E*X*X2
         RETURN
         END
C ******************************************

         SUBROUTINE CSTSUM
C
C  FOR SATLIQ START WITH EA,SA,AT TA,INTEGRATE FROM TA TO T.
C  YIELDS DEN,E,H,S,CV,CP,CSAT,W AT T FOR THE SATDLIQUID
       COMMON/B03/DPDT,D2PDT2,DPSDT,DPMDT,DPDD,DPDR,DTSDR,DTHDR
       COMMON/B05/DDSDT
       COMMON/B07/TA,TB,PB,EA,HA,SA,HB,SB,TY1,TY2,DYH,DYS
       COMMON/B08/IN,IK,P,T,DEN,E,H,S,CV,CP,CSAT,W,WK
       E=EA
       S=SA
       TR=T-TA
       IF(TR.EQ.0.0) GO TO 9
       N=ABS(TR)/4.0+2.0
       DT=TR/N
      DO 8 J=1,N
        TJ=TA+(J-0.5)*DT
        C=CPSL(TJ)
        S=S+C*DT/TJ
        PS=VAPRES(TJ)
        D=DENLOF(TJ)
        DD=DDSDT*DT
        E=E+C*DT+100.0*PS*DD/D/D
  8     CONTINUE
  9     CSAT=CPSL(T)
      DEN=DL=DENLOF(T)
      DDLDT=DDSDT
 10   PS=PVTFUN(T,DL,1)
      H=E+100.0*PS/DL
 11   CV=CSAT+100.0*T*DPDT*DDLDT/DL/DL
 12   CP=CV+100.0*T/DPDD*(DPDT/DL)**2
 15   W=SQRT(WK*CP*DPDD/CV)
      RETURN
      END
C  ******************************************

      FUNCTION CUBERT(X)
C
C  CUBE ROOT MISSING FROM 6600 COMPUTER LIBRARY
      E=1.0/3.0
      IF(X) 2,3,4
  2   CUBERT=-ABS(X)**E
      RETURN
  3   CUBERT=0.0
      RETURN
  4   CUBERT=X**E
      RETURN
      END
C  ******************************************

       REAL FUNCTION DENGSF(T)
C
C  PROPANE SATURATED VAPOR DENSITY(DENGSF(T))
C  DEN=(DC*TC/T)*EXP(-YNG*Y)
C  YNG=LN(DC*TC/DGAT/TTRP)
C  X=(TC-T)/(TC-TT)
C  U=(TC/T-1)/(TC/TT-1)
C  Y=U+(XE-X)*(A1+A2*X/XE+A3*X+..+A6*X4)
       COMMON/B05/DDSDT
       DIMENSION A(6)
       DCRT=4.96
       TTRP=85.47
       TCRT=369.8
       E=0.35
       DGAT=4.221626E-10
       YNG=24.65103315
       A(1)=0.072453281
       A(2)=0.170534468
       A(3)=-0.278060163
       A(4)=0.438982342
       A(5)=-0.841080253
       A(6)=0.405105441
  1    FORMAT(1H0,9X,'T EXCEEDS TCRT IN DENGSF(T).',/)
       IF(TCRT-T) 3,4,5
  3    WRITE(6,1)
```

```
      STOP
  4   DENGSF=DCRT
      DDSDT=1.0E+10
      RETURN
  5   DCT=DCRT*TCRT
      XN=TCRT-TTRP
      X=(TCRT-T)/XN
      X1T=-1.0/XN
  6   UN=TCRT/TTRP-1.0
      U=(TCRT/T-1.0)/UN
      U1T=-TCRT/UN/T/T
      XE=X**E
      V=XE-X
      V1=E*XE/X-1.0
      W=A(1)+A(2)*X/XE
      W1=A(2)*(1.0-E)/XE
      DO 10 K=3,6
      L=K-2.0
      XL=X**L
      W=W+A(K)*XL
 10   W1=W1+A(K)*L*XL/X
      Y=U+V*W
      Y1T=U1T+(V*W1+V1*W)*X1T
 12   DENGSF=DCT/T*EXP(-YNG*Y)
 15   DDSDT=-(YNG*Y1T+1.0/T)*DENGSF
      RETURN
      END
C  ******************************************

      REAL FUNCTION DENLQF(T)
C
C  PROPANE SATURATED LIQUID DENSITIES(MOL/LITRE)
C  DEN=DCRT+YNL*(X+(XE-X)*Y)
C  YNL=DTRP-DCRT
C  Y=A+B*X2+C*X3
C  X=(TC-T)/(TC-TT)
      COMMON/B05/DDSDT
      TTRP=85.47
      TCRT=369.80
      DCRT=4.96
      DTRP=16.62
      E=0.35
      A=0.775396679
      B=-0.167912979
      C=0.081166807
  1   FORMAT(1H0,9X,'T EXCEEDS TCRT IN DENLQF(T)',/)
  2   IF(TCRT-T) 3,4,5
  3   WRITE(6,1)
      STOP
  4   DENLQF=DCRT
      DDSDT=-1.0E+10
      RETURN
  5   XN=TCRT-TTRP
      X=(TCRT-T)/XN
      X2=X*X
      X1T=-1.0/XN
  6   XE=X**E
      V=XE-X
      V1=E*XE/X-1.0
      YNL=DTRP-DCRT
```

```
    7     Y=A+B*X2+C*X*X2
          Y1=2.0*B*X+3.0*C*X2
    8     DENLQF=DCRT+YNL*(X+V*Y)
    9     DDSDT=YNL*(1.0+V*Y1+V1*Y)*X1T
          RETURN
          END
C   ***********************************************
          FUNCTION EDELF(L,N,T,DA,DB)
C
C   GET CHANGE OF E,S,CV WITH DENSITY ALONG ISOTHERMS.
C   GET EDELF,DELS,DELCV FROM DA TO DB ALONG ISOTHERM T.
          COMMON/B03/DPDT,D2PDT2,DPSDT,DPMDT,DPDD,DPDR,DTSDR,DTHDR
          COMMON/B12/DELS,DELCV
          G=0.0831434
          DX=(DB-DA)/N
          IF(DX.EQ.0.0) GO TO 10
          E=S=CV=0.0
          DO 9 J=1,N
            DN=DA+(J-0.5)*DX
            DXN=DX/DN/DN
            P=PVTFUN(T,DN,0)
            E=E+(P-T*DPDT)*DXN
            CV=CV-D2PDT2*DXN
            IF(L.NE.0) GO TO 7
            S=S-DPDT*DXN
            GO TO 9
    7       S=S+(G-DPDT/DN)*DX/DN
    9       CONTINUE
          EDELF=100.0*E
          DELS=100.0*S
          DELCV=100.0*T*CV
          RETURN
   10     EDELF=DELS=DELCV=0.0
          RETURN
          END
C***********************************************
          REAL FUNCTION FINDEN(T,P)
C
C   ON ISOTHERM T,FIND DEN,MOL/L,TO MINIMIZE(P-PC) VIA
C   THE EQATION OF STATE
          COMMON/B01/AL,BE,GA,DE,DCRT,TCRT,PCRT,DGAT,DTRP,TTRP,PTRP
          COMMON/B03/DPDT,D2PDT2,DPSDT,DPMDT,DPDD,DPDR,DTSDR,DTHDR
          DM=17.2
          GKK=0.0831434
   41     FORMAT(1H0,9X,'FINDEN=0,FAILS TO CONVERGE.',/)
   42     FORMAT(1H0,9X,'FINDEN=DCRT,DP/DR ZERO OR NEG.',/)
   43     FORMAT(1H0,9X,'FINDEN=0,DOUBLE -VALUED AT P=PSAT.',/)
          IF(P.LE.0) GO TO 35
    1     IF(T-TCRT) 2,5,8
    2     DG=DENGSF(T)
          DL=DENLQF(T)
          PS=VAPRES(T)
          IF(P-PS) 3,32,4
    3     D=DG/2
          GO TO 11
    4     D=(DL+DTRP)/2
          GO TO 11
    5     DG=DL=DCRT
```

```
      PS=PCRT
      IF(P-PS) 6,33,7
    6 D=DCRT/2
      GO TO 11
    7 D=2*DCRT
      GO TO 11
    8 IF(T.GE.400.0) GO TO 10
    9 PC=PVTFUN(T,DCRT,0)
      IF(P-PC) 6,33,7
   10 D=DCRT
   11 DO 30J=1,50
        DP=P-PVTFUN(T,D,1)
        IF(ABS(DP/P)-1.0E-5) 31,31,12
   12   IF(DPDD.LE.0) GO TO 34
   13   DD=DP/DPDD
        IF(ABS(DD/D)-1.0E-5) 31,31,14
   14   D=D+DD
        IF(D.GT.0.0) GO TO 16
   15   D=P/GKK/T
        GO TO 30
   16   IF(D.LE.DM) GO TO 18
   17   D=DM
        GO TO 30
   18   IF(T-TCRT) 19,24,30
   19   IF(P.GE.PS) GO TO 22
   20   IF(D.LE.DG) GO TO 30
   21   D=DG
        GO TO 30
   22   IF(D.GE.DL) GO TO 30
   23   D=DL
        GO TO 30
   24   IF(P.GE.PCRT) GO TO 27
   25   IF(D.LT.DCRT) GO TO 30
   26   D=DCRT-0.02
        GO TO 30
   27   IF(D.GT.DCRT) GO TO 30
   28   D=DCRT+0.02
   30   CONTINUE
       WRITE(6,41)
       STOP
   31 FINDEN=D
      RETURN
   32 WRITE(6,43)
      STOP
   33 FINDEN=DCRT
      RETURN
   34 FINDEN=DCRT
      WRITE(6,42)
      RETURN
   35 FINDEN=DPDT=D2PDT2=0
      DPDD=GKK*T
      DPDR=DPDD*DTRP
   36 RETURN
      END
C  ********************************************
        REAL FUNCTION FINDTM(P)
C
C---GIVEN P ON THE MELTING LINE . FIND T .
      COMMON/B01/AL,BE,GA,DE,DCRT,TCRT,PCRT,DGAT,DTRP,TTRP,PTRP
      DATA A,E /7180.0, 1.283/
      X = (P-PTRP)/A + 1.0
      FINDTM = TTRP*X**(1.0/E)
      RETURN
      END
C ************************************

      REAL FUNCTION FINDTS(P)
C
C  GIVEN THE VAPOUR PRESSURE P,ITERATE T TO MINIZE (P-PC)
      COMMON/B01/AL.BE,GA.DE.DCRT.TCRT.PCRT.DGAT.DTRP.TTRP.PTRP
      COMMON/R03/DPDT,D2PDT2,DPSDT.DPMDT,D?DD.DPDR,DTSDR,DTHDR
    1 FORMAT(1H0,9X,'FINDTS=0.FAILS TO CONVERGE.',/)
    2 FORMAT(1H0,9X,'FINDTS=0,P EXCEEDS PCRT.',/)
      IF(P-PCRT) 4,11,12
    4 T=250
      DO 9 J=1,50
        DP=P-VAPRES(T)
        ADP=ABS(DP)
    5   IF(ADP/P-1.0E-5) 10,6,6
    6   IF(ADP/DPSDT/T-1.0E-5) 10,7,7
    7   T=T+DP/DPSDT
        IF(T-TCRT) 9,9,8
    8   T=TCRT
    9   CONTINUE
      WRITE(6,1)
      STOP
   10 FINDTS=T
      RETURN
   11 FINDTS=TCRT
      RETURN
   12 WRITE(6,2)
      STOP
      END
C ********************************************

      SUBROUTINE GENOUS
C
C  GIVEN P,T FOR THE HOMOGEGEOUS DOMAIN
C  GET THE DEN AND FUNCTIONS AT ANY TEMPERATURE
      COMMON/B03/DPDT,D2PDT2,DPSDT,DPMDT,DPDD,DPDR, DTSDR,DTHDR
      COMMON/R08/IN,IK,P,T,DEN,E,H,S,CV,CP,CSAT,W,WK
      COMMON/B12/DELS,DELCV
      COMMON/R99/TI,EZZ,EZ,SZ,CVZ,HZ,CPZ
      Q=1.01325
      G=0.0831434
      TI=T
      CALL IDEAL
      IF(P.LE.0.0) GO TO 10
    4 DEN=DB=FINDEN(T,P)
      N=DB*20+10
    5 E=EZZ+EZ+EDELF(1,N,T,0.0,DB)
      H=E+100.*P/DB
    6 S=SZ+DELS-100.0*G*ALOG(G*T*DB/Q)
    7 CV=CVZ+DELCV
      PX=PVTFUN(T,DB,1)
      CP=CV+100.0*T/DPDD*(DPDT/DB)**2
      W=SQRT(WK*CP*DPDD/CV)
      RETURN
   10 DEN=S=0
```

```
      E=EZZ+EZ
      HG=EG+100.0*G*T
      CV=CVZ
      CP=CPZ
   12 W=SQRT(WK*CP*G*T/CV)
      RETURN
      END
C   **********************************************

      SUBROUTINE IDEAL
C
C  PROPANE IDEAL GAS (1 ATM) THERMO FUNCTIONS VIACHAD (1973)
C  (HZ-HZZ)/RT=4.0+(A+B/Q+C/Q2+D/X)*EXP(-E/X), WHERE
C  X=T/100,Q=CUERT(X)
      COMMON/B99/TI,EZZ,EZ,SZ,CVZ,HZ,CPZ
      DIMENSION A(6)
      E=3.0
      R=8.31434
      SI=32.552
      A(1)=24.11012
      A(2)=94.40550
      A(3)=-585.32814
      A(4)=980.124065
      A(5)=-678.64094
      A(6)=170.42778
      X=TI/100
      Q=CUBERT(X)
      DQDX=Q/3/X
      XP=EXP(-E/X)
      H=4.0
      SUM=SM1=0
      DO 7 K=1,6
        H=H+A(K)*XP*Q**(1-K)
        L=4-K
        QL=Q**L
        SUM=SUM+A(K)*QL
        SM1=SM1+A(K)*L*QL*DQDX/Q
    7   CONTINUE
      CP=4.0+(E*SUM/X/X+SM1)*XP
C  S=S(300)+INTEGRAL(CP/X)*DX FROM T=310 UP TO TI.
   10 N=ABS(TI-300)/4+4
      DX=(X-3)/N
      S=SI
   12 DO 22 J=1,N
        X=3.0+(J-0.5)*DX
        Q=CUBERT(X)
        DQDX=Q/3/X
        XP=EXP(-E/X)
        SUM=SM1=0
        DO 19 K=1,6
          L=4-K
          QL=Q**L
          SUM=SUM+A(K)*QL
          SM1=SM1+A(K)*L*QL*DQDX/Q
   19     CONTINUE
        CPX=4.0+(E*SUM/X/X+SM1)*XP
   20 S=S+CPX*DX/X
C  CONVERT TO DIMENSIONED RESULTS .JOULES .MOLES,KELVINS.
   22   CPZ=R*CP
        SZ=R*S
      HZ=R*TI*H
      CVZ=CPZ-R
      EZ=HZ-R*TI
      RETURN
      END
C     *****************************************
      REAL FUNCTION PVTFUN(T,D,M)
C
C THE EQUATION OF STATE FOR PROPANE
C PVTFUN=PRESSURE(BAR)
C  M=0 YIELDS DP/DT AND D2PDT2 M=1 YIELDS ALSO DP/DD
C  EONSTATE,P-PSAT=S*GK*(T-TSAT)+S*S*GK*TCRT*F(R,T)
C  WHERE F(R,T)=B(S)*XBF(R,T)+E(S)*XEF(R,T)
C  AND B(R)=B1+B2*R+B3*R2+B4*R3
C  E(R)=E1*(R-1)*(R-ER)*EXP(-GA*R4)
      COMMON GK,GKK,B1,B2,B3,B4,E1,ER
      COMMON/B01/AL,BE,GA,DE,DCRT,TCRT,RCRT,DGAT,DTRP,TTRP,PTRP
      COMMON/B03/DPDT,D2PDT2,DPSDT,DPMDT,DPDD,DPDR,DTSDR,DTHDR
      COMMON/B04/XB1,XB2,XE1,XE2,DXBDR,DXEDR
      COMMON/B06/TSAT,THETA,PSAT
      COMMON/B20/B,BD,ED,XB,XE,F1
      DCRT=4.96
      IF(D.GT.0.0) GO TO 40
      PVTFUN=DPDT=D2PDT2=0.0
      DPDD=GKK*T
      DPDR=DPDD*DTRP
      RETURN
   40 R=S=D/DCRT
      R2=R*R
      R3=R2*R
      R4=R2*R2
      SN=S-1.0
      SR=S-ER
      TC=TCRT
      RG=R*GK
      GKT=GK*TC
      DSDR=DTRP/DCRT
      TS=TSAT=TSATF(D)
      PS=PSAT=VAPRES(TS)
      THETA=THETAF(D)
      XB=XBF(T,D)
      XE=XEF(T,D)
      B=(B1+B2*R+B3*R2+B4*R3)*R2
      XP=EXP(-GA*R4)
      SM=SN*R2*SR
      E=E1*SM*XP
      F=B*XB+E*XE
      F1=B*XB1+E*XE1
      F2=B*XB2+E*XE2
      PVTFUN=PS+RG*(T-TS)+GKT*F
      DPDT=RG+GK*F1
      D2PDT2=GK*F2/TC
      IF(M.EQ.0.0) RETURN
      BD=(2.0*B1*R+3.0*B2*R2+4.0*B3*R3+5.0*B4*R4)*DSDR
      XP1=-4.0*GA*R3
      SM1=SN*R2+(3.0*R-2.0)*R*SR
      ED=(SM*XP1+SM1)*E1*XP*DSDR
      F1=B*DXBDR+BD*XB+E*DXEDR+ED*XE
      DPDR=(DPSDT-RG)*DTSDR+(T-TS)*GK*DSDR+GKT*F1
      DPDD=DPDR/DTRP
      RETURN
      END
C ******************************************
      REAL FUNCTION QVAP(T)
C
C     PROPANE HEATS OF VAPORIZATION,(J/MOLE)
C     VIA PROGRAM QVAP-C3,DEC.15,1976 AT 14.31,USING-
C     DATA FROM PTHERM4,DEC.13,1976 AT 10.31.
C     QVAP/QTRP=X+(XE-X)*(A+B*X/XE+C*X),WHERE-
C     X=(TC-T)/(TC-TT)
C     XE=X**E
C
      REAL E,QT,TTRP,TCRT,XN,A,B,C,T,XE,X,S
C     DECLARING THE CONSTANTS
C       QT=HEAT OF VAPORIZATION AT THE TRIPLE POINT
        E=0.38
        QT=23.906
        TTRP=85.47
        TCRT=369.800
        XN=284.33
        A=0.98373471
        B=0.41758440
        C=-0.30674140
C     CACULATING THE QVAP HEAT OF VAPORIZATION
        IF(T.GE.369.800) GO TO 5
    2    X=(TCRT-T)/XN
         XE=X**E
         S=A+B*X/XE+C*X
    3    QVAP=QT*1000.0*(X+(XE-X)*S)
         RETURN
    5    QVAP=0.0
         RETURN
         END
C ******************************************************
      SUBROUTINE REMSAT
C
C---MEMORIZE FUNCTIONS ON THE SATURATED LIQUID BOUNDARY.
C---STORE DK,EK,SK,CVK, EVERY 10 K FROM 90 THRU 360 K.
C
        COMMON/B08/IN,IK,P,T,DEN,E,H,S,CV,CP,CSAT,W,WK
        COMMON/B11/DK(40),EK(40),SK(40),CVK(40)
       J = IFIX(T/10.0)
       T = 10.0*J
        CALL COEXST
        DK(J) = DEN
        EK(J) = E
        SK(J) = S
        CVK(J) = CV
       RETURN
       END
C ********************************************
      REAL FUNCTION THETAF(DEN)
C
C     THETA=TSAT*EXP(U(S))
C     LET Q=(S-1.0)/(ST-1.0),WHERE ST=DTRP/DCRT.THEN-
C     IF S.LT.1.0, U=AL*Q**3,AND IF S.GT.1.0, U=-AL*Q**3.0
```

```
      COMMON/B01/AL,BE,GA,DE,DCRT,TCRT,PCRT,DGAT,DTRP,TTRP,PTRP
      COMMON/B03/DPDT,D2DT2,DPSDT,DPMDT,DPDD,DPDR,DTSDR,DTHDR
      COMMON/B06/TSAT,THETA,PSAT
    1 S=DEN/DCRT
      DSDR=DTRP/DCRT
      C=DSDR-1.0
    2 Q=(S-1.0)/C
      Q2=Q*Q
      U=AL*Q*Q2
      U1=AL*3.0*Q2*DSDR/C
      IF(Q) 5,9,4
    4 U=-U
      U1=-U1
    5 XP=EXP(U)
      THETAF=TSAT*XP
    6 DTHDR=(TSAT*U1+DTSDR)*XP
      RETURN
    9 THETAF=TCRT
      DTHDR=0.0
      RETURN
      END
C   ****************************************

      REAL FUNCTION TSATF(DEN)
C
C   ITERATE TEMPERATURE TO MINIMIZE (DEN-DCLAC)
C   VIA DENGSF(T),DENLQF(T).
      COMMON/B01/AL,BE,GA,DE,DCRT,TCRT,PCRT,DGAT,DTRP,TTRP,PTRP
      COMMON/B03/DPDT,D2PDT2,DPSDT,DPMDT,DPDD,DPDR,DTSDR,DTHDR
      COMMON/B05/DDSDT
    1 FORMAT(1H0,9X,'TSATF FAILS TO CONVERGE',/)
      Q=2.0
      FN=6.3890561
C   NOTE , FN=EXP(Q)-1.0
      S=DEN/DCRT
      YN=TCRT/TTRP-1.0
      IF(DEN-DCRT) 3,30,4
    3 ST=DGAT/DCRT
      F=ALOG(S)/ALOG(ST)*((1.0-S)/(1.0-ST))**2.0
      GO TO 5
    4 ST=DTRP/DCRT
      U=((S-1.0)/(ST-1.0))**3.0
      F=(EXP(Q*U)-1.0)/FN
    5 T=TCRT/(1.0+YN*F)
    6 DO 15 J=1,50
        IF(DEN-DCRT) 7,30,8
    7   DD=DEN-DENGSF(T)
        GO TO 9
    8   DD=DEN-DENLQF(T)
    9   IF(ABS(DD/DEN).LT.1.0E-6) GO TO 16
   10   DT=DD/DDSDT
        TEST=ABS(DT/T)
        IF(TEST.LT.1.0E-6) GO TO 16
   11   T=T+DT
        IF(T) 12,12,13
   12   T=TTRP
        GO TO 15
   13   IF(T.LT.TCRT) GO TO 15
   14   T=TCRT-0.10
   15   CONTINUE
```

```
            WRITE(6,1)
            STOP
      16    TSATF=T
            DTSDR=DTRP/DDSDT
            RETURN
      30    TSATF=TCRT
            DTSDR=0.0
            RETURN
            END
C ***************************************
            REAL FUNCTION VAPRES(T)
C
C     PROPANE VAPOR PRESSURE (BARS)
C      LN(P/PT)=A*X+(B*U+C*U2+D*U3)*(1-U)**E
C      ARGS.,U=(T-TT)/(TC-TT)
C             X=(1-TT/T)(1-TT/TC)
C      TTRP=TRIPLE POINT TEMP
C      TCRT=CRITICAL POINT TEMP
C      PTRP=PRESSURE AT TRIPLE POINT
            REAL E,PTRP,TTRP,TCRT,A,B,C,D,UN,U,U2,UIT
            REAL XN,X,X1T,V,T,Z,Z1,W1,W,F,F1T,DPSDT,VPRES
            COMMON/B03/DPDT,D2PDT2,DPSDT,DPMDT,DPDD,DPDR,DTSDR,DTHDR
C
C      DECLARING THE CONSTANTS
C
            E=1.3
            PTRP=3.0E-9
            TTRP=85.47
            TCRT=369.80
            A=23.37228380
            B=5.71668788
            C=-8.51170714
            D=3.97587379
C
C      CALCULATING THE VAPOUR PRESSURE
C
       2    UN=TCRT-TTRP
            U=(T-TTRP)/UN
            U2=U*U
            UIT=1.0/UN
       3    XN=1-TTRP/TCRT
            X=(1-TTRP/T)/XN
            X1T=TTRP/XN/T/T
       4    V=1.0-U
            IF(V.LT.0.0) GO TO 5
            IF(V.EQ.0.0) GO TO 6
            IF(V.GT.0.0) GO TO 7
       5    VAPRES=0.0
             WRITE(6,1)
            RETURN
       6    Z=Z1=0.0
            GO TO 8
       7    Z=V**E
            Z1=-E*Z/V
       8    W=B*U+C*U2+D*U*U2
            W1=B+2*C*U+3*D*U2
       9    F=A*X+W*Z
            F1T=A*X1T+(W*Z1+W1*Z)*UIT
      10    VAPRES=PTRP*EXP(F)
```

THE UNIVERSITY OF NEW BRUNSWICK

```
      DPSDT=F1T*VAPRES
      RETURN
    1 FORMAT(1H0,9X,'T EXCEEDS TCRT IN VAPRES')
      END
C ****************************************

      REAL FUNCTION XBF(T,D)
C
C   XBF=SQRT(T/TC)*LN(T/TS)=Q(T)*Z(R,T)
      COMMON/B01/AL,BE,GA,DE,DCRT,TCRT,PCRT,DGAT,DTRP,TTRP,PTRP
      COMMON/B03/DPDT,D2PDT2,DPSDT,DPMDT,DPDD,DPDR,DTSDR,DTHDR
      COMMON/B04/XB1,XB2,XE1,XE2,DXBDR,DXEDR
      COMMON/B06/TSAT,THETA,PSAT
      TC=TCRT
      TS=TSAT
      X=T/TC
      U=T/TS
      U1X=TC/TS
      U1R=-U*DTSDR/TS
      Z=ALOG(U)
      Z1R=U1R/U
      Z1X=U1X/U
      Z2X=-Z1X*Z1X
      Q=SQRT(X)
      Q1=0.5/Q
      Q2=-Q1/2.0/X
      XBF=Q*Z
      DXBDR=Q*Z1R
      XB1=Q*Z1X+Q1*Z
      XB2=Q*Z2X+Q1*2.0*Z1X+Q2*Z
      RETURN
      END
C   **************************************

      REAL FUNCTION XEF(T,D)
C
C   XEF(T,D)=PSI(T,D)-PSISAT(D),
C   WHERE PSI=DE/X=(1-DE)*(1-W+W*LN(W))
C   W=(1-TH/T)
      COMMON/B01/AL,BE,GA,DE,DCRT,TCRT,PCRT,DGAT,DTRP,TTRP,PTRP
      COMMON/B03/DPDT,D2PDT2,DPSDT,DPMDT,DPDD,DPDR,DTSDR,DTHDR
      COMMON/B04/XB1,XB2,XE1,XE2,DXBDR,DXEDR
      COMMON/B06/TSAT,THETA,PSAT
      A=DE
      B=1.0-A
      TC=TCRT
      TH=THETA
      TS=TSAT
      X=T/TC
      X2=X*X
      XS=TS/TC
      XS1=DTSDR/TC
      W=1.0-TH/T
      IF(W) 30,30,5
    5 W1R=-DTHDR/T
      W1X=TH/T/X
      W2X=-2.0*W1X/X
      G=ALOG(W)
      G1R=W1R/W
      G1X=W1X/W
```

```
                G2X=W2X/W-G1X*G1X
                P=A/X+B*(W*G-W+1.0)
                P1R=B*(W*G1R+W1R*G-W1R)
                XE1=-A/X2+B*(W*G1X+W1X*G-W1X)
                XE2=2.0*A/X/X2+B*(W*G2X+2.0*W1X*G1X+W2X*G-W2X)
                WS=1.0-TH/TS
                IF(WS) 20,20,21
          20    PS=1.0
                PS1=0.0
                GO TO 25
          21    GS=ALOG(WS)
                PS=A/XS+B*(WS*GS-WS+1.0)
          22    PS1=-A*XS1/XS/XS+B*(TH*DTSDR/TS-DTHDR)*GS/TS
          25    XEF=P-PS
                DXEDR=P1R-PS1
                RETURN
          30    XEF=XE1=XE2=DXEDR=0.0
                RETURN
                END
       C ***************************************************


TANK PRESSURE           =      9.997 BARS
MASS OF PROPANE (L+V)=  10000.000 KG.
VOL. OF PROPANE (L+V)=     30.000 CUBIC METERS

IFLAG                   =      2

SATURATED LIQUID STATE

TEMPERATURE             =    300.000 K
DENSITY                 =   489.2559 KG/M**3
DP/DT                   =   5.095484 BAR/K
DP/DD                   =     3.0540 BAR-M**3/KG
INTERNAL ENERGY(E)      =     591.06 KJ/KG
SPECIFIC ENTHALPY(H)    =     593.10 KJ/KG
SPECIFIC ENTROPY(S)     =      4.516 KJ/(KG-K)
SPECIFIC HEAT(CV)       =       1.69 KJ/(KG-K)
SPECIFIC HEAT (CP)      =       2.76 KJ/(KG-K)
VELOCITY OF SOUND       =      705.6 M/SEC

LATENT HEAT OF EVAP.    =      333.3 KJ/KG

MASS OF LIQUID          =    9925.71 KG
VOLUME OF LIQUID        =      20.29 M**3

SUPERHEATED VAPOR STATE

TEMPERATURE             =    700.000 K
DENSITY                 =     7.6472 KG/M**3
DP/DT                   =   0.014693 BAR/K
DP/DD                   =     1.2971 BAR-M**3/KG
INTERNAL ENERGY(E)      =    1830.84 KJ/KG
SPECIFIC ENTHALPY(H)    =    1961.57 KJ/KG
SPECIFIC ENTROPY(S)     =      7.740 KJ/(KG-K)
SPECIFIC HEAT(CV)       =       3.05 KJ/(KG-K)
SPECIFIC HEAT (CP)      =       3.25 KJ/(KG-K)
VELOCITY OF SOUND       =      371.7 M/SEC

MASS OF VAPOR           =      74.29 KG
```

SITY OF NEW

```
VOLUME OF VAPOR        =       9.71 M**3

STATEMENTS EXECUTED=    19401
CORE JSAGE       OBJECT CODE=   43736 BYTES,ARRAY AREA=    2260 BYTES,TOTAL AREA AVAILABLE=  131072  BYTE
DIAGNOSTICS          NUMBER OF ERRORS=         0, NUMBER OF WARNINGS=          0, NUMBER OF EXTENSIONS=       33
COMPILE TIME=     0.76 SEC,EXECUTION TIME=     0.35 SEC,     11.03.36    TUESDAY        6 JUL 82    WATFI

        C$STOP
```

```
**************************************************************************************************
C ****************************************************
C **                                                **
C **         SIMULATED MAIN PROGRAM                 **
C **   TO COMPUTE  THERMAL CONDUCTIVITY, VISCOSITY, **
C **       AND SURFACE TENSION OF PROPANE           **
C ****************************************************
C
C     INPUT TEMPERATURE (T, K) AND DENSITY (D, KG/M**3)
C
      T = 300.00
      D = 440.0
C
      DMOL = D/44.1
      TC = CONDUC(T,D)
      VISC = VISCOS(T,D)
      ST = SURFT(T)
      WRITE(6,110)T,D,DMOL,TC,VISC,ST
  110 FORMAT(1X,'TEMPERATURE            = ',E12.5,' K',/,
     @       1X,'DENSITY (KG/M**3)      = ',E12.5,' KGM/M**3',/,
     @       1X,'DENSITY (MOL/L)        = ',E12.5,' MOL/L',/,
     @       1X,'THERMAL CONDUCTIVITY = ',E12.5,' MILLIWATT/M-K',/,
     @       1X,'VISCOSITY              = ',E12.5,' MICROGRAM/CM-S',/,
     @       1X,'SURFACE TENSION        = ',E12.5,' DYNES/CM',/)
      STOP
      END
      FUNCTION VISCOS(T,RO)
C
C------FUNCTION TO CALCULATE VISCOSITY (MICROGRAM/CM-SEC)
C        T  = TEMPERATURE, K
C        RO = DENSITY IN KG/M**3
C
      REAL*8 A,B,C,E,F,AJ1,AJ2,AJ3,AJ4,AJ5,AJ6,AJ7,GV(9)
      RO = RO*0.001
C
      A = 0.0
      B = 0.0
      C = 1.12
      E = 1.0
      F = 358.9
      ROCR = 0.211
C
      GV(1) =-0.1132608333D 07
      GV(2) = 0.8465572850D 06
      GV(3) =-0.2314345388D 06
      GV(4) = 0.2089338580D 05
      GV(5) = 0.2693257510D 04
      GV(6) =-0.8709423636D 03
      GV(7) = 0.9216623121D 02
      GV(8) =-0.4593654004D 01
      GV(9) = 0.9088758027D-01
C
      AJ1 =-0.1496346267D 02
      AJ2 = 0.2179858583D 02
      AJ3 =-0.2566988314D 05
      AJ4 = 0.1527903946D 04
      AJ5 =-0.2112678461D 00
      AJ6 = 0.2127695241D 03
      AJ7 = 0.55159879190D 05
C
      ROR = RO/ROCR
      THETA = ROR-1.0
C
C-----CALCULATE DILUTE GAS VISCOSOTY (V0)
C
      VAR = T**(-4.0/3.0)
      V0 = 0.0
      DO 20 IH=1,9
      VAR = VAR*T**(1.0/3.0)
      V0 = V0+GV(IH)*VAR
   20 CONTINUE
C
C-----CALCULATE MODERATE DENSITY CONTRIBUTION (V1)
C
      V1 = (A+B*(C-DLOG(T/F))**2)*RO
C
C-----CALCULATE HIGH DENSITY CONTRIBUTION (V2)
C
      V2 = E*DEXP(AJ1+AJ4/T)*(DEXP(RO**0.1*(AJ2+AJ3/T**1.5)+
     @     THETA*SQRT(RO)*(AJ5+AJ6/T+AJ7/(T*T)))-1.0)
C
C-----CALCULATE BACKGROUND VISCOSOTY
C
      VHAN = V0+V1+V2
      VISCOS = VHAN
C
        RO = RO*1000.0
        RETURN
        END
        FUNCTION CONDUC(T,RO)
C
C----- FUNCTION TO CALAULATE THERMAL CONDUCTIVITY, MILLIWATT/M-K
C         T  = TEMPERATURE, K
C         RO = DENSITY, KG/M**3
C
        REAL*8 A,B,C,D,F,AK1,AK2,AK3,AK4,AK5,AK6,AK7,GT(9)
        RO = RO*0.001
C
        A =-1.149813131
        B = 0.788531221
        C = 1.12
        D = 1.0
        F = 358.9
        ROCR = 0.211
C
        GT(1) =-0.10893811030D 07
        GT(2) = 0.83432978290D 06
        GT(3) =-0.22709027360D 06
        GT(4) = 0.16678663680D 05
        GT(5) = 0.43473205650D 04
        GT(6) =-0.11777846710D 04
        GT(7) = 0.12154258330D 03
        GT(8) =-0.60405969210D 01
        GT(9) = 0.12073736810D 00
C
        AK1 =-0.10924494640D 02
        AK2 = 0.14806220800D 02
      AK3 =-0.1874097856D 05
      AK4 = 0.1269709514D 04
      AK5 =-0.9598486895D-01
      AK6 = 0.1389024749D 03
      AK7 = 0.2554581504D 05
C
C-----CALCULATE THERMAL CONDJCTIVITY BY HANLEY'S CORRELATION
C
      ROR = RO/ROCR
      THETA = ROR-1.0
C
C-----CALCULATE DILUTE GAS THERMAL CONDUCTIVITY (TC0)
C
      VAR = T**(-4.0/3.0)
      TC0 = 0.0
      DO 20 IH=1,9
      VAR = VAR*T**(1.0/3.0)
      TC0 = TC0+GT(IH)*VAR
   20 CONTINUE
C
C-----CALCULATE MODERATE DENSITY CONTRIBUTION (TC1)
C
      TC1 = (A+B*(C-DLOG(T/F))**2)*RO
C
C-----CALCULATE HIGH DENSITY CONTRIBUTION (TC2)
C
      TC2 = D*DEXP(AK1+AK4/T)*(DEXP(RO**0.1*(AK2+AK3/T**1.5)+
     @      THETA*SQRT(RO)*(AK5+AK6/T+AK7/(T*T)))-1.0)
C
C-----CALCULATE BACKGROUND THERMAL CONDUCTIVITY
C
      TCHAN = TC0+TC1+TC2
      CONDUC = TCHAN
C
       RO = RO*1000.0
       RETURN
       END

       FUNCTION SURFT(T)
C
C------FUNCTION PROGRAM TO CALCULATE SURFACE TENSION OF PROPANE.
C         SURFT = SURFACE TENSION, DYNES/CM
C         T     = TEMPERATURE, K
C
C------DEFINE COEFFICIENTS.
C
       ST0 = 27.870112
       AMU = 0.8645988
       B   = 0.2133452
       TCR = 369.8
C
C------CALCULATE SURFACE TENSION
C
       X = 1.0-T/TCR
       SURFT = (ST0*X**AMU)*(1.0+B*X)
       RETURN
       END

EMPERATURE          =  0.30000E 03 K
```